NTNU

Norwegian University of
Science and Technology

Investigation of metallic bipolar plates for PEM fuel cells

Sigrid Lædre

Chemical Engineering and Biotechnology

Submission date: June 2011

Supervisor: Frode Seland, IMTE

Co-supervisor: Anders Ødegård, SINTEF

Ole Edvard Kongstein, SINTEF

Norwegian University of Science and Technology

Department of Materials Science and Engineering

Preface

This master thesis is written as part of the course TMT 4900 at the Department of Material Science and Engineering, NTNU. The work leading up to this report was done in cooperation with SINTEF. I, Sigrid Lædre, declare that the work described in this report has been done according to the regulations at NTNU.

I want to take this opportunity to thank my supervisor, associate professor Frode Seland, for guidance and support throughout the entire project. I also want to give thanks to Dr. Anders Ødegård and Dr. Ole Edvard Kongstein from SINTEF for helping me during the experimental work in the lab.

I would like to thank Julian Tolchard, for education in how to use the SEM apparatus. I also want to thank Rebecca Williams for helping me with proofreading of the report. Finally, I want to thank Camilla Sommerseth, Toril Nyhus and Inga Askestad for help and support throughout the entire project.

Trondheim 09.06.2011

Sigrid Lædre

Abstract

High cost and a short lifetime are the two main reasons why the PEM fuel cell is yet to be commercialized. The bipolar plate in a PEM fuel cell is alone responsible for about 45% of the cost and 85% of the total weight of a single cell [3]. stainless steel has been suggested as material for the bipolar plate because of its good mechanical properties, easy manufacturing and relatively low price. A problem with stainless steel is the Chromium oxide film formed on the surface which causes a high contact resistance. In order to prevent this oxide formation, the stainless steel can be coated. Gold has been suggested as coating, but it is too expensive to be considered a viable alternative.

The objective of this thesis was to investigate stainless steel as bipolar plate material for PEM fuel cells. In cooperation with SINTEF polarization tests were done on stainless steel bipolar plates with and without two different coatings; gold and Coating A. The tests were performed in H_2SO_4 electrolytes with different molarities and additives. Before and after each polarization test Interfacial Contact Resistance (ICR) measurements where done to see how the oxide layer on the stainless steel surface changed during polarization. Gold coated stainless steel was chosen as standard for both the polarization tests and the ICR measurements because of its corrosion resistance.

The results obtained from both polarization tests and corresponding ICR measurements showed that the reproducibility was not as good as one had hoped, but this can be explained by low absolute values of the current densities. Gold coated steel proved to be a good standard for the ICR measurements, but due to pitting corrosion the corresponding polarization results were not as promising. The pH in an operating fuel cell was found to be approximately 3.5, and the tests done at different molarities showed that at a lower pH the oxide layer seemed to be thinner and the stainless steel surface thus became more exposed to corrosion. Additions of fluoride and chloride in the amounts expected in an operating fuel cell did not seem to cause any changes for neither the polarization results nor the contact resistance measurements.

Stainless steel plates with Coating A showed very small changes in contact resistance after being put trough the polarization tests, but at low potentials the current densities in the polarization test were very high, indicating that components in the coating either catalyzed hydrogen evolution or were reduced themselves. Out of all the ICR measurements, gold coated stainless steel was the only plate satisfying US department Of Energy's (DOE) resistance requirement for bipolar plates of less than 10 $m\Omega\ cm^2$. The stainless steel plates with Coating A were close to DOE's requirements for both corrosion current and contact resistance. Non-coated stainless steel was ruled out as bipolar plate material due to high contact resistance measurements.

Abbreviations

Term	Definition
AFC	Alkaline Fuel Cell
BSE	Backscattered Electron Mode in the SEM
DOS	US department of energy
EDS	Energy Dispersive Spectrometer
ICR	Interfacial Contact Resistance
MCFC	Molten Carbonate Fuel Cell
OCV	Open Circuit potential
PAFC	Phosphoric Acid Fuel Cell
PEM	Proton Exchange Membrane
PEMFC	Proton Exchange Membrane Fuel Cell
PPM	Parts Per Million
SE	Secondary Electron Mode in the SEM
SHE	Standard Hydrogen electrode
SEM	Scanning Electron Microscopy
SOFC	Solid Oxide Fuel Cell

Nomenclature

Symbol	Description	Unit
U	Potential	V
I	Current	A
i	Current density	A cm^{-2}
P	Pressure	N cm^{-2}
E	Potential	V
t	seconds	s
Ω	Resistance	Ohm

Contents

1. Introduction

Fuel cells are electrochemical devices that efficiently convert chemical energy to electrical energy, and have become an important contribution to the development of more environmental friendly energy sources. PEMFCs, short for Proton Exchange Membrane Fuel Cells, operate in the low temperature window yielding a fast response time desired in several applications, and if fed with pure hydrogen and oxygen, only emit water, heat and some unused gases. The PEM fuel cell (Figure 1) combines hydrogen and oxygen to form electrical energy from electrochemical reactions at the electrodes. Compared to combustion of fossil fuels, PEM fuel cells operated with pure hydrogen release little or no greenhouse gases. Additionally, the efficiency of a fuel cell is significantly improved compared to a hydrogen combustion engine. This makes PEM fuel cells attractive in today's environmental-concerned society, and a great deal of research is done to make PEM fuel cells more efficient and applicable in e.g. portable electronic equipment, as well as mobile and stationary applications. Today, most emphasis of fuel cells is in the transportation sector.

There are several challenges to overcome in order to make PEM fuel cells more efficient. The two main setbacks of PEMFCs are short lifetime and high costs. The lifetime of a PEM fuel cell is highly dependent on the degrading of the different components in the fuel cell, and the environment inside the PEM fuel cell is acidic, which means that corrosion resistant components are required for the cell to operate over longer periods of time. Noble metals, such as platinum and ruthenium, are thus often used as electrocatalysts in PEM fuel cells. These catalysts, along with the carbon separators and acid tolerant gaskets, effectively increase the material and manufacturing cost of the cells.

As a direct consequence of the environment, the cost of a fuel cell is highly dependent on the bipolar plate (Figure 3), which stands for about 45 % of the total cost of a PEMFC today [3]. Most commercialized bipolar plates made today are carbon based, but they are expensive to produce. Metal bipolar plates are cheaper to produce than the carbon based plates, and they are usually very good electric conductors (section 2.3). But the metal plates tend to degrade over time, mainly due to corrosion. To avoid this degrading, metal bipolar plates are often coated with corrosion resistant coatings. Gold is a corrosive resistant metal, and is often used as coating for bipolar plates. However, gold is expensive and a lot of effort is put into the development of new, cheaper coatings.

The research described in this report was done by corrosion- and contact resistance testing of stainless steel bipolar plates, with and without coating. The research was performed in cooperation with SINTEF, as part of an ongoing international project. The primary objective of this project is inspired by DOS targets for PEM fuel cells (Table 1), in order to develop new, more cost efficient coatings for stainless steel bipolar plates, preferably with lifetimes of longer than 10 000 hours. The objective of the project described in this report was to study how stainless steel bipolar plates behave in a simulated PEM fuel cell environment, and how the contact resistances of the plates changed after going through these tests.

Table 1 : US department of energy's targets for PEM fuel cell bipolar plates [4, 5].

Properties	Units	2005	2010	2015
Cost	$ kW^{-1}	10	5	3
Weight	Kg kW^{-1}	0.36	<0.4	<0.4
H_2 permeation flux	cm^3 sec^{-1} cm^{-2} @ 80 ^oC, 3 atm	$<2x10^{-6}$	$<2x10^{-6}$	$<2x10^{-6}$
Corrosion	µA cm^{-2}	<1	<1	<1
Electrical conductivity	S cm^{-1}	<600	<100	<100
Resistivity	Ω cm^2	<0.02	<0.01	<0.01
Flexural strength	MPa	<34	<25	<25
Flexibility	% deflection at mid-span	1.5-3.5	3-5	3-5

2. Theory

This section of the report contains basic theory about fuel cells and bipolar plates. In addition, the theory required to perform the experimental work (section 3) and discuss the results is presented. Whenever it is relevant, the subsections contain previous work and description of experimental setups used in previous research.

2.1 Fuel Cells

In a fuel cell, an electrochemical reaction takes place to produce electrical current, and chemical energy is transformed into electrical energy. Two reactants are fed into the cell and combined, and the product is continuously taken out. The main difference between batteries and fuel cells is that the fuel is continuously fed to the fuel cell, while a battery is sealed with a limited amount of fuel inside it. The fuel cell can thus be operated over longer periods of time without any down time as long as reactants are being fed. The reaction that takes place inside a fuel cell depends on the type of fuel used. In the hydrogen fuel cell, hydrogen and oxygen (usually fed as air) reacts and water is the main product along with the converted electrical energy:

$$O_2 + 4e^- + 4\mathrm{H}^+ \rightarrow 2H_2O \qquad (1)$$

There are several types of fuel cells, including Proton Exchange Membrane- (PEMFC), Alkaline- (AFC), Phosphoric Acid- (PAFC), Molten Carbonate- (MCFC) and Solid Oxide (SOFC) fuel cells. They are separated into groups, typically by the operational temperature dictated by the electrolyte and charge carrier. The first fuel cell to be commercialized was the PAFC. This cell runs at about 200 ^{0}C, thus being situated between the high temperature (MCFC, SOFC) and the low temperature (PEMFC, AFC) cells. Some PAFC systems have experienced long lifetimes, by running for periods of over one year, with little or no maintenance needed. This is important, because the short lifetime of a fuel cell is one of the main obstacles to overcome prior commercial breakthrough. [6]

2.2 PEM fuel cells

PEM stands for Proton Exchange Membrane (Figure 1), and in this fuel cell the polymer membrane works as a solid electrolyte [6]. The working part of the fuel cell consists of a membrane with appropriate electrodes attached to each side, anode and cathode, and is usually referred to as the Membrane Electrode Assembly (MEA). A membrane made of Nafion is often used in PEM fuel cells. A PEMFC depends on liquid water to facilitate ion conductivity (H^+) and operates at temperatures between 30 ^{0}C to 100 ^{0}C, placing them in the low-temperature fuel cell group [6]. Figure 1 shows the schematic of a single cell, including MEA. The hydrogen is fed into the Anode side of the cell, and the oxygen (air) to the cathode side. Electrochemical reactions take place on both anode and cathode side:

Anode reaction: $H_2 \rightarrow 2H^+ + 2e^-$ (2)

Cathode reaction: $O_2 + 4e^- + 4\mathrm{H}^+ \rightarrow 2H_2O$ (3)

The membrane is proton conducting, and functions as an electron barrier between the anode and cathode in the fuel cell, letting only the hydrogen ions produced at the anode side through the membrane to the cathode side. On the cathode side the hydrogen ions and oxygen combine together with the electrons, from the anode, to form water. The electrons are forced to travel in an outer circuit from the anode to the cathode side, enabling electrical energy to be harvested from the chemical energy present in the hydrogen and oxygen. On both cathode and anode side of the cell there are catalysts to help the reduction and oxidation reactions, in order to minimize the loss (released as heat). The most common catalysts used in PEM fuel cells are platinum based. This is primarily due to the highly acidic environment within the fuel cell, where stability and corrosion resistance is an issue. This acid environment also limits the material selection for cell and stack components.

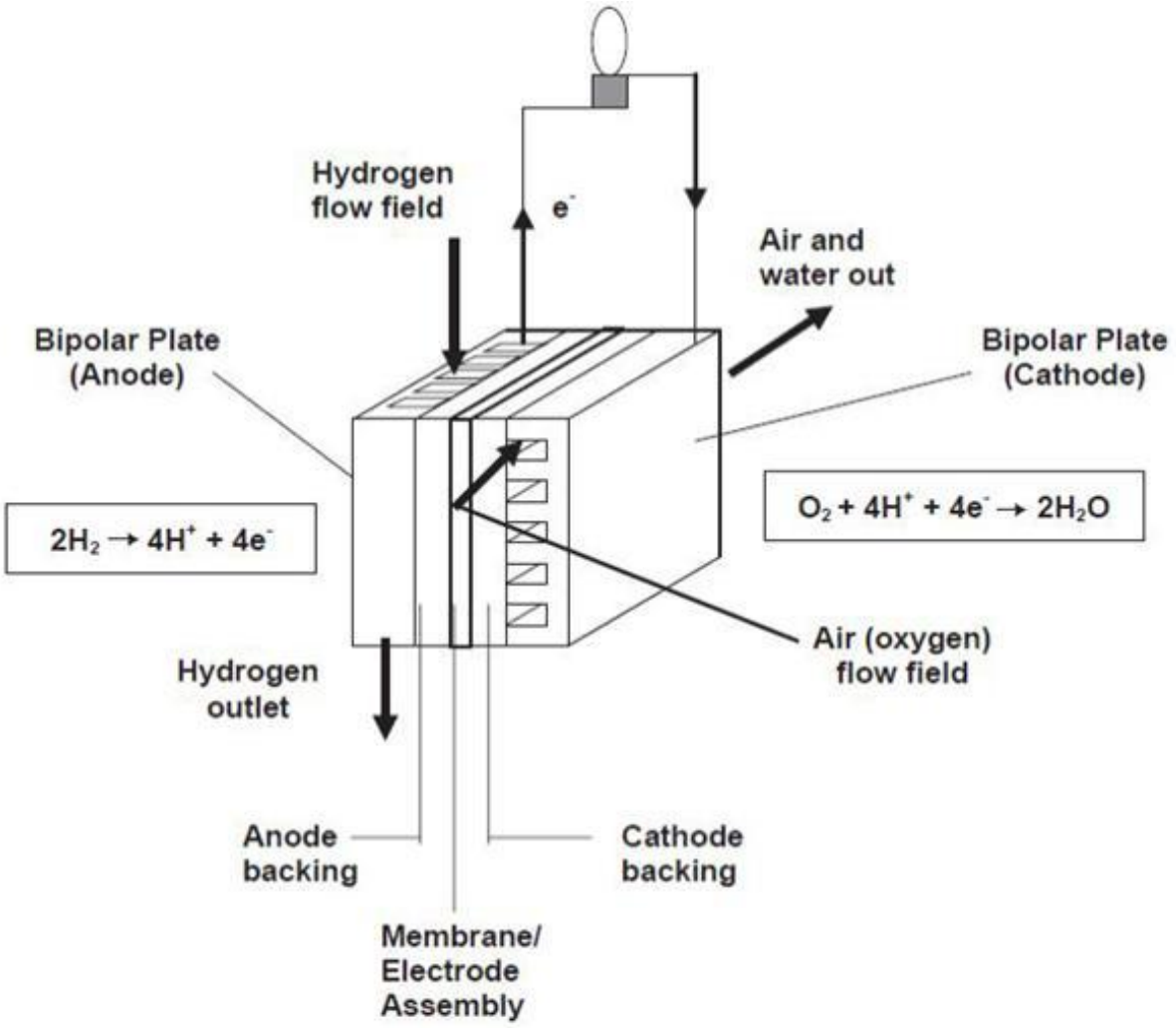

Figure 1: The PEM fuel cell. The hydrogen and oxygen is fed into the cell, and hydrogen ions are formed. The hydrogen ions are led trough the membrane, while the electrons travel in an outer circuit. [3]

An important term used for fuel cells, is the three-phase area. This refers to the gas-solid interface where the fuel gas meets the electrolyte membrane (containing H^+) and the solid electrode/catalyst (electron carrier). Both H_2 and O_2 are poorly soluble in the membrane, which limits the mass-transport. By creating a three-phase area, the concentration of the gas can become sufficient to sustain a high current density. A good way of increasing the three-phase area is to use a porous electrode material impregnated with the electrolyte membrane. The porous electrode must not be completely filled with water during operation of the fuel cell, and the gas flow should not get high enough to dry out the electrolyte within the pore. In order to obtain a high current density, both gas and electrolyte need to be accessible within the pores. For this system to work, the catalyst needs to be as active as possible. [6, 7]

Commercialized fuel cells systems are usually built up by several single cells in a so-called stack (Figure 2). The motivation for combining several fuel cells together in series is to customize the desired power output. In between each cell there is a bipolar plate (section 2.3), working as an anode on the hydrogen side and cathode on the oxygen side.

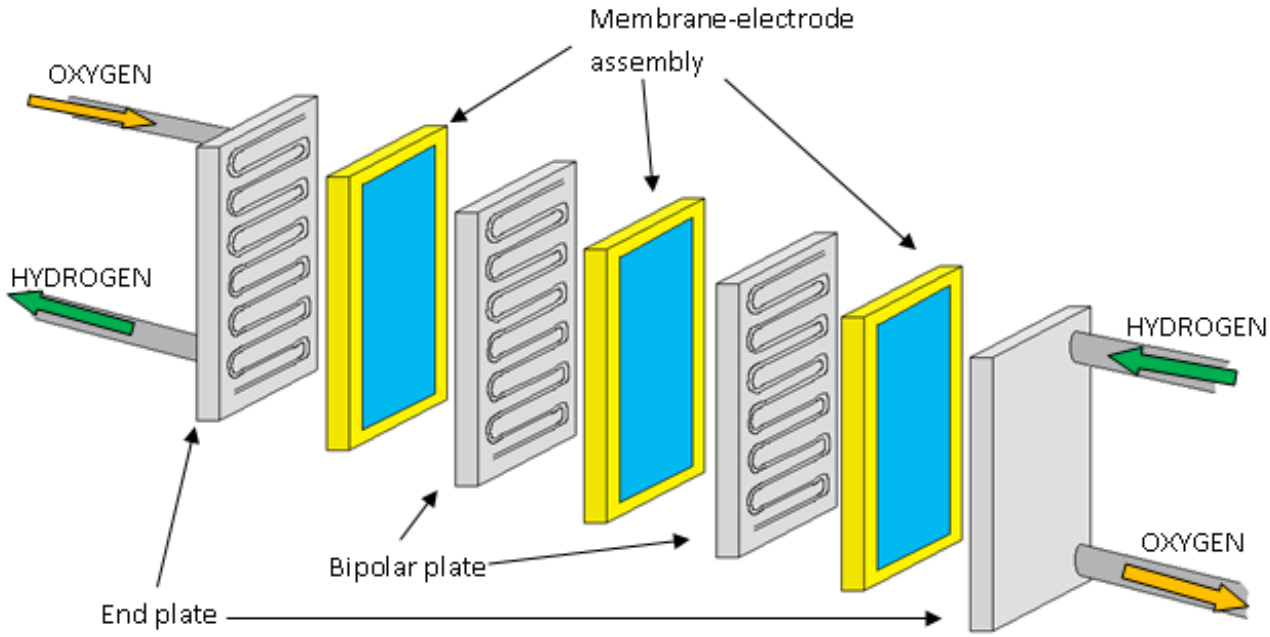

Figure 2: Several single cells put together in a stack. The bipolar plates work as separators between each single cell. [1]

2.2.1 Water management

It is necessary to humidify the cells in order to operate them over time. The protons formed at the anode needs water in order to be able to go through the membrane. Proton conductivity is directly proportional to the water content. If there is too much water inside the cell, the active sites in the catalytic layer may be blocked, and no reaction can take place. Ideally there would be enough water produced during the reaction to humidify the cell. But due to electro-osmotic drag, where the H^+ drags water from the anode to the cathode side, the humidity on the anode side is severely reduced. Another problem occurs at high temperatures, above 60 degrees, as the hot air dries out the electrodes faster than new water can be produced within the cell. All of these factors suggest that one has to use some sort of humidifier to humidify the gas before it enters the fuel cell. This extra amount of water comes out with the excess gas on the anode side and with the produced water and excess gas on the cathode side of the cell. [6]

2.2.2 Problems and challenges

There are two important issues which keep the PEM fuel cell from being more attractive as an electrochemical energy conversion device; lifetime and cost. To improve the lifetime of a PEMFC, more watt-hours per kg material has to be produced. The two components that contribute the most in decreasing the lifetime of the cells are the catalyst and the membrane. Both the catalyst and the membrane degrades over time [8]. By controlling the conditions under which the cell is operated (potential, temperature, humidity etc.), the lifetime of the MEA can be increased [8]. But big improvements have to be made if the lifetime is to be significantly increased. It is also desirable to get more watts per currency spent on the fuel cell. The cost of the PEMFC is highly affected by the catalyst. Platinum catalyst, which are often used in PEMFC's, are very expensive. The bipolar plates are also expensive, and stand for about 45% of the cost in the PEM fuel cells used today. Hopefully this cost can be reduced in the future by using metal bipolar plates instead of the carbon based ones that are most common today. [3]

2.3 The bipolar plate

The bipolar plate (Figure 3) is a very important component in the PEMFC stack (Figure 2), accounting for the vast amount of research done to improve them. The bipolar plate accounts for about 80% of the total cell-weight and ca. 45% of the cell cost [3]. The tasks of the bipolar plate is to distribute the gas in the cell, manage the water in the cell, remove heat from active areas, prevent leakage and to conduct the current away from each cell [3].

Figure 3: Nitrided metallic bipolar plate. The plate conducts the current between each cell in a stack, and the flowfield leads the gas trough the cell. [9]

When the gas enters a fuel cell stack (oxygen from one side, and hydrogen from the other), it comes in contact with the bipolar plate. The gas is led into the flow field, which is a pattern on the bipolar plate (Figure 3) that leads the gas trough the cell. When the gas is moving through the flow field, most of it will react and move through the membrane as H^+. The rest of the gas will move on to the next cell in the stack (Figure 2). The plates at the end of a stack have a flow field on one side, and are thus monoploar. The bipolar plates in between single cells have flow fields on both sides (one for oxygen and one for hydrogen), and are thus bipolar.

2.3.1 Design and material choice

When it comes to the design and flow fields of the bipolar plates, there are a lot of alternatives to be considered. Most common flow field patterns are column, serpentine (Figure 3 shows a quadruple serpentine flow field pattern) and iterdigitated. One can study the effect of gas flow utilizing various flow field designs. The flow field on the bipolar plate varies from company to company, and is usually a well kept secret.

When choosing which material to use in bipolar plates, there are some important factors that need to be taken into consideration. First off, the material has to be electrically conducting. The material should also be fairly resistible to corrosion. This causes problems because many good electrical conductors (e.g. metals) are easily corroded. The cost of the material needs to be kept as low as possible, to be able to commercialize the product. If a particular PEM fuel cell is to be used in e.g. a car, the total prize of this car should not be much more than other cars with the same performance and equipment. Figure 4 gives an overview over materials used in bipolar plates, and they are also categorized into different classes of materials.

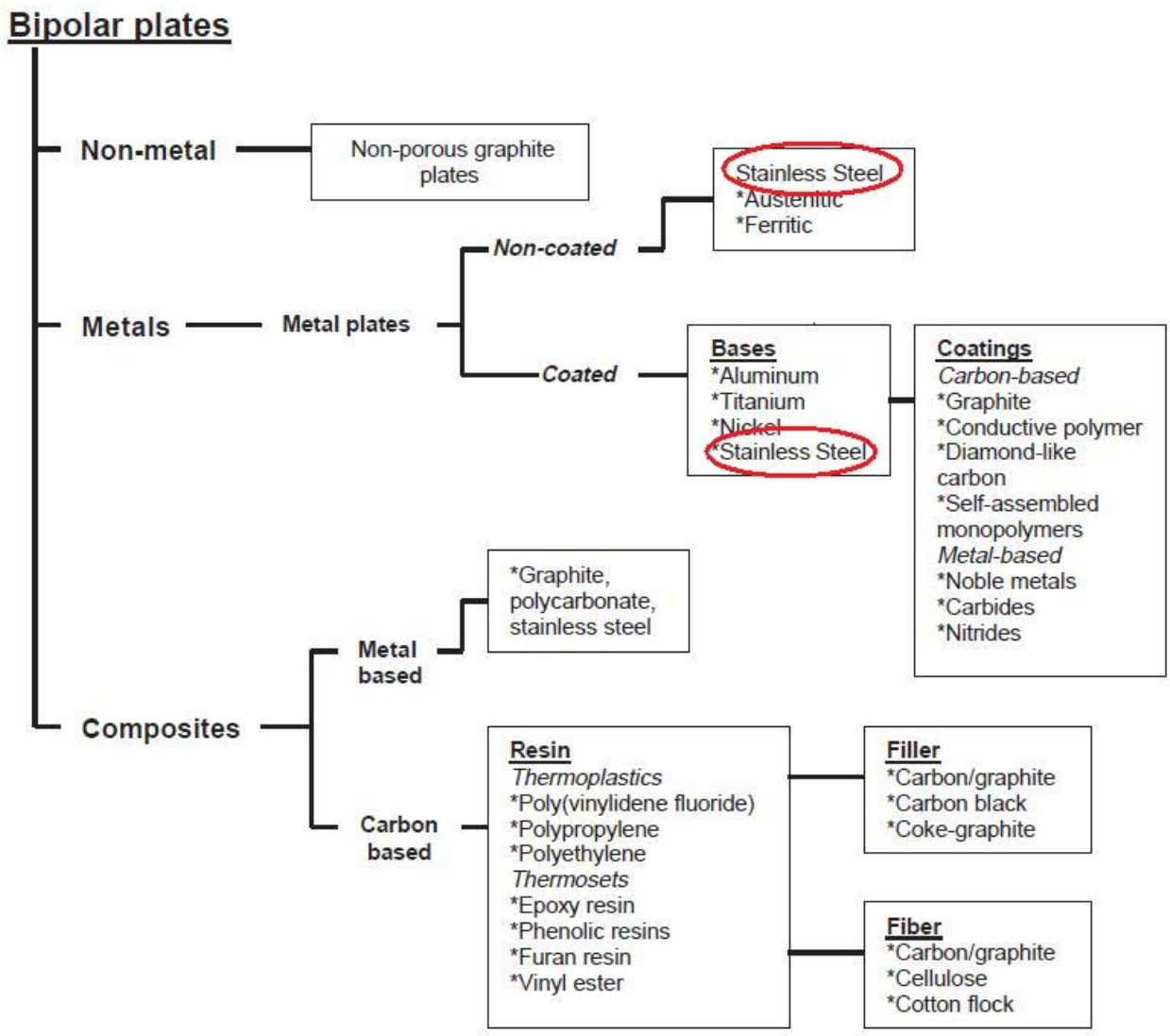

Figure 4: Classification of materials for bipolar plates used in PEMFC's [3].

Most commercialized bipolar plates today are carbon based, as they have a good chemical stability and low resistivity. The production of these plates, however, is expensive. Other materials used are metals and polymer composites. Polymer composites are lightweight and are easily molded into desired shape and size. Carbon based composites have already been extensively studied. [3]

A lot of research is done on metal bipolar plates, because they are simple and cheaper than carbon plates to mass produce. Stainless steel, Aluminum and Titanium are some of the metals used in bipolar plates (Figure 4). Metal bipolar plates show a high mechanical stability, and they are also highly conducting. The main problems with metal bipolar plates are that they corrode and dissolute due to the highly corrosive environment inside the fuel cell. One solution to these problems is to use a coating on the metal plate, which still allows for fast manufacturing of these plates. [3]

Stainless steel bipolar plates

The composition of 316L steel is presented in Table 2. Note that there is room for some variation in composition within the 316L grade steel.

Table 2: Chemical composition of 316L stainless steel [2].

C	Cr	Ni	Mn	Mo	Si	N	Cu	Co	Fe
<0.028	16.20-16.80	10.10-10-30	1.7-1.95	2.03-2.25	0.45-0.65	0.02-0.04	<0.5	<0.5	The rest

Stainless steel has a relatively high strength, low gas permeability, high chemical stability, a wide range of alloy choices and it is relatively cheap to produce [3]. There are however some drawbacks when it comes to using stainless steel in a PEM fuel cell. In the acidic environment (pH=2-3) and at temperatures around 80 ^{o}C [3], stainless steel may corrode. An oxide film may also form on the surface, which increases the contact resistance [10]. The contact resistance increases with the thickness of this oxide layer [10].

2.3.2 Coated metal bipolar plates

The coating used on metal bipolar plates needs to be conducting, and it is important that the contact resistance between coating and metal, as well as between coating and backing, is small. To avoid formation of cracks and pores when the plates are heated, the thermal expansion coefficient of the coating should be close to the substrate metals. There are different processes used to coat bipolar plates. Some of these are prone to pinhole defects, and new coatings techniques are under development to avoid these types of problems. [10]

There are a number of different materials used for bipolar plate coating, most of them are metal- or carbon-based. Graphite and diamond-like carbon are some of the carbon-based coatings. Metal-based coatings include noble metals, metal nitrides and metal carbides [10]. Gold coated stainless steel plates have shown performances similar to the carbon based plates [3], but gold is expensive and other coatings should be considered instead.

2.4 Degrading mechanisms of a metallic bipolar plate

2.4.1 Oxide layers and Passivity

Passivity is a phenomenon where metals form a thin, oxidized, protective layer on their surfaces in corrosive environments. Passivity protects the metal from corrosion by formation of a thin surface film under oxidizing conditions at high anodic polarization. Metals that form this protective oxide layer without being polarized are not considered to be passive. [11]

In stainless steel the oxide layer is formed by Chromium and Oxygen (Cr_2O_3), and can be formed in air, without anodic polarization. This layer is what makes the stainless steel rustproof, but as described above the oxide layer only makes the stainless steel passive when it is under anodic polarization. The Chromium content is crucial for the formation of the oxide layer in stainless steel, and minimum 12 % is needed for the layer to form at all. If too much Chromium is added the steel becomes brittle because of the formation of a brittle σ phase. The passivated film formed on stainless steel can be decomposed if the pH, temperature or concentration of certain compounds in the solution is changed. A change in potential can also cause the passivated film to decompose. [12]

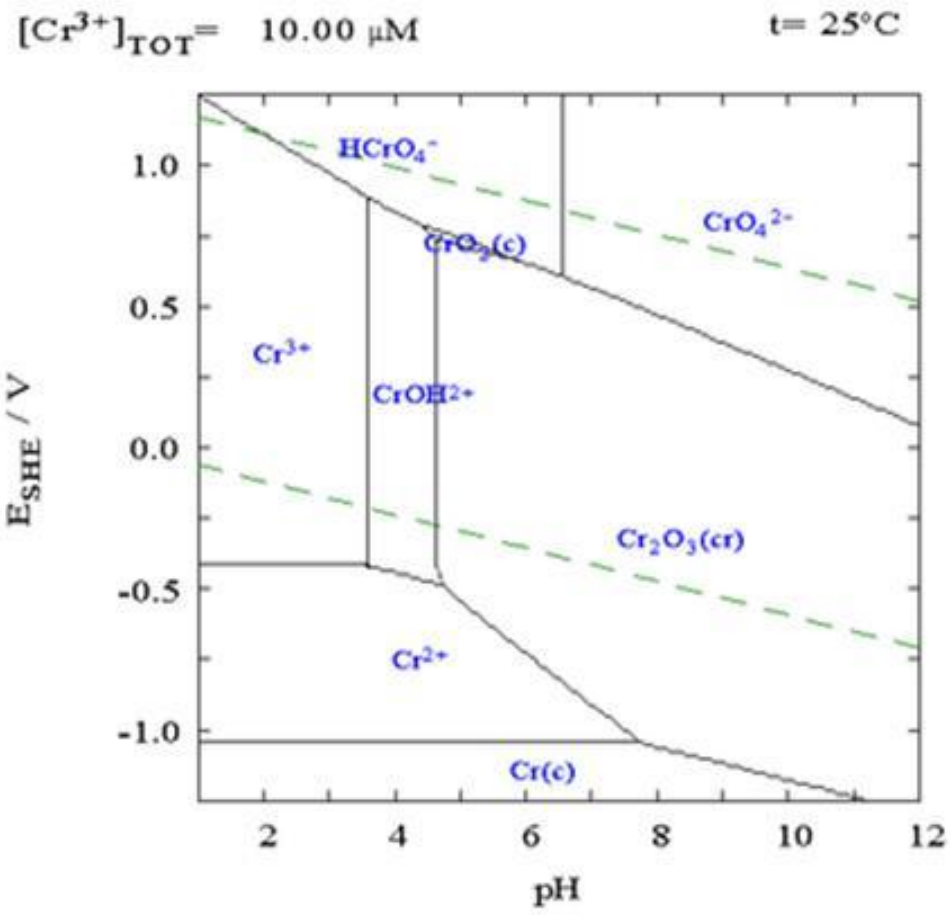

Figure 5: Pourbaix diagram, Chromium [13].

In order to understand the oxide layer formation of stainless steel the Pourbaix diagram of chromium must be considered. In Figure 5 the Pourbaix diagram of Chromium is displayed. A Pourbaix diagram presents the relationship between pH in the solution and the applied potential. The largest area in the figure shows the stability region of Cr_2O_3, and it is evident that below a certain pH, and between certain potentials, this protective oxide layer will no longer be formed. The Pourbaix diagram in Figure 5 is for pure Chromium, and the Pourbaix diagram for chromium in stainless steel would look a little different because of the other components in stainless steel. Figure 5 can however be used to illustrate how the different Chromium compounds are formed under different conditions. This has to be taken into consideration when ex-situ corrosion tests (section 2.5.3) are designed for investigation of corrosion in stainless steel.

2.4.2 Pitting corrosion

Pitting corrosion appears on more or less passivated metals and alloys (section 2.4.1). Narrow pits, with radius no larger than the depth of the pit, can grow deep into the material. The shape of the pit may vary, but it usually has sharp edges (Figure 6). Pitting corrosion is hard to predict, because it accelerates very quickly and can work through the entire depth of a material before it is even noticed. Figure 7 shows how pitting corrosion in 300 stainless steel looks in the SEM. The pits are circled in the picture. [12]

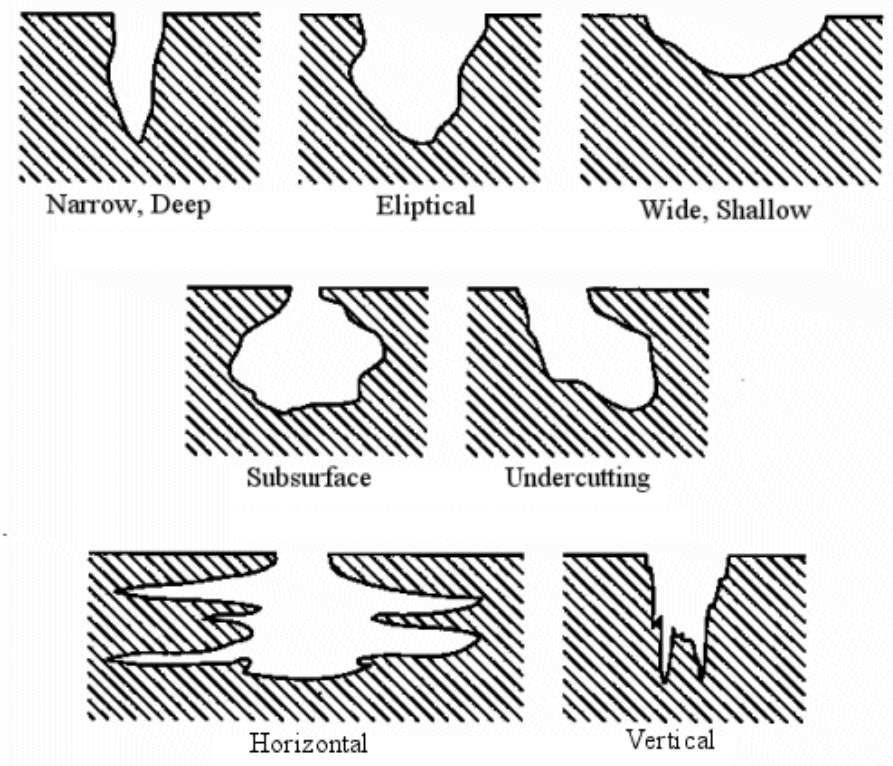

Figure 6: Different types of pitting corrosion [14].

Figure 7: SEM (Backscatter mode) image showing pitting corrosion in 300 stainless steel [13].

2.5 Characterization of bipolar plates

2.5.1 In-situ interfacial contact resistance (ICR) measurements

In-situ contact resistance measurements were conducted by Makkus et al. [15] by attaching a gold wire to the backing inside a Solid Polymer Fuel Cell as shown in Figure 8. The potential drop between the gold wire and the bipolar plate was measured during cell operation. The Contact resistance was calculated from these results (see appendix E). By using this setup, the calculated contact resistance also includes the contribution from the backing. [15]

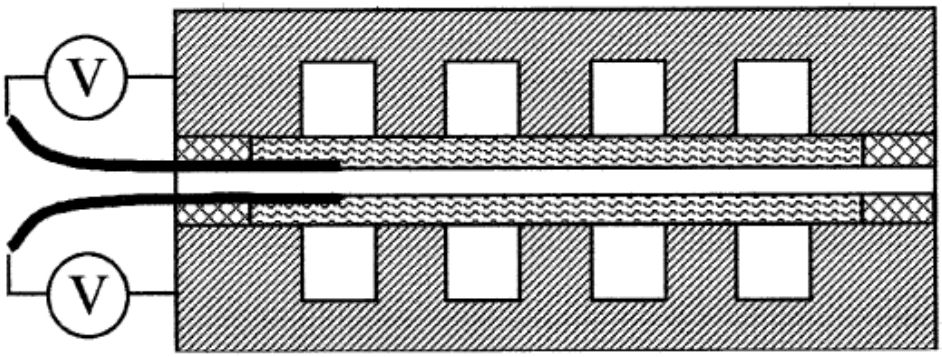

Figure 8: Schematic of method for measuring of potential drop over backing and contact with the bipolar plate [15].

Makkus et al. [15] did contact resistance measurements at 3 bar and 30 bar pressure, and the resulting contact resistances for 316L stainless steel (UNS code 1.4404) was found to be 10 Ωcm^2 on both anode and cathode side at 30 bar, and 25 $\Omega\ cm^2$ on the anode and 50 $\Omega\ cm^2$ on the cathode side at 3 bar.

Ihonen et al. [16] performed in-situ contact resistance measurements of plated and unplated 316 stainless steel in a PEM fuel cell. The results are presented in Figure 9, along with the cell potentials at different temperatures. They found that the in-situ measurements showed considerable scattering, because the pressure over the MEA in the operating fuel cell was hard to control.

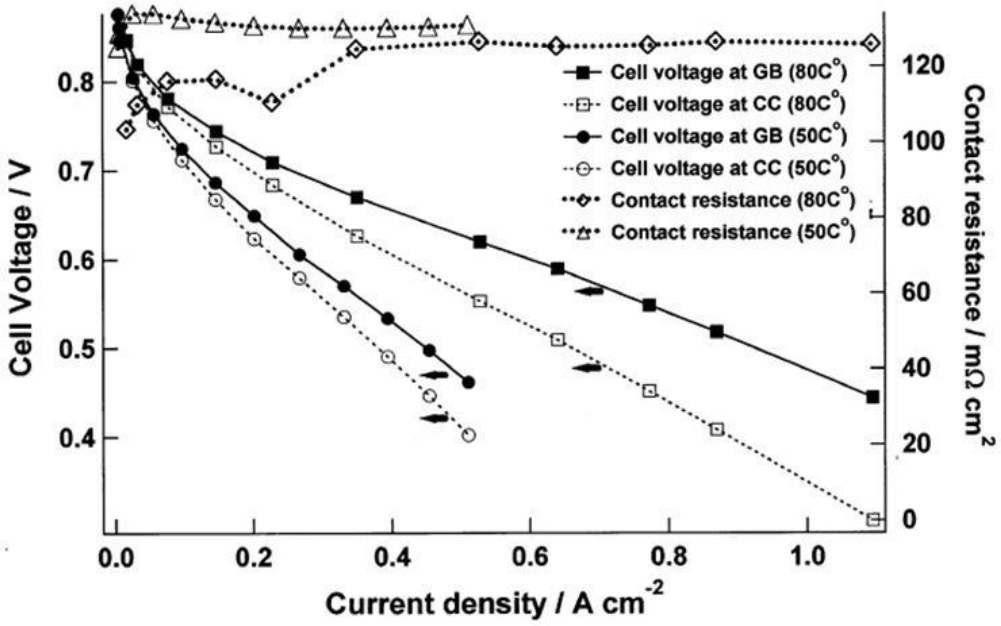

Figure 9: Cell potential and contact resistance as a function of current density [16].

2.5.2 Ex-situ interfacial contact resistance (ICR) measurements

316L stainless steel contains considerable amounts of Chromium (around 16.5 %), which reacts with oxygen to form oxides at certain pH values and during polarization (section 2.4.1). This oxide layer protects the steel against corrosion, but it can cause problems in a fuel cell as it increases the contact resistance. When a stainless steel plate is put into a PEM fuel cell and the cell is operated, oxygen and water is in constant contact with the bipolar plate. This is necessary in order to get the electrical reaction needed to run the fuel cell, but it makes it easy for chromium oxide layer to form. In order to find out how this oxide layer affects the current flowing between bipolar plates in a PEM fuel cell, one can measure the interfacial contact resistance between two bipolar plates.

Setup of the contact resistance testing equipment

Several articles describe setups for Contact Resistance Testing (ICR). Wang et al [2] used the setup shown in Figure 10.

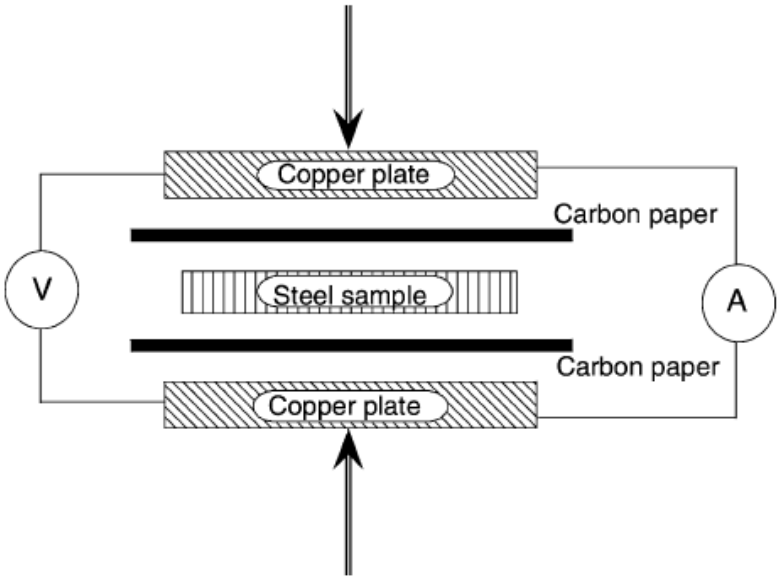

Figure 10: Setup for ICR measurements [2]

Lee et al [17] used a similar setup shown in Figure 11.

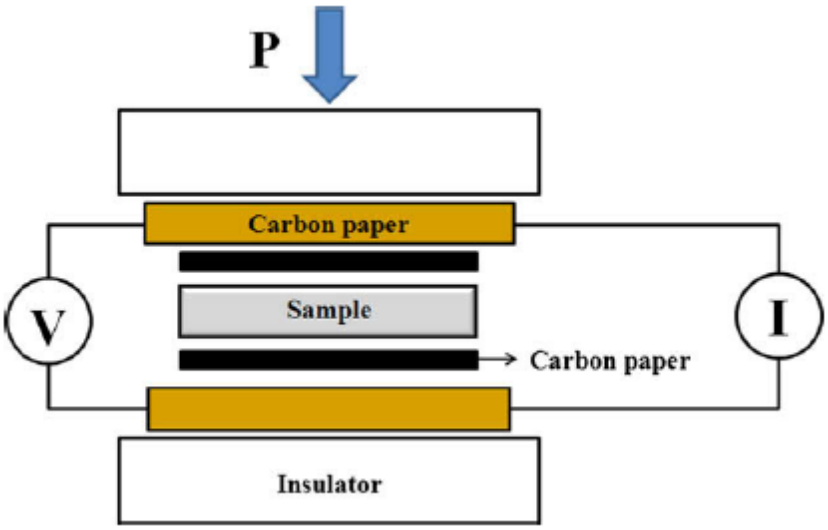

Figure 11: Setup for ICR measurements [17].

Wang et al [18] used the setup shown in Figure 12 for ICR testing, which was inspired by the setup made by Wang et al [2] (Figure 10). All of the three setups described here use a system where current is sent through the whole setup, and where the potential is measured trough a different circuit. Both Wang et al [2] and Wang et al [18] used copper plates as conducting end pieces for the setup, while Lee et al [17] used carbon paper. The principle is still the same; the test specimen (regardless of material) was put in the middle with carbon paper on each side, and a conducting outer element on top of this.

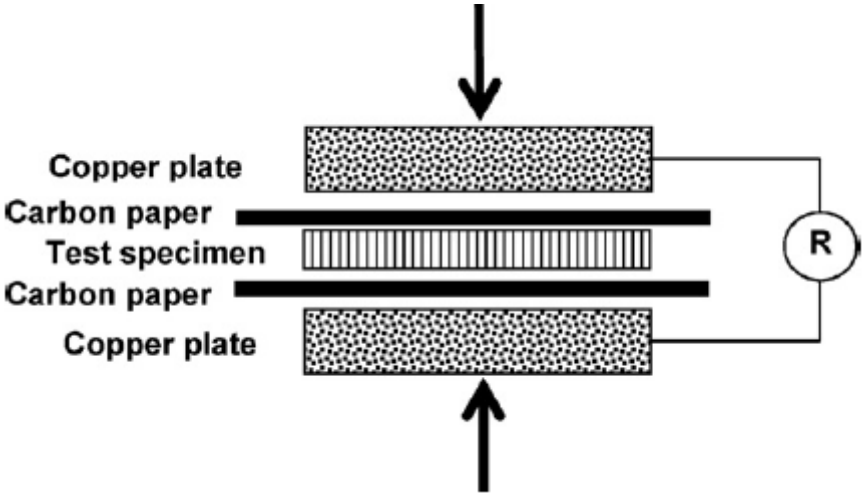

Figure 12: Setup for ICR measurements [18].

Results from previous ICR testing

Wang et al [2] found the contact resistance of stainless steel bipolar plates after pre-treating them under potentiostatic conditions at 0.6 V for different lengths of time. They found that after 60 minutes at 0.6 V the contact resistance at 140 N cm^{-2} (14 bar) was 250 mΩ cm^2, and the tests done for different lengths of time showed very similar results.

Lee et al [17] performed ICR measurements on stainless steel bipolar plates coated with a polymer made from a PAI matrix with Carbon black as electrical filler. The contact resistance was measured to between 25 mΩ cm^2 and 850 mΩ cm^2 where low content of carbon black resulted in the highest values and vice versa for high content of carbon black.

Wang et al [18] tested the contact resistance of bare stainless steel and stainless steel coated with different coatings. They found the contact resistance for bare stainless steel to be approximately 210 mΩ cm^2. The coated stainless steel all showed a lower contact resistance, which is expected due to the badly conductive passivated oxide layer found on stainless steel.

Kumagai et al [19] corrosion tested nickel free stainless steel with high chromium content (23 wt %) in a 0.05 M H_2SO_4 + 2ppm HF solution at 80 ^oC. They found the contact resistance to be 40 mΩ cm^{-2} at 140 N cm^{-2} before the corrosion test and 800 mΩ cm^2 after.

Yoon et al [20] also performed corrosion tests by running a sweep from -1 V to 1 V at 1 mV s^{-1} scan rate in a H_2SO_4 solution (ph=2) at 80 ^oC. Stainless steel plates with electroplated gold coating showed a contact resistance of 4-5 mΩ cm^1 after the corrosion tests.

Few contact resistance measurements have been conducted in the exact same way and with the same materials, but the order of magnitude of the results might still be useful for comparison. Note that some of the previous results are obtained from surface treated- and/or coated stainless steel bipolar plates, and that the ICR results depend on whether or not a corrosion test was performed on the bipolar plates before measuring the contact resistance.

What is evident from all this previous research is that different ways of performing the ICR tests show different results. The pretreatment of the stainless steel plays an important role, making it difficult to compare the results from different articles. Only one of these articles show results that satisfy the DOE requirement (Table 1) for resistivity. This requirement is set to 10 mΩ cm^2, and the gold coated stainless steel plates investigated by Yoon et al [20] showed a contact resistance of 4-5 mΩ cm^1.

2.5.3 Ex-situ polarization testing

Choice of electrolyte - pH-values and additives

Table 3 shows the compositions of some electrolytes described in the literature for polarization testing of different materials, with and without coating. What is evident from this table is that most of the electrolytes have a 1 M or 0.5 M H_2SO_4 base. Wang et al [2] state their reason for using sulfuric acid by referring to earlier tests done in the field; the membranes are pretreated with sulfuric acid, which makes the environment inside the cell acidic [2].

Additives like Chloride and Fluoride have also been added in different amounts to the electrolyte. Wang et al [2] and Rivas et al [21] both added 2 ppm fluoride to their sulfuric acid solution because fluoride had been detected in water analysis done on an operating fuel cell [2]. Ofstad et al [22] evaluated the stability of different types of platinum surfaces in the presence of chloride [22]. They added 10, 20 and 50 ppm chloride in the form of hydrochloric acid to a 0.5 M H_2SO_4 solution, where their electrochemical measurements were done [22]. Chloride is used during the production and preparation of the MEA, and traces of Cl^- are to be expected inside the PEM fuel cell.

The temperature used for the polarization tests often correspond with the temperature in an operating PEM fuel cell [2], usually lying between 70 and 80 ^oC.

Table 3: Electrolyte compositions used for polarization tests on stainless steel.

Authors	Coating	Molarities of H_2SO_4 [mol L^{-1}]	Fluorides (F^-) [ppm]	Chlorides (Cl^-) [ppm]	Temperature [^oC]
Wang et al. [2]	None	1M	2	-	70
Rivas et al. [21]	None	0.5M	2	-	50
Wang et al. [18]	Titanium nitride	0.5 M	-	-	70
Yang-bok Lee and Dae-Soon Lim [17]	Carbon/PAI	1 M	-	-	80
Kumangai et al. [19]		0.05M	2	-	80
Yoon et al [20]	Gold	PH=2 (ca. 0.01 M)	-	-	80
Ofstad et al. [22]		0.5 M	-	10, 20 and 50	-
This thesis	Gold and Coating A	0.1 mM, 1 mM, 0.1 M and 1 M	2	10 and 100	75

Results from some of the tests presented in table 3

Wang et al [2] performed potentiostatic polarization experiments in a three electrode system, where the reference electrode was a saturated calomel electrode (SCE).

Andrè et al [23] obtained polarization curved by cyclic voltammetry between -150 and 1050 mV/SHE at 10mV/min. An Hg/Hg_2SO_4 electrode was used to avoid contamination of chloride, and different types of stainless steel were tested. The polarization curves are presented in Figure 13.

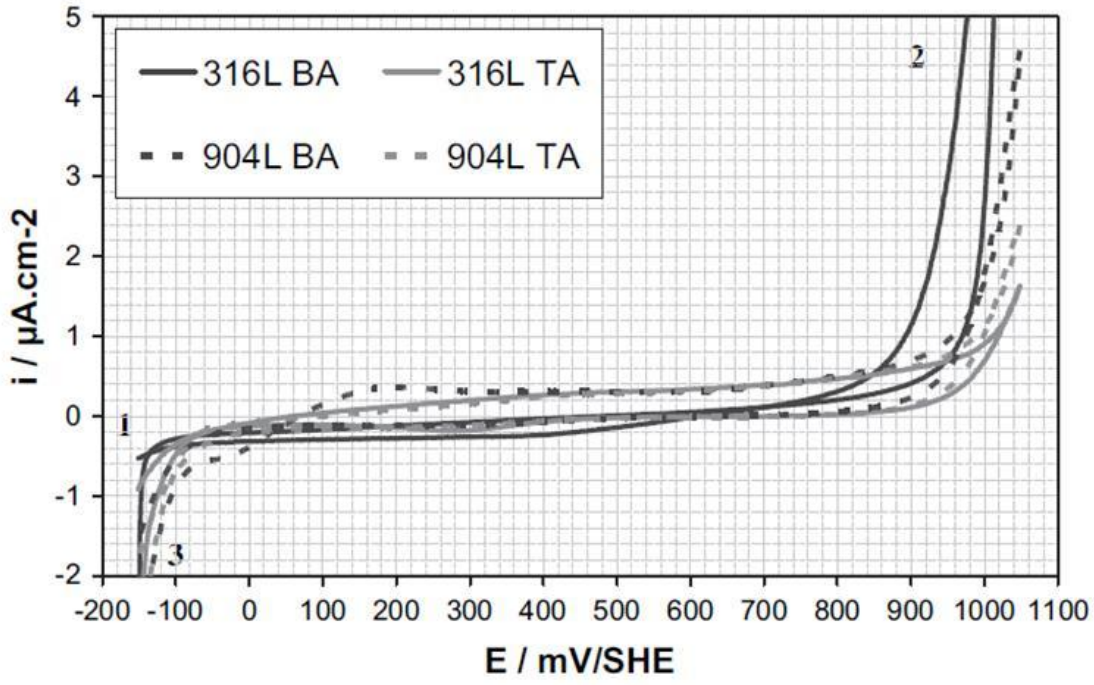

Figure 13: Polarization curves of 316L and 904L alloy with bright annealed and TA surface states in desaerated anodic electrolyte.

Rivas et al [21] used a Hg/Hg_2SO_4 electrode as the reference during their corrosion testing of Mo coated stainless steel. Constant tests were conducted at 100 mV for anodic media and 800 mV for cathodic media. The results for the anodic polarization are presented in Figure 14.

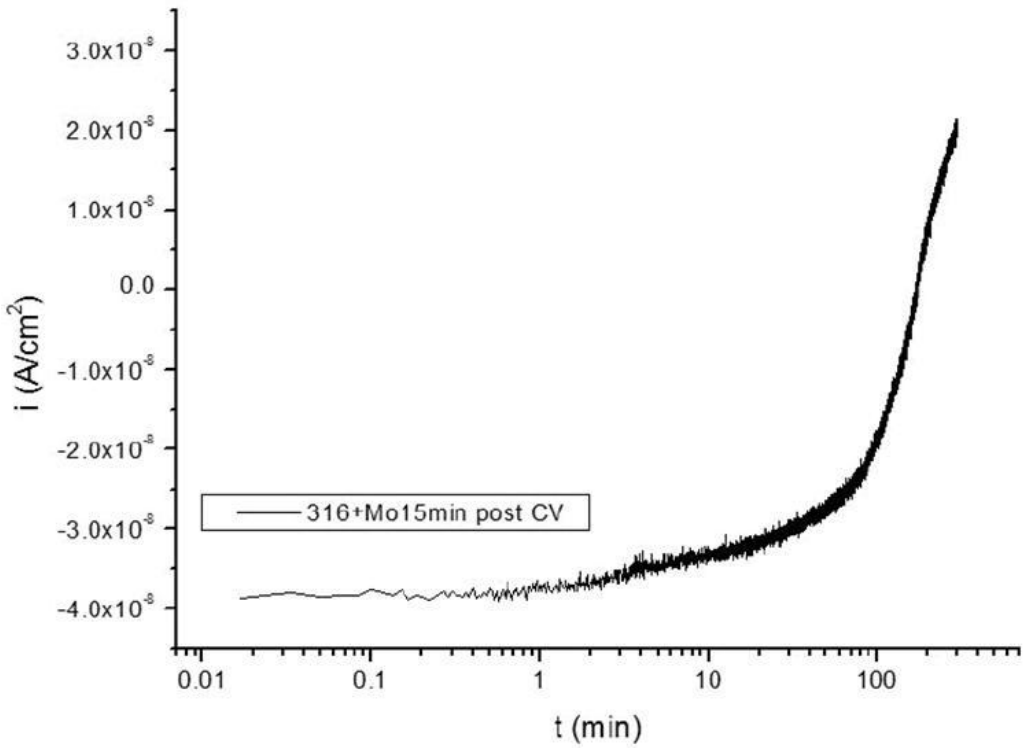

Figure 14: The anodic polarization of Mo coated stainless steel [21].

Linear sweep voltammetry

Voltammetry is an electrochemical technique where the current is studied as a response to an applied potential ramp. Voltammetry can be used to provide information about kinetics of electrochemical reactions. Linear sweep voltammetry is the simplest form of voltammetry, and it is done by varying the potential between the working electrode and reference electrode (Figure 16) linearly with time, from a potential where no reaction occur to a potential where you typically have a diffusion controlled reaction, while the current response is measured. The scan rate is often kept fairly low, around 5 mV s^{-1} is normal. Linear sweep voltammetry can give both quantitative and qualitative information, but the linear sweep voltammetry curves described in this report was mainly used to compare to each other. [24]

2.6 Scanning electron microscopy (SEM)

The SEM microscope (Figure 15) is used when one wishes to study very small topographic details, which are not visible to the naked eye, as well as element analysis of the surface layers. Electrons are used to analyze the sample, and a SEM microscope is a rather complicated device. The most important parts of the SEM are the electron source and the different detectors that detect the electrons and phonons reflected from the sample. [25]

Figure 15: SEM apparatus.

The most commonly used detectors in the SEM are those that detect secondary electrons, backscattered electrons and X-ray. Secondary electrons are defined as emitted electrons with less energy than 50 eV. These electrons come from a fairly small volume of the sample, and can be generated by either primary electrons (the electrons emitted from the electron source) or backscattered electrons.

Backscattered electrons are primary electrons that reflect back instead of entering the sample. By using this detector, atomic number contrast will make it possible to separate different elements within in one sample. This is because different atomic numbers is seen as different shades of gray in the microscope image. [25]

X-ray beams arise when the electron beam hits the material and the electrons interact with the orbitals of the atoms in the sample. The primary electrons can cause the electrons in an inner orbital to be excited. When the electron then moves back to the orbital it came from, energy is released as photons or auger electrons. These x-ray beams are then detected by an energy dispersive spectrometer (EDS), and the different elements in the sample can be determined. [25]

3. Experimental apparatus and procedure

3.1 Polarization measurements

3.1.1 The setup

The setup for the polarization testing equipment is shown in Figure 16, and a picture of the setup is shown in appendix A. This setup was made to simulate the environment experienced by the bipolar plates inside a fuel cell. Sulfuric acid was used as electrolyte because the MEA used in an operating fuel cell is pretreated in sulfuric acid, which in turn makes the environment inside the fuel cell acidic. The calculations done before preparing the electrolytes are shown in appendix B. An IM6 potentiostat (Zahner electric) was used and the reference electrode was a Mercury/mercury sulfide ($Hg/HgSO_4$) electrode. This electrode was chosen because it, compared to a lot of other reference electrodes, does not contain chloride. It was desirable to avoid any chloride in the electrolyte in order to avoid any undesired reactions. To make completely sure the reference electrode did not cause any unwanted reactions, it was connected to the electrolyte via a salt bridge (Figure 16). The counter electrodes were made of platinum, and two of these electrodes were necessary to compensate for the large surface area of the stainless steel plate (working electrode).

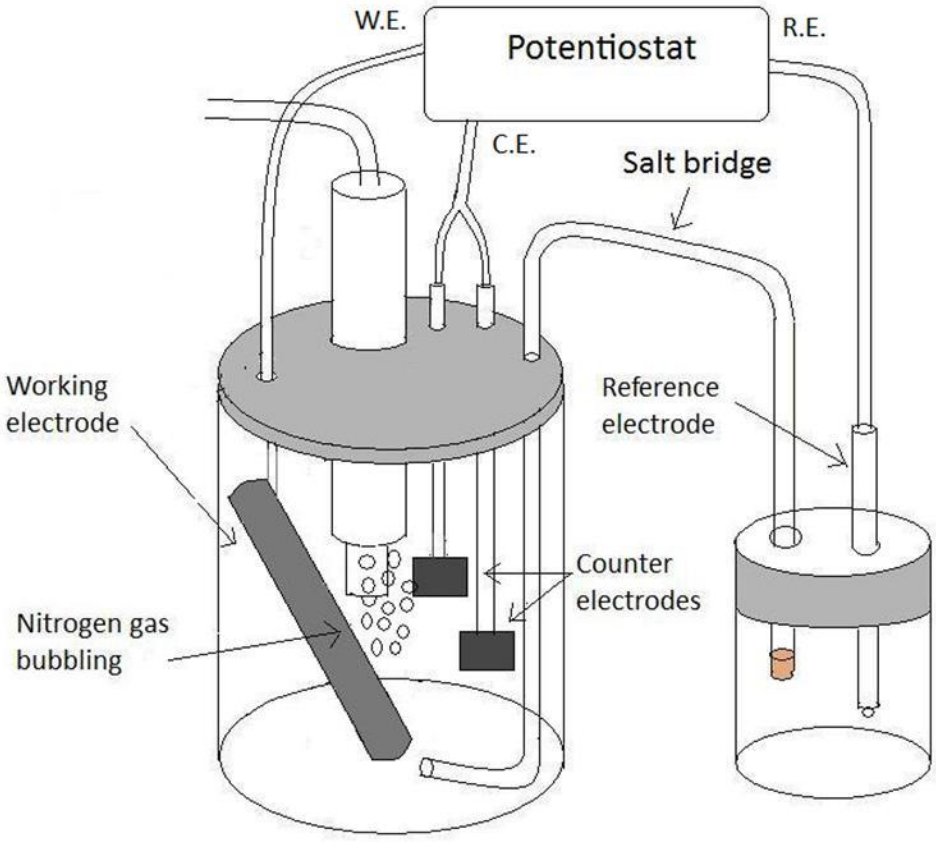

Figure 16: Setup of corrosion testing equipment with electrolyte, working electrode, counter electrodes, salt bridge and reference electrode.

3.1.2 Preparation of the bipolar plate

In the single test cells used for the in situ testing leading up to this project work, only one side of the stainless steel plate was exposed to the corrosive environment; the side facing the acidic membrane. To compensate for this, one side of the plate was coated with varnish, before putting into the electrolyte (Figure 17). This had to be done after the pre-polarization contact resistance test (section 3.1). The varnish also had to be taken off after finishing the corrosion test, in order to do test the contact resistance again. The varnish was taken off by use of acetone in a VWR ultrasound cleaner.

Figure 17: a) Stainless steel plate coated with nail varnish to avoid corrosion on both sides. b) The front side of the bipolar plate which was not coated with nail varnish.

3.1.3 Standardized tests designed for this project work

The temperature in the cell was set to 75 ^{o}C, and when the electrolyte had reached this temperature, the nail varnish coated stainless steel plate (section 3.2) was put into the electrolyte. The platinum wire already welded to the bipolar plate was connected to the potentiostat along with the wires from the counter- and reference electrodes. To avoid oxygen reduction, nitrogen gas was continuously bubbled into the electrolyte during the experiments. This was also done during the heating of the electrolyte.

The program used to run the potentiostat from a computer was called Thales, and the startup procedure for the polarization tests in this program is described in appendix C. 5 different pre-designed tests were used in this project work and they are described in Table 4. The tests were chosen according to different criterions. Test number 1 is a linear sweep test (see section 2.5.3), where the potential was set to run between -0.9 V and 0.4 V vs. $Hg/HgSO_4$ at 2 mV s^{-1}. The highest potential was chosen because in an operating fuel cell, even with maximum overpotential, the voltage should never be higher than 0.4 V vs. $Hg/HgSO_4$. The lowest potential was set to -0.9 V to cover the lower region voltage in an operating PEM fuel cell.

Test number 2 (Table 4) was made to simulate the potential at the anode in a fuel cell. Hydrogen ions are formed on the anode side of the fuel cell, and the electrochemical potential for this reaction is 0 if a standard hydrogen electrode is used as a reference. This potential relates to the pH in the electrolyte trough equation 4. The pH close to the MEA is approximately 1, and it is assumed that this is the pH "seen" by the anode reaction. This means that the potential at the anode side is -0.059 vs. SHE corresponding to -0.717 V vs. the $Hg/HgSO_4$ electrode used as reference in this project work.

$$E = E^0 - \log[C] \cdot pH \qquad (4)$$

The potential used in test number 3 was chosen to be as close to the open circuit potential in a PEM fuel cell as possible, which is usually around 1 V vs. SHE. The OCV potential was found by adding 1 V to the hydrogen reaction potential (-0.717 vs. $Hg/HgSO_4$), but by mistake 1.01 V was added and the resulting potential then became 0.293 V $Hg/HgSO_4$. This miscalculation was not discovered until late in the project work, but it was assumed that it did not cause any big problems for the obtained results. Note that the corrosion results first and foremost were compared to each other in the results and discussion section, and it should thus not have caused any problems that the high voltage was set 0.01 V higher than first planned.

Table 4: The different potentials and durations of the standardized tests.

Standard test number	Potentials [V] vs. $Hg/HgSO_4$	Duration/speed	Description
1	-0.9 to 0.4	2 mV/s	A swipe between the maximum and minimum potentialss recorded from the PEM fuel cells.
2	-0.717	60 min	Low potential to simulate the anode reaction.
3	0.293	60 min	High potential to simulate the cathode reactions
4	-0.717	1080 min	Low potential over time to see whether the current density stabilized or not.
5	0.293	1080 min	High potential over time to see whether the current density stabilized or not.

Test number 4 and 5 were similar to test 2 and 3, except they were set to 18 hours instead of 1 hour. These tests were done once to make sure that the current densities that were measured after one hour, did not change much over the next 17 hours.

All the corrosion tests done as part of this project work are described in table D1 appendix D. Not all of them are discussed in section 4.1, but table D1 gives an overview over all the work done for this master thesis. The test numbers refer to the test numbers in Table 4.

3.1.4 Gold coated stainless steel – standard

Because gold is an unreactive metal, it should not corrode in the fuel cell environment and there are no oxide layers formed on its surface. In addition, gold conducts current well, which indicates that it would work well as a corrosion protective coating for a bipolar plate in a PEM fuel cell. Gold coated stainless steel plates were chosen as the standard for all the testing done later on in the project. Test 1, 2 and 3 (Table 4) were done on gold coated stainless steel plates in a 1 mM H_2SO_4 solution, and the results are described in section 4.1.1 and 4.2.1. Gold is expensive and even though tests were done on gold coated plates, gold is too expensive for use in commercialized fuel cells.

3.1.5 Reproducibility of non-coated stainless steel

Most of the tests described in this report were done on non-coated stainless steel plates. It was thus important to find out whether the different tests were reproducible or not. Test 1, 2 and 3 (Table 4) were repeated 3 times each in a 1 mM H_2SO_4 solution, where the conditions were kept as similar as possible from test to test. The results are presented in section 4.1.2 and 4.2.2.

3.1.6 1 vs. 18 hours

The passivated layer that forms on the stainless steel plates was expected to stabilize early on in the corrosion tests at both low and high potentials. But in order to confirm this, corrosion tests were run over several hours. One 18 hour test was conducted at a low potential (test 2), and one 17.5 hour test was conducted at a high potential (test 3). The reason why the tests did not run for the same length of time, was that the test at high potential stopped by itself after 17.5 hours due to problems with the computer connected to the potentiostat. This was not seen as problem, because the exact lengths of the tests were not important for the discussion later on. The results from these tests are presented in section 4.1.3 and 4.2.3.

3.1.7 pH variations

The pH within an operating fuel cell is hard to measure, but measurements done on the water leaving the fuel cell, showed that the pH was always higher than 3.5 (Figure 18). These results indicated that the simulated tests should be done in a solution with pH around 3.5. Testing described in the literature (see section 3.5.3) has often been done in an electrolyte with pH=0 (1 M H_2SO_4) or pH=0.5 (0.5 M H_2SO_4). Some authors had used electrolytes with low pH values to increase the degrading rate of the plates, but it was suspected that a decrease in pH could cause different surface reactions which would not have happened in an electrolyte with a higher, and in our case, more realistic pH. We decided to do most of our

testing in the 1mM H_2SO_4 (pH=2.87) electrolyte, which should be a lot more realistic, but still conservative.

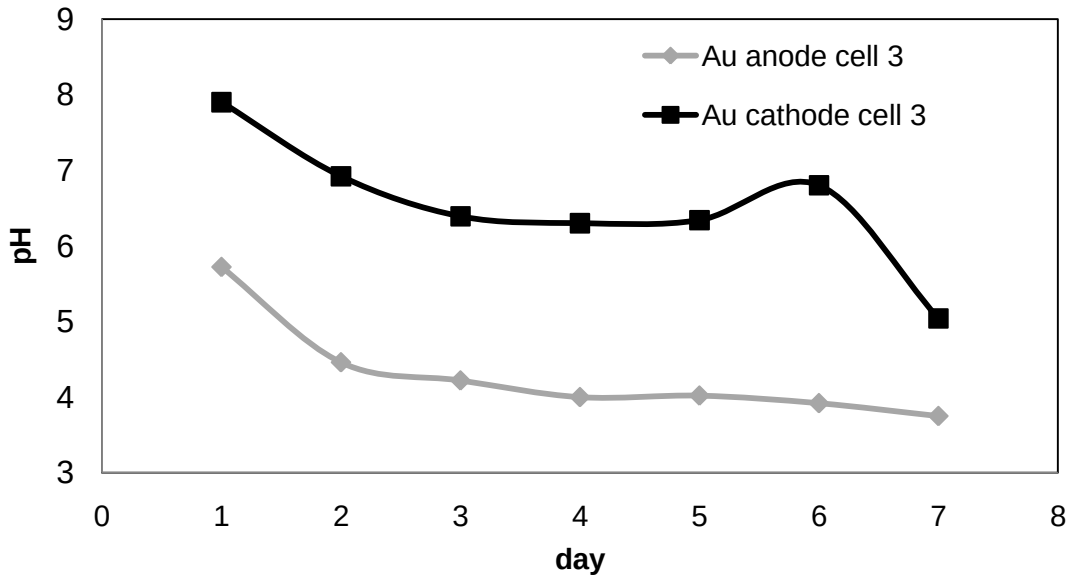

Figure 18: pH values measured from the water leaving a fuel cell running of several days.

Although most of the polarization test in this thesis work was done in a 1 mM H_2SO_4 solution, tests were also done in sulfuric acid solutions with other molarities (pH values). This was to compare the different molarities and evaluate whether the chosen molarity was the best fitted. Test 1, 2 and 3 (Table 4) were done in solutions with molarities of 0.1 mM, 1 mM, 0.1 M and 1 M. The results from these tests are presented in section 4.1.4 and 4.2.4.

3.1.8 Addition of Fluoride and Chloride to the electrolyte

Corrosion tests done on stainless steel plates have previously been done with additives of fluoride and chloride because these ions are found in a real PEM fuel cell (section 2.4.2.1). Corrosion tests 1, 2 and 3 (Table 4) were thus done in 1 mM H_2SO_4 with 2 ppm fluoride and in 1 mM H_2SO_4 with 10 ppm chloride. Even though more than 10 ppm Chlorine would be unrealistic to detect in a PEM fuel cell, tests were done in a 1 mM H_2SO_4 solution with 100ppm chloride. This was just to see if chloride could have an effect at all on the stainless steel plates in 1 mM H_2SO_4 solution. The fluoride was added as NaF and the chloride was added as NaCl, and in appendix B the calculations for the amounts of fluoride and chloride are presented. The results from these tests are discussed in section 4.1.5 and 4.2.5.

3.1.9 Coating A

One new coating was tested as part of this project work. The coating was called Coating A and had been made by one of the partners in the SINTEF project. Standard test 1, 2 and 3 were run on stainless steel plates coated with Coating A. The composition of the coating was not known, and the plates that had been coated with it did not look any different from the non-coated plates. The results are presented in section 4.1.6 and 4.2.6.

3.2 Contact resistance measurements

The interfacial contact resistance (ICR) was measured before and after each corrosion test. One bipolar plate was used for one corrosion test, and thus for two ICR tests. That way, new plates were used for each corrosion test. The setup of the contact resistance equipment is shown in Figure 19, and pictures of the equipment are shown in Figure 21a-d. The setup was designed to simulate the fuel cells used to test the bipolar plates in-situ. The gold coated bipolar plate (Figure 19) was used as standard, and the contact resistance was measured between this plate, the backing and the bipolar test plate. The top part of the setup was easy to remove, which made it easy to take out and put in the bipolar test plates.

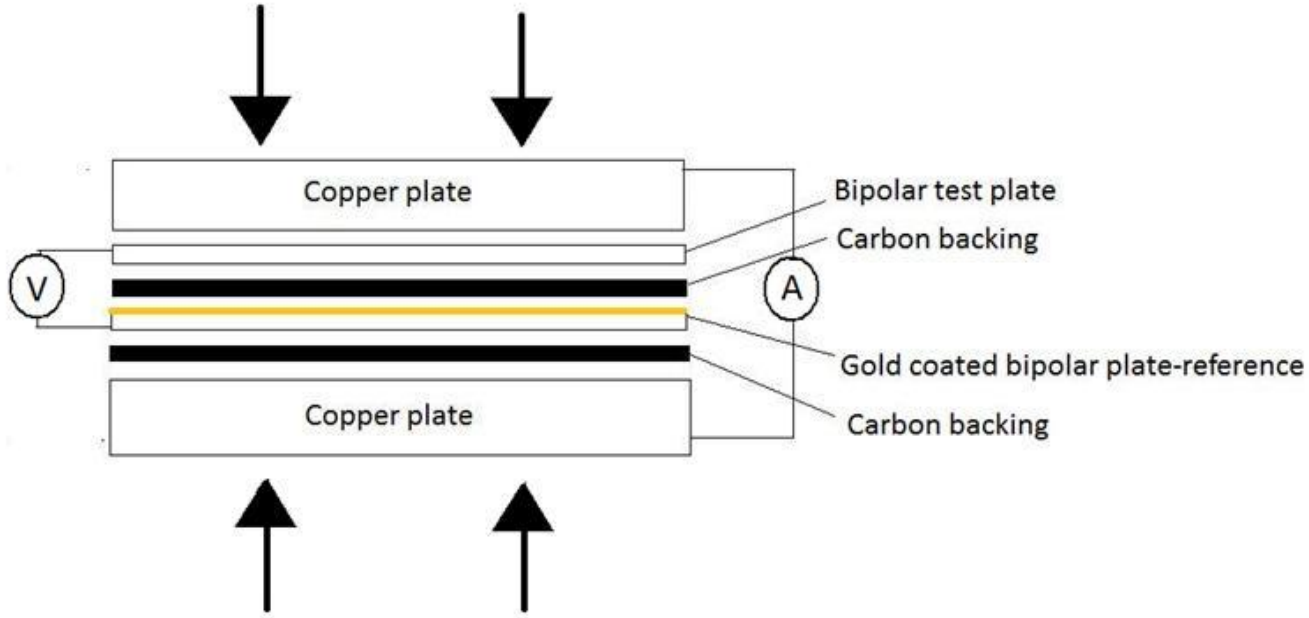

Figure 19: Contact resistance testing setup, built to simulate the PEM fuel cell.

A XDL 56-4 DC power supply (Xantex) was connected to the Copper plates in order to send current through the whole setup, and the resulting voltage was measured with a multimeter (Fluke 76 True RMS) between the two bipolar plates. Platinum wires were welded to both plates as shown in Figure 20.

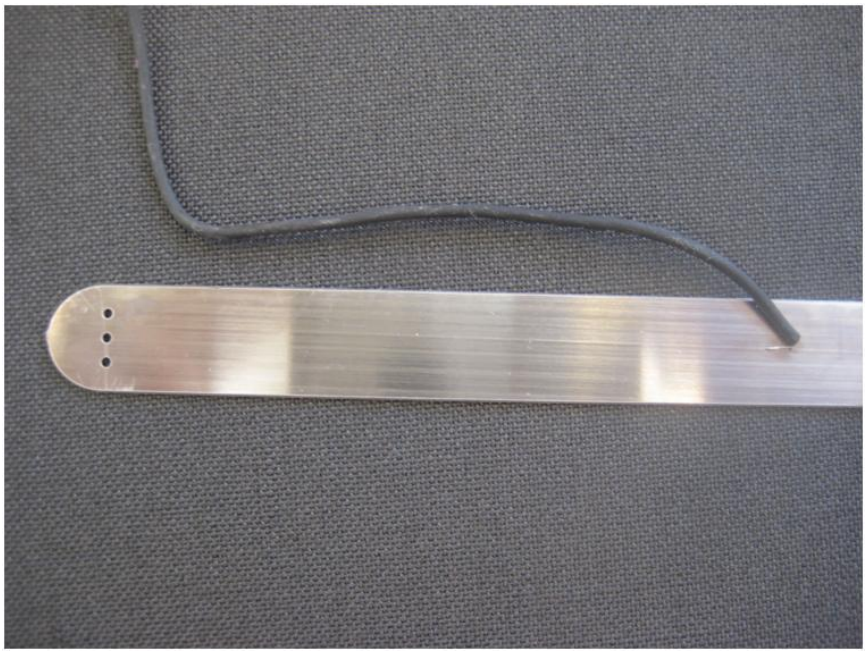

Figure 20: Bipolar plate with a platinum wire welded to it. The wire was needed for the contact resistance measurements.

To test the contact resistance between the test bipolar plate and the gold coated bipolar plate used as standard, the plate was placed as shown in Figure 21a. The top part was then placed on top of the bottom part, and screws were used to keep the whole setup together (Figure 21c). The wire welded to the bipolar plate was put through holes in the copper and steel plate, and connected to the multimeter. Pneumatic pressure was then applied from underneath the setup, and potentials were recorded between the two plates as the pneumatic pressure was increased. These potentials were used to calculate the contact resistance as described in appendix E.

a

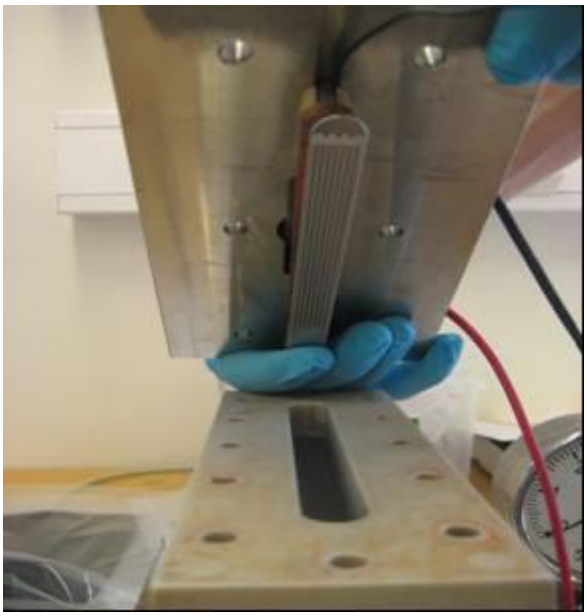

b

c

d

Figure 21: a) The bottom part of the setup. b) The top part of the setup with the bipolar test plate. c) The setup put together with screws. d) The power supply (Xantex) used to run current trough the setup.

3.3 SEM

3.3.1 Preparing the sample

The bipolar plates were made of stainless steel and were thus good electrical conductors. This made the preparation of the plates very simple. It was important to make sure that the plate had been cleaned properly, before putting it in the SEM. Gloves were used during the entire preparation process. First the plate was washed with ethanol and distilled water. To remove any last traces of backing on the surface, the bipolar plate was put in an ultrasound bath for a couple of minutes. There were at times still traces of the backing on the surface, but it was hard to get it all off without scratching the bipolar plate surface.

Carbon stickers were used to attach the bipolar plate to the sample table (Figure 22). The height of the sample was measured before installing it in the SEM, to avoid crashing the electron canon into the sample when it was inside the SEM. The sample was put into the apparatus and the vacuum was turned on. A picture of the SEM apparatus is shown in Figure 15.

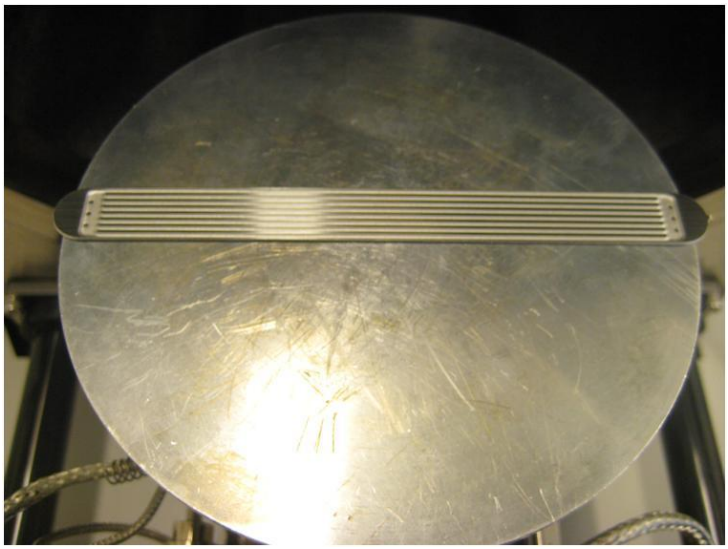

Figure 22: The bipolar plate attached to the sample table by carbon stickers.

3.3.2 Running the SEM

The SEM used during this project was a Hitachi S-3400N. After logging into the computer and starting the software, the distance from the electron gun to the sample was adjusted to 10 cm. The different parameters (probe current, vacuum etc.) were set to obtain the best possible image. Pictures were taken at different magnifications, depending on the areas of the plates that were studied. The main focus of using the SEM, was to find any traces of wear or corrosion on the stainless steel plates.

4. Results and discussion

This part of the report has been divided into several parts. The first part consists of the results obtained from the polarization tests and the discussion comparing these results with each other (section 4.1). Towards the end (section 4.1.7) there is a concluding part which sums up the corrosion discussion (section 4.1.7). The second part is where the results from the ICR testing are presented and discussed (section 4.2), and at the end there is a sum up of the discussion concerning the ICR results (section 4.2.7). To conclude the entire discussion part, there is a chapter at the end where the corrosion and ICR results are compared and discussed together (section 4.3).

4.1 Polarization measurements

4.1.1 Gold coated stainless steel

The gold coated stainless steel bipolar plate was chosen as standard because gold does not form oxide layers like stainless steel does, and gold coated steel should not corrode in the simulated fuel cell environment. The results from the sweep polarization test (test 1, Table 4) of the gold coated stainless steel plate is shown in Figure 23.

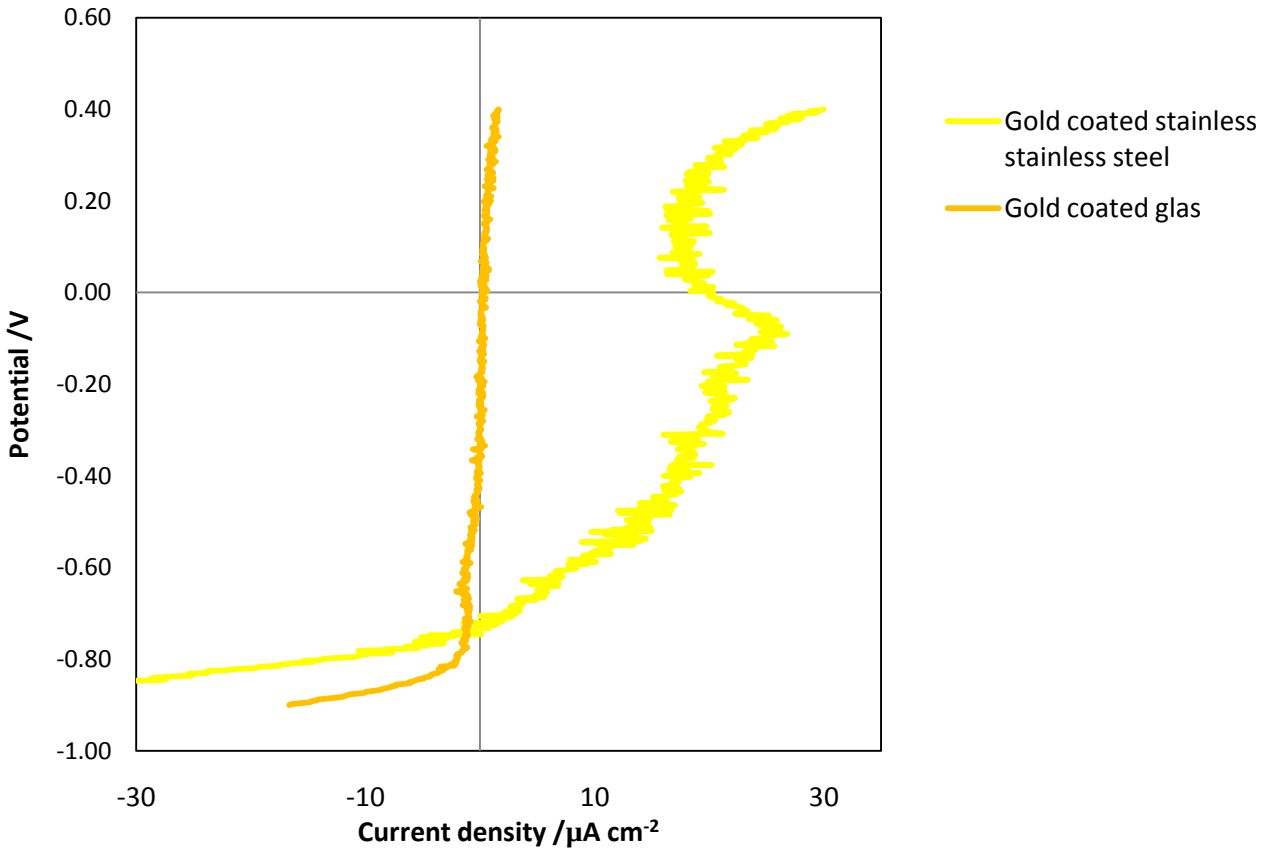

Figure 23: Gold coated glass and gold coated stainless steel, test 1; -0.9V to 0.4 V vs. Hg/$HgSO_4$ at 2 mV s^{-1}.

The assumption that gold is an ideal coating when little or no corrosion is the objective holds when the gold coating adheres well to the stainless steel surface. The polarization test performed on the gold coated stainless steel plate did, however, not result in as low current densities as would be expected (Figure 23). Further studying of these plates showed that the gold coating had come off in some areas of the plate (Figure 24a). Just by handling the plates, some of the gold seemed to come off. This indicated that the gold did not adhere well to the stainless steel, which could in turn have caused pitting corrosion (section 2.4.1) in certain areas of the plate during the polarization test. This pitting could in turn have increased the corrosion current. Pitting is most common in passivated materials, and the gold coating protects against corrosion in much the same way as e.g. an oxide layer. When very small pieces of gold coating are worn off, pitting corrosion can thus occur.

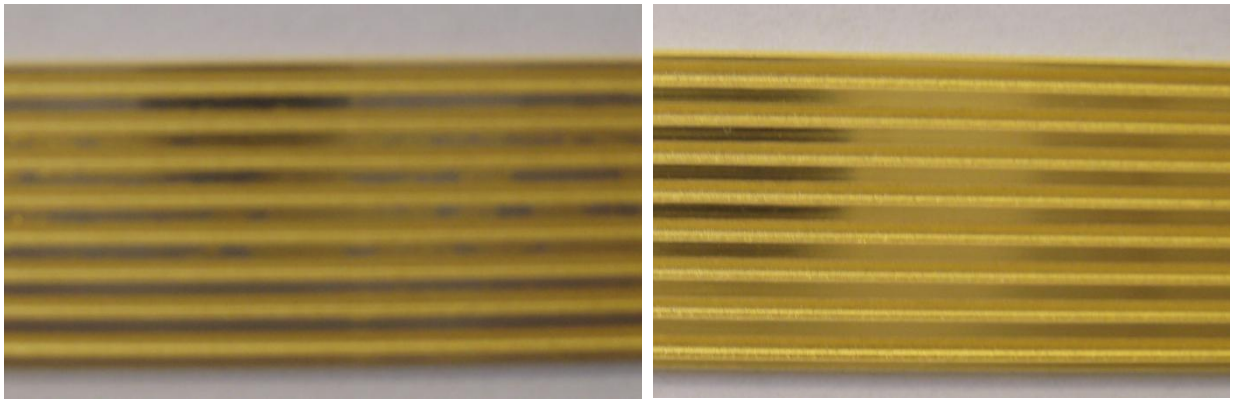

Figure 24: a) Used gold coated stainless steel plate where the gold has been worn off. b) New gold coated stainless steel plate.

Gold coated glass plates were run from -0.9 V to 0.4 V vs. $Hg/HgSO_4$ (test 1) in the same way as the gold coated stainless steel plates, and the results are presented in Figure 23. These sweeps show that the gold coated glass produces a much lower current density throughout the entire sweep than the gold coated stainless steel, and this gives good reason to assume that there had in fact occurred pitting corrosion on the gold coated stainless steel. The sweep results from gold coated glass will be included in the further discussion, because they show more ideal results than the gold coated stainless steel plates.

4.1.2 Reproducibility of non coated stainless steel

Test number 1, 2 and 3 (Table 4) were performed three times each on new stainless steel plates, that had been pretreated in a hydrochloric acid solution, to check whether these tests were reproducible or not. The results are presented in Figure 25, Figure 26 and Figure 27. At a low potential (Figure 25) the three reproduced tests seem to overlap well. The current densities start off at high absolute values, and as the oxide layer (section 2.3.1.1) stabilizes the surface the current densities levels off and approach a steady value. After the current density has stabilized, it was very low, almost non-existing. This means that even small variations in current densities between the three curves are in the same order of magnitude as the absolute value of one test at a given time. This makes it hard to determine whether the reproducibility is good or not.

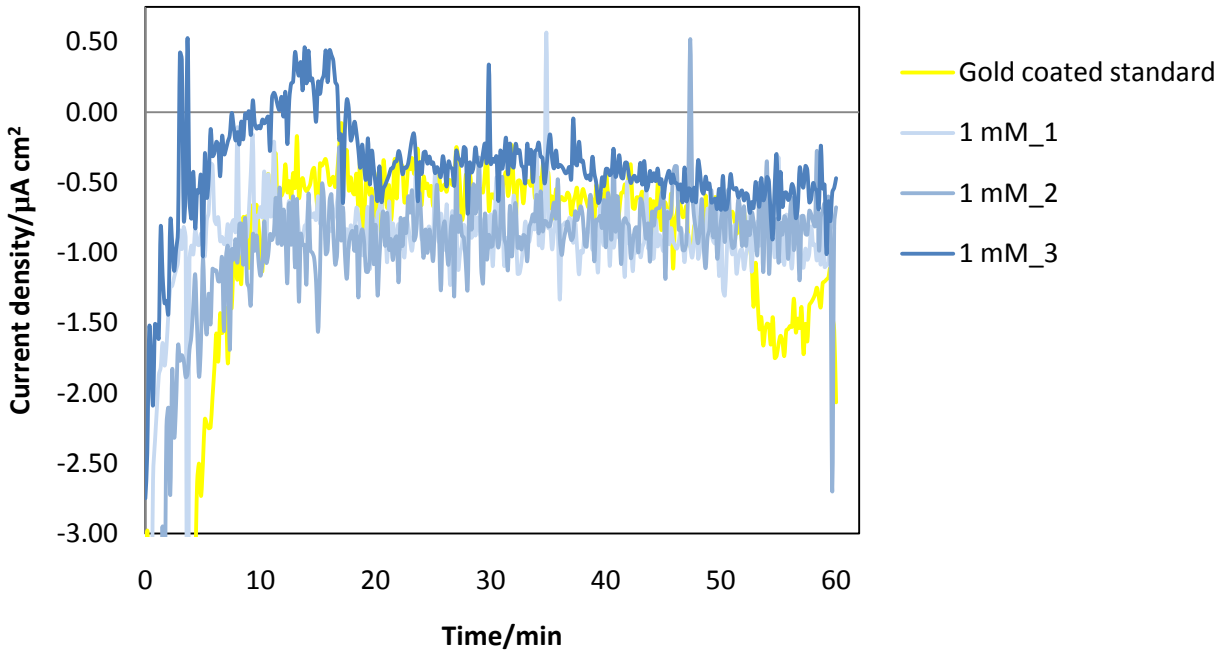

Figure 25: Reproducibility, test 2; -0.717 V vs. $Hg/HgSO_4$ for 1 hour

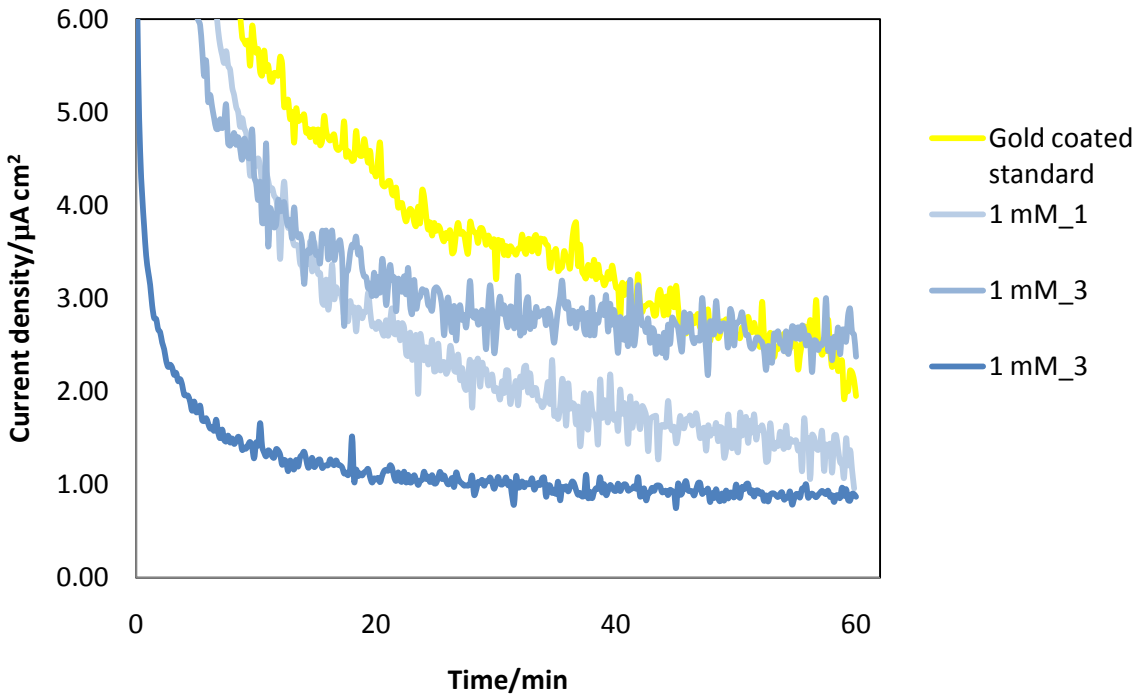

Figure 26: Reproducibility, test 3; 0.293 V vs. Hg/$HgSO_4$ for 1 hour

At a higher potential (Figure 26) the stabilized absolute values of the current densities are a little higher than at a low potential. There is some variation in current density between the three tests, but the absolute values are still fairly small. The variations are, like at low potentials, almost as big as the absolute value of the current density.

The variations between the three reproduced tests in Figure 25 and Figure 26 could be caused by several factors such as fluxuating temperature in the electrolyte, composition variations in the stainless steel, variation in oxide layer thickness before the corrosion test was started, uneven mixing and even the power grid. The power grid in the lab where the tests were performed was not stable, and other equipment used on the same grid could thus cause instabilities. We also see that when the current density is low, each curve show great instability, while at higher absolute values of the current densities (Figure 26) the graphs show less noise. The noise is most likely in the same order of magnitude regardless of the absolute value of the current density, and at lower current densities it becomes more apparent.

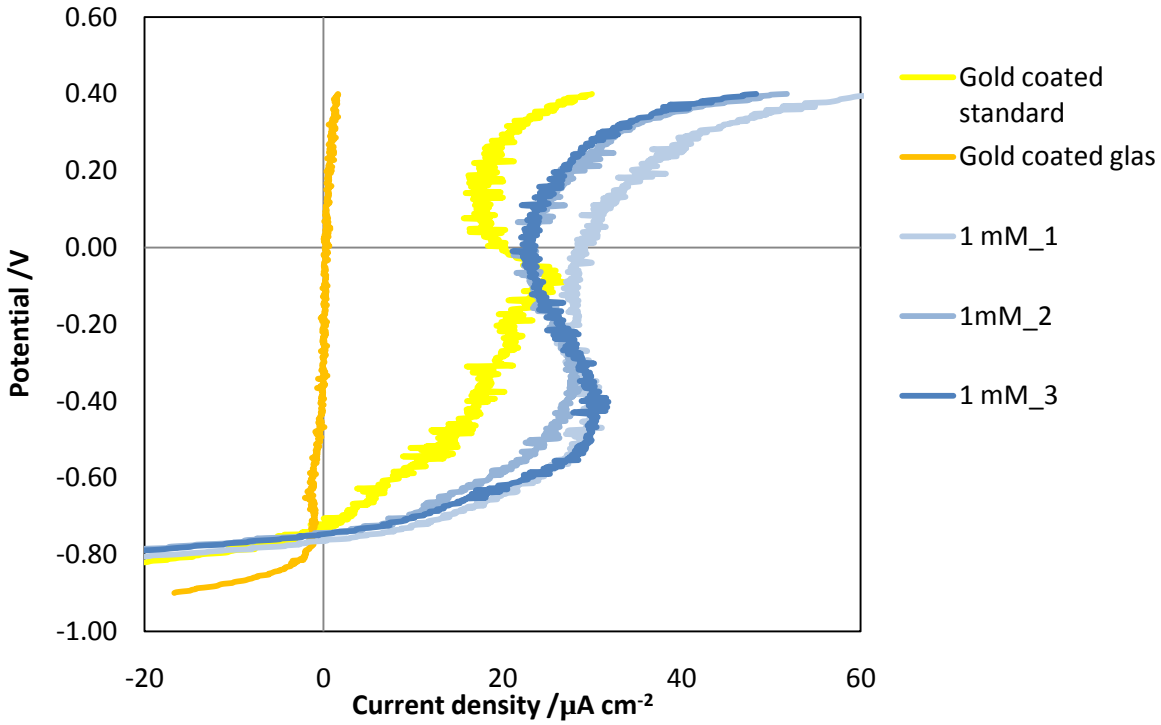

Figure 27: Reproducibility, test 1; -0.9V to 0.4 V vs. $Hg/HgSO_4$ with a scan rate of 2 mV s^{-1}.

The polarizations from low to high potentials (Figure 27) show some variation between the three reproduced tests, but the shape of the curves and the maximum values do not differ that much. By comparing them to the sweep from the gold coated glass, the three reproduced curves are very similar. All tree curves seem to have an increase in current density at around 0.4 V vs. $Hg/HgSO_4$. At this potential, the oxide layer probably dissolves and thereby increases the corrosion current. This way, even though the three curves don't follow each other all the way, they still superimpose towards the end of the polarization.

The current densities for the three tests before the current density has stabilized are very similar. At these high current densities the variation between the three tests are much smaller than the absolute value of the current density. This could be due to a number of reasons, but it might just show that the magnitude of the noise not scale with the current, which makes the noise more apparent at lower current densities. When the oxide layer is stable the current density produced is very low, which makes it hard to differentiate between absolute values and standard deviation.

4.1.3 1 vs. 18 hours

The 17,5 and 18 hour corrosion tests were conducted in order to defend the chosen length of all the other corrosion tests (1 hour), and they were both done in a 1 mM sulfuric acid solution. It was decided early on in the project that 1 hour should be long enough for each test, because the corrosion current seemed to stabilize after about 20-30 minutes. Figure 28 shows the curve from the test performed at -0.717 V vs. $Hg/HgSO_4$ for 18 hours. As expected the current density seems to stabilize after some time. The current density stabilizes at about -3 μAcm^{-2}, which is a little higher in absolute value compared to the 1 hour tests (Figure 25)**.** This means that even though the test at 18 hours takes longer to stabilize, it still stabilized at a higher absolute current density value than the reproduced 1 hour tests did.

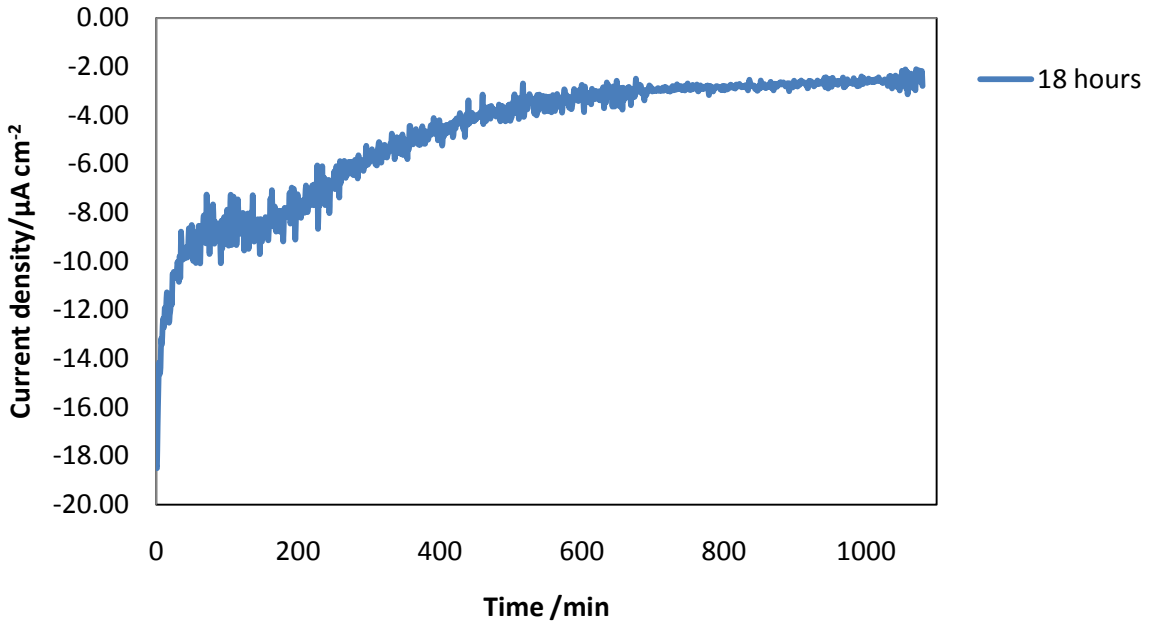

Figure 28: 1 vs. 18 hours, test 2; -0.717 V vs. $Hg/HgSO_4$ for 18 hours.

There is one more aspect of the curve in Figure 28 that is different from the curves in Figure 25; the current density does not seem to become completely stable until after about 600 minutes (about 10 hours) in the 18 hour test. This is different from the 1 hour curves which stabilize after only 15 minutes. There seems to be a stabilized current density that starts at around 50 minutes and stays put for about 2 hours in the 18 hour test. This could indicate that the stabilized current density in the 1 hour tests is in fact not the final stabilized current, but just an intermediate level of stabilization.

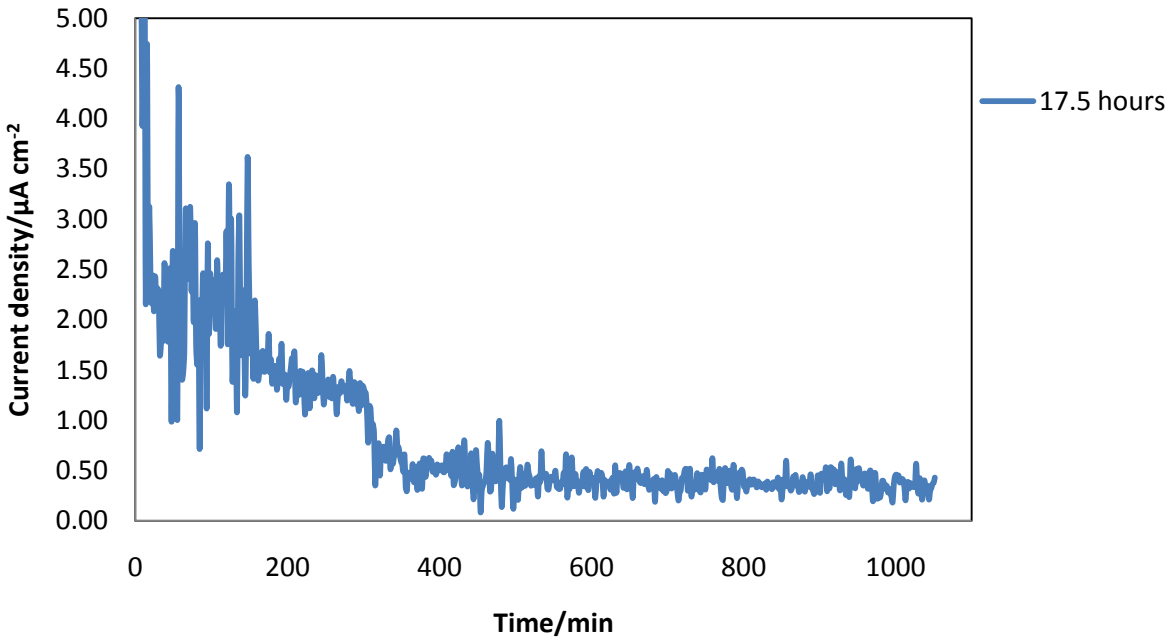

Figure 29: 1 vs. 18 hours, test 3; 0.293 V vs. $Hg/HgSO_4$ for 17.5 hours.

Compared to the starting absolute value of the current density in Figure 28 (-0,717 V vs. $Hg/HgSO_4$), the starting absolute value in Figure 29 (0.293 V vs. $Hg/HgSO_4$) decreases rapidly. It comes down to under 3 μAcm^{-2} within the first 20 minutes. This is where the current density started to stabilize in the 1 hour tests as well (Figure 26), and it indicates that the corrosion current stabilizes after around 20 minutes. However, the same intermediate stabilization as was seen in Figure 28 is also seen in Figure 29, which could mean that the current needs more than 1 hour to stabilize.

The reason why the 17.5 hour test at 0.293 V vs. $Hg/HgSO_4$ seem to take longer to reach the stabilized current density than the 1 hour test, could be that the current takes this long to stabilize, and the 1 hour tests might not reach the lowest current value possible. The absolute value of the current density after 20 minutes in both the 17.5 hour test and the 1 hour tests are so small that it might not make a difference. The differences in current densities between the reproduced tests at high potentials (Figure 26) are greater than the change in current density in the 17.5 hour tests from 20 min to 5 hours, and it is thus assumed that the 1 hour tests are sufficient for the testing done in this thesis. All the other tests during this project work were 1 hour tests, and as most of the discussion is bases on comparison between the tests performed within this project, the 1 hour tests were not a bad choice. If all the tests should have been 18 hour tests, there would not have been enough time to do all the tests planned.

The plates used in the long term tests were reused, in contrast to the plates used for the 1 hour tests. It was assumed that the stainless steel plates could be reused as long as they were treated in hydrochloric acid in between each corrosion test. After the long term tests were done, new plates were used for each new test performed, to make sure there would be no leftover oxide layer on the stainless steel plates when starting a new test. It was only the long term tests that were performed with used stainless steel plates. The electrolyte was also made in the same way for each test, but if the electrolyte was used for a lot of tests before being exchanged, some of the current density produced at the 18 hour test could come from leftover ions in the electrolyte that should not have been there.

4.1.4 pH variations

The solutions used during the pH variation tests were made from Sulfuric acid and ion-changed distilled water. The pH values were measured in each solution, and the results are presented in Table 5.

Table 5: The different molarities and their corresponding pH value.

Molarity	0.0001 M	0.001 M	0.1 M	1 M
pH	3.77	2.87	1.01	0.36

Because the minimum pH in an operating PEM fuel cell was measured to be around 3.5 (section 3.1.7), a 1 mM (pH=2.87) solution of H_2SO_4 was used during most of the tests described in this report. However, most of the corrosion tests described in the literature (section 2.5.3) have been done in 1 M or 0.5 M H_2SO_4 electrolytes, and because of this tests were done at different molarities (and thus different pH values) here as well. The results are presented in Figure 30, Figure 31 and Figure 32.

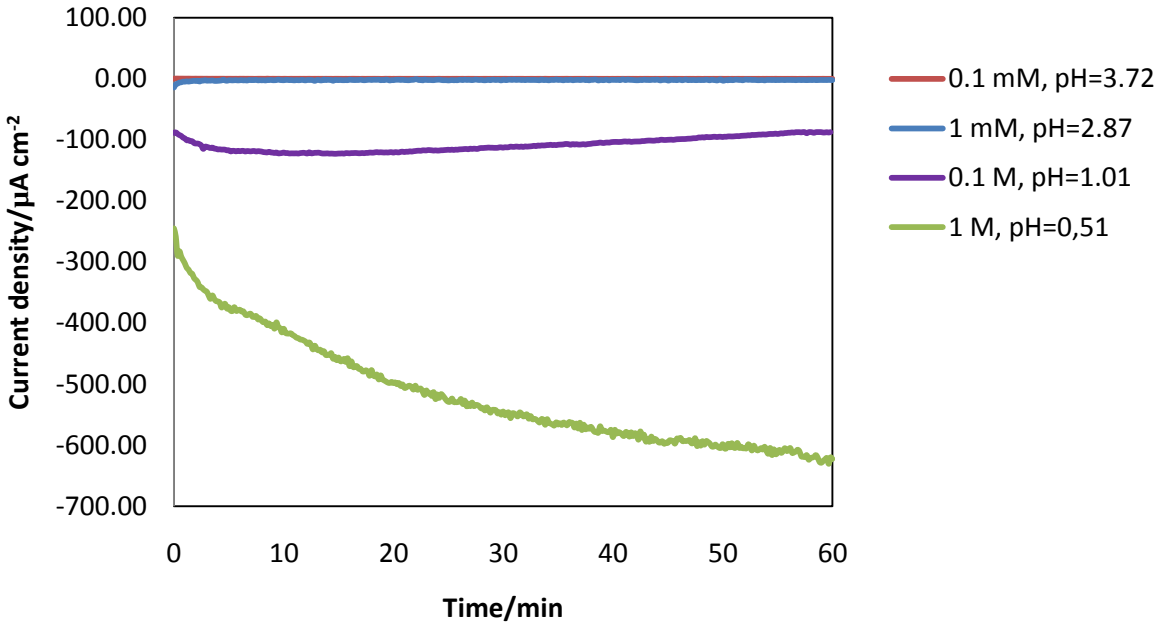

Figure 30: pH variations, test 2, -0.717 V vs. $Hg/HgSO_4$ for 1 hour

Earlier research has aimed to accelerate the corrosion and degrading rate for the stainless steel plates by using a stronger acid. Both Figure 30 and Figure 31 show that the current density, and in Figure 31, the corrosion current, for a 1 M sulfuric acid solution are much higher in absolute values than all the other molarities tested. This result by itself could suggest that the increase in acidity did accelerate the degrading and corrosion of the stainless steel plates. During test 2 (Figure 30), performed in a 1mM H_2SO_4 solution, the

absolute current density stabilized after a short period of time (less than half an hour), while the absolute current density seems to keep increasing at higher acidities (1M), even after 1 hour. At the low potential test (Figure 31) hydrogen evolution should be the main reaction, and the increased current is probably not due to corrosion.

When a strong acidic solution is used, the passivated oxide layer could destabilize (section 2.4.1). If this happens, the oxide layer could start to dissolve, and the stainless steel surface might come in direct contact with the electrolyte. This could in turn open up corrosion reactions on the stainless steel surface that would not have taken place in an electrolyte with lower pH.

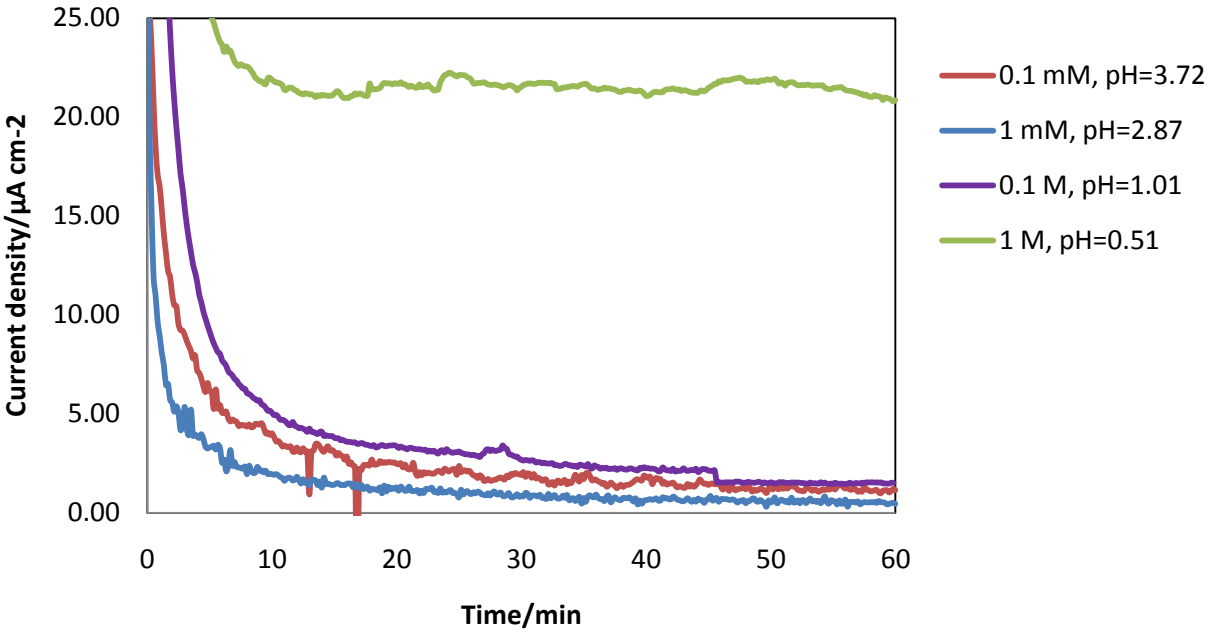

Figure 31: pH variations, test 3; 0.293 V vs. $Hg/HgSO_4$ for 1 hour

At a high potential (0.293 V vs. $Hg/HgSO_4$, Figure 31), in the 1 M solution, the current density seems to stabilize, but at a much higher value than for the other molarities. At this potential, corrosion might occur. As for the low potential test at 1 M, the oxide layer on the stainless steel surface might dissolve and make the surface exposed directly to the electrolyte. This could mean that by increasing the acidity of the electrolyte, one does accelerate the corrosion and thus degrading of the bipolar plate. This might not have happened at all when operating a fuel cell, because the acidity experienced by the bipolar plates within an operating PEM fuel cell is probably never as high as 1 M. As can be seen for the tests performed in the 0.1 mM and 1 mM H_2SO_4, at both high and low voltages, the current densities stabilize after very short time.

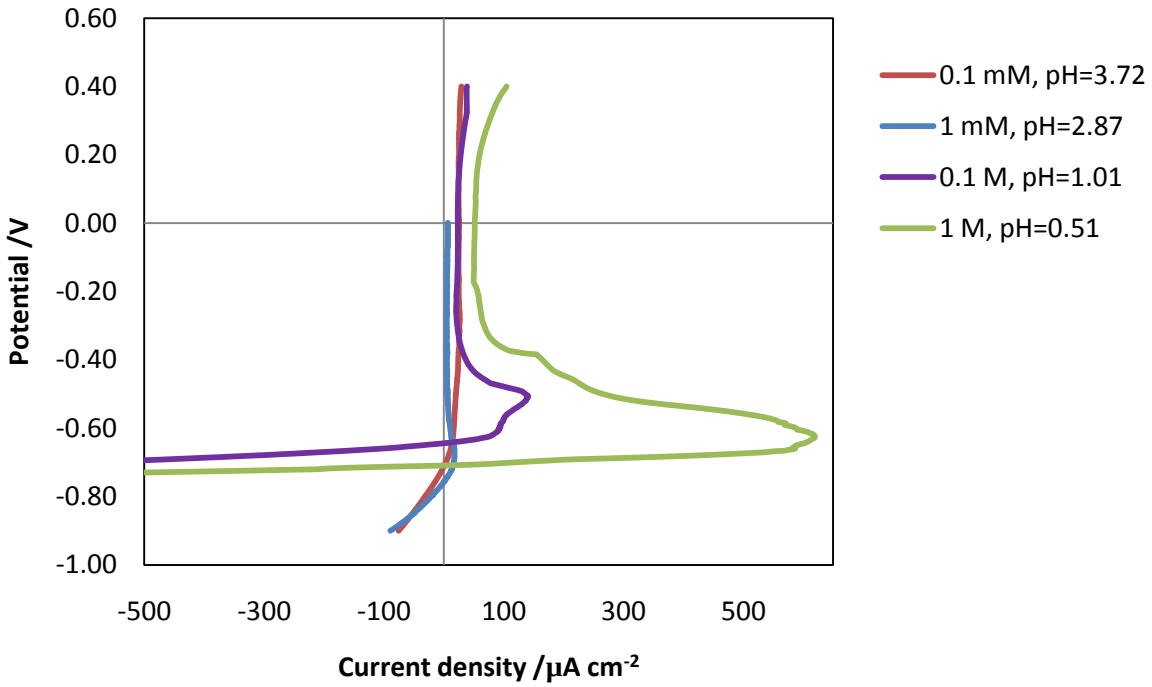

Figure 32: pH variations, test 1; -0.9V to 0.4 V vs. $Hg/HgSO_4$ with a scan rate of 2 mV s^{-1}.

The sweeps from low to high voltage are shown in Figure 32. Both the 0.1 M and 1 M polarization tests show an increase in current density between -0.717 V and -0.4 V, which confirm the results from the high voltage tests in Figure 31. This increase was not found in the 0.1 mM and 1 mM curves in Figure 32, which also corresponds well with the results in Figure 31.

Figure 33a shows the plate that was tested in the 1 M solution of sulfuric acid when the potential was set to -0.717 V vs. $Hg/HgSO_4$ for 1 hour. This black color came from a layer that had formed on the stainless steel plates. This plate did not look like any of the other plates that had been tested. The layer could have consisted of some sort of iron oxide, which would show good conductivity compared to the chromium oxide layer usually formed on stainless steel. The conductivity of the stainless steel plates after the corrosion tests will be further discussed in section 4.2.4. The iron oxide layer could have increased the current densities to values that one would never find in an operating fuel cell. This could indicate that using a 1M sulfuric acid solution to accelerate the reactions that takes place inside a fuel cell, would actually provoke reactions that would never happened in a real fuel cell.

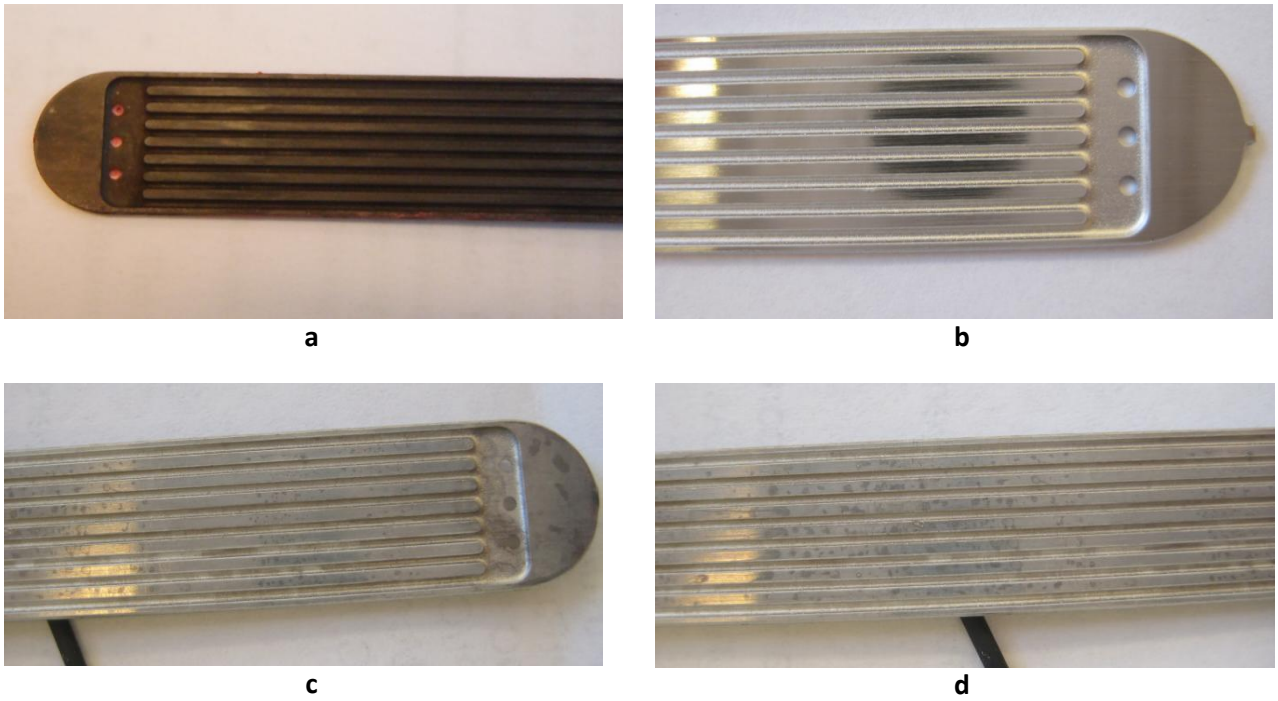

Figure 33: a) Used stainless steel bipolar plate, 1 M H_2SO_4 at -0.717 V vs. $Hg/HgSO_4$ for 1 hour. b) New stainless steel bipolar plate. c) Used stainless steel bipolar plate, 1mM H_2SO_4 at 0.293 V vs. $Hg/HgSO_4$ for 1 hour. d) Used stainless steel bipolar plate, 0.1 mM H_2SO_4 at -0.717 V vs. $Hg/HgSO_4$ for 1 hour.

4.1.5 Addition of Fluoride and Chloride to the electrolyte

Figure 34, Figure 35 and Figure 36 present the results obtained from the polarization tests performed with additions of fluoride and chloride to the sulfuric acid electrolyte. In both Figure 34 and Figure 35 the tests performed in the electrolyte with 2 ppm addition of fluoride and 10 ppm addition of chloride seem to produce currents in the same order of magnitude as the reproducibility tests (section 4.1.2). This indicates that the fluoride and chloride amounts found in a PEM fuel cell does not create any extra current. The similar tests performed by Wang et al [2] and Rivas et al [21] (section 2.4.3) were not done to see whether or not fluoride affected the reaction, and it is thus hard to compare the results here to their results. Previous research done in electrolytes containing chloride was focused on the degrading of platinum and not stainless steel.

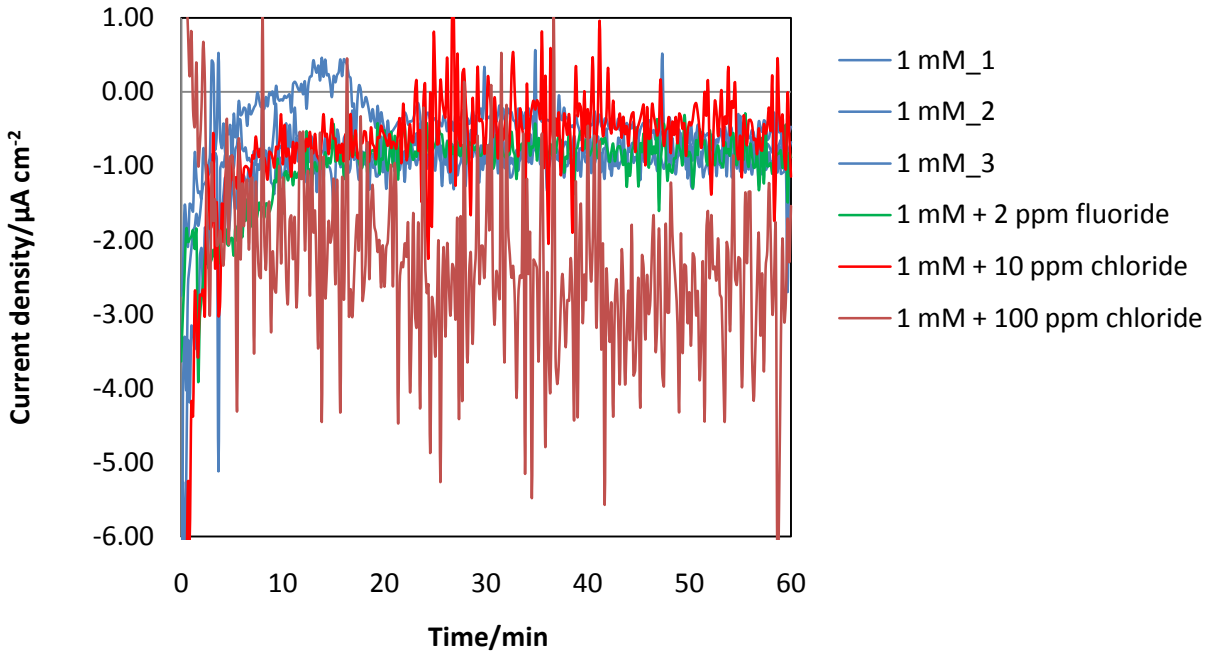

Figure 34: Addition of F^- and Cl^-, test 3; -0.717 V vs. $Hg/HgSO_4$ for 1 hour

By comparing Figure 34 and Figure 35 it is clear that the 100 ppm chlorine addition has a greater effect when the potential is high (0.293 V vs. $Hg/HgSO_4$) than when it is low (-0.717 V vs. $Hg/HgSO_4$). At low potentials the current density is not expected to cause any corrosion current because at this potential hydrogen evolution is the only expected reaction. At higher potentials (Figure 35) corrosion can occur, and Figure 35 shows that the plate tested in the electrolyte containing 100 ppm chloride produced a much higher corrosion current than any of the other test in the same figure. But the chloride content within a fuel cell will, however, probably never exceed 10 ppm, and thus the corrosion at 100 ppm should not be an issue when running the fuel cells.

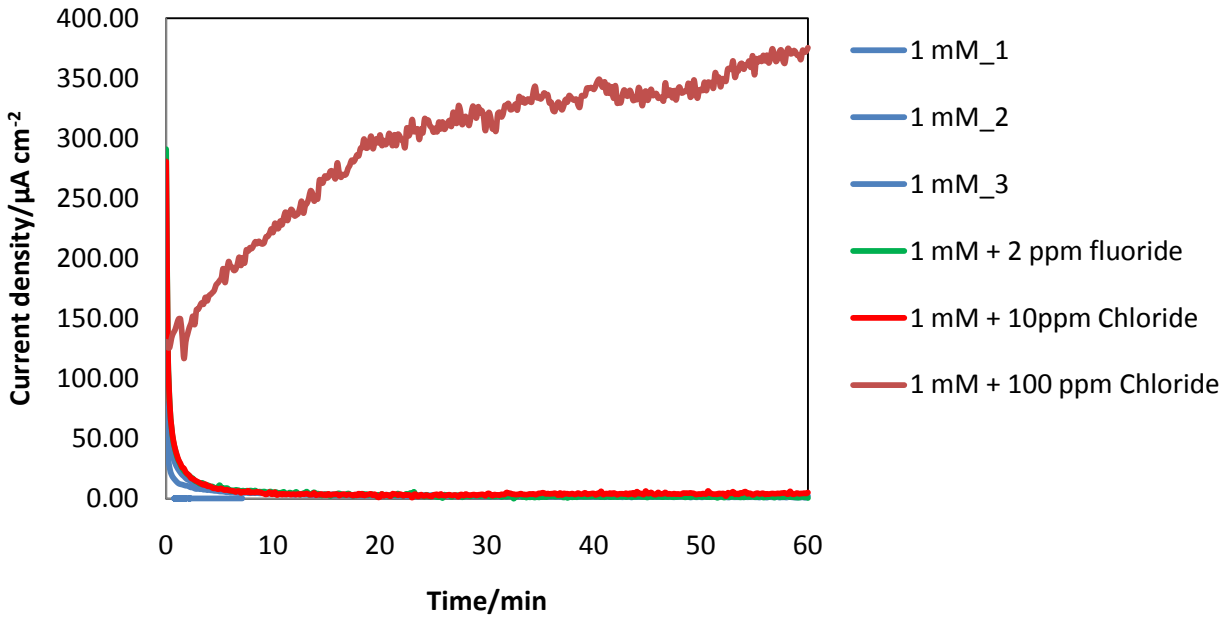

Figure 35: Addition of F^- and Cl^-, test 3; 0.293 V vs. $Hg/HgSO_4$ for 1 hour

Figure 36 shows the sweep of the fluoride and chloride tests together with some of the tests presented earlier in the report. The shape of the 2 ppm fluoride and 10 ppm chloride curves are almost identical to the 1 mM test. The 100 ppm chloride curve is a little different, with a more emphasized current peak at around 0.6 V. This peak indicates a higher corrosion current, and confirms that 100 ppm chloride affects the steel more than 10 ppm. If the 100 ppm curve is compared to the gold coated glass curve, it is clear that much higher currents were detected for the test done on stainless steel in the electrolyte containing 100 ppm chloride.

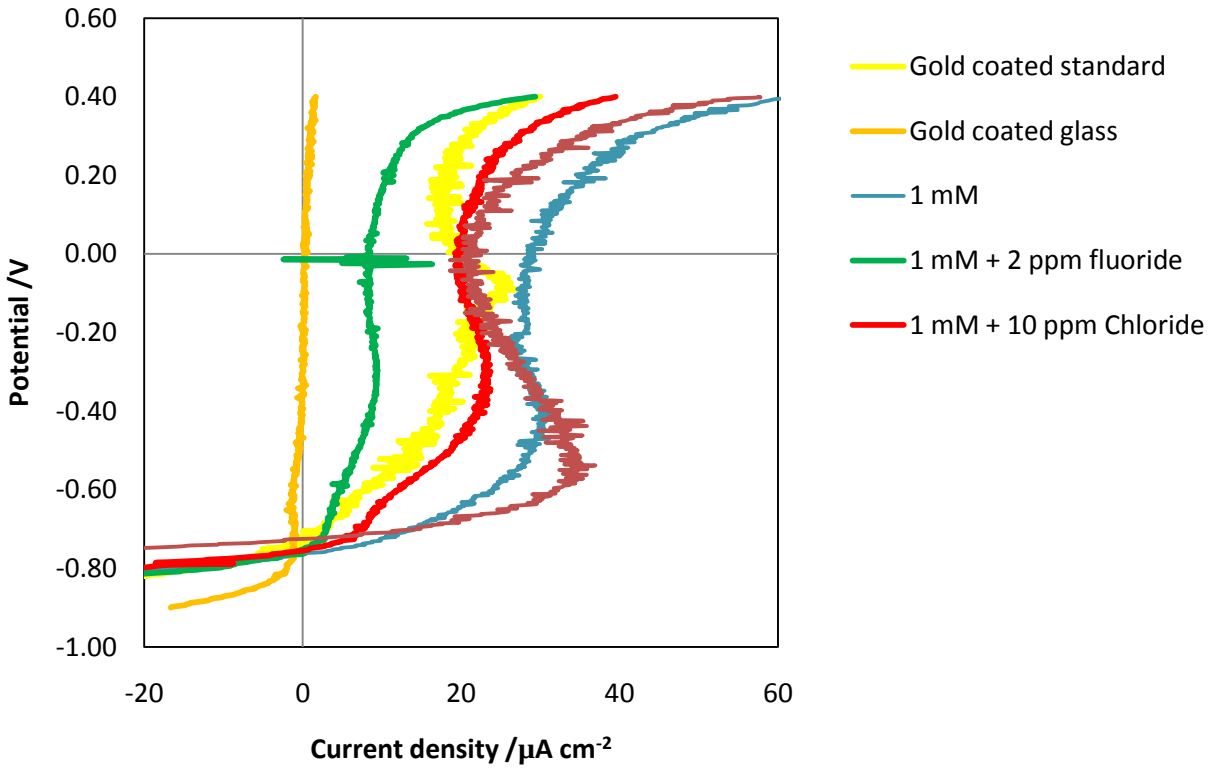

Figure 36: Addition of F^- and Cl^-, test 1; -0.9V to 0.4 V vs. $Hg/HgSO_4$ with a scan rate of 2 mV s^{-1}.

Towards the end of each sweep, the curves seem to flat out around the same potential. This is interesting because it might show that the oxide layer on the stainless steel plates start to dissolve. The same phenomenon was also observed in section 4.2.3, where reproducibility was tested. The area of the graphs where the curves are close to vertical the oxide layer is probably stable and no more or less current is created. Around 0.3 V all the curves seem to turn and the current density increases again. As suggested in section 4.2.3 this could be because the oxide layer dissolves at this potential. This is an important factor to know about, but the PEM fuel cells used in the NORCOAT project has never been run at this high potential, and it should thus not affect this project either.

When the stainless steel plates used for the test at 0.293 V vs. $Hg/HgSO_4$ in a sulfuric acid solution with 100 ppm chloride were taken out of the solution after the test was done, tiny dots on the surface were revealed. These dots where very hard to see with the naked eye, and the plates were thus investigated in the SEM. Figure 37b-d are images of the dots observed, and they appear as dark areas in the SEM images. By comparing them to Figure 7 in section 2.4.1, one might suggest that these dark areas could come from pitting corrosion. This could in turn explain why the corrosion current for the solution containing 100ppm chloride at 0.293 V vs. $Hg/HgSO_4$ is so much higher than the other tests presented in Figure 35.

As described in section 2.4.1, pitting corrosion often accelerates quickly once it has initiated and can be crucial for the construction in which it occurs. This should however not cause any problems when operating a PEM fuel cell because more than 10 ppm is very unlikely to be found in a PEM fuel cell [22]. For comparison a picture of a new stainless steel bipolar plate that has never been used is shown in Figure 37a.

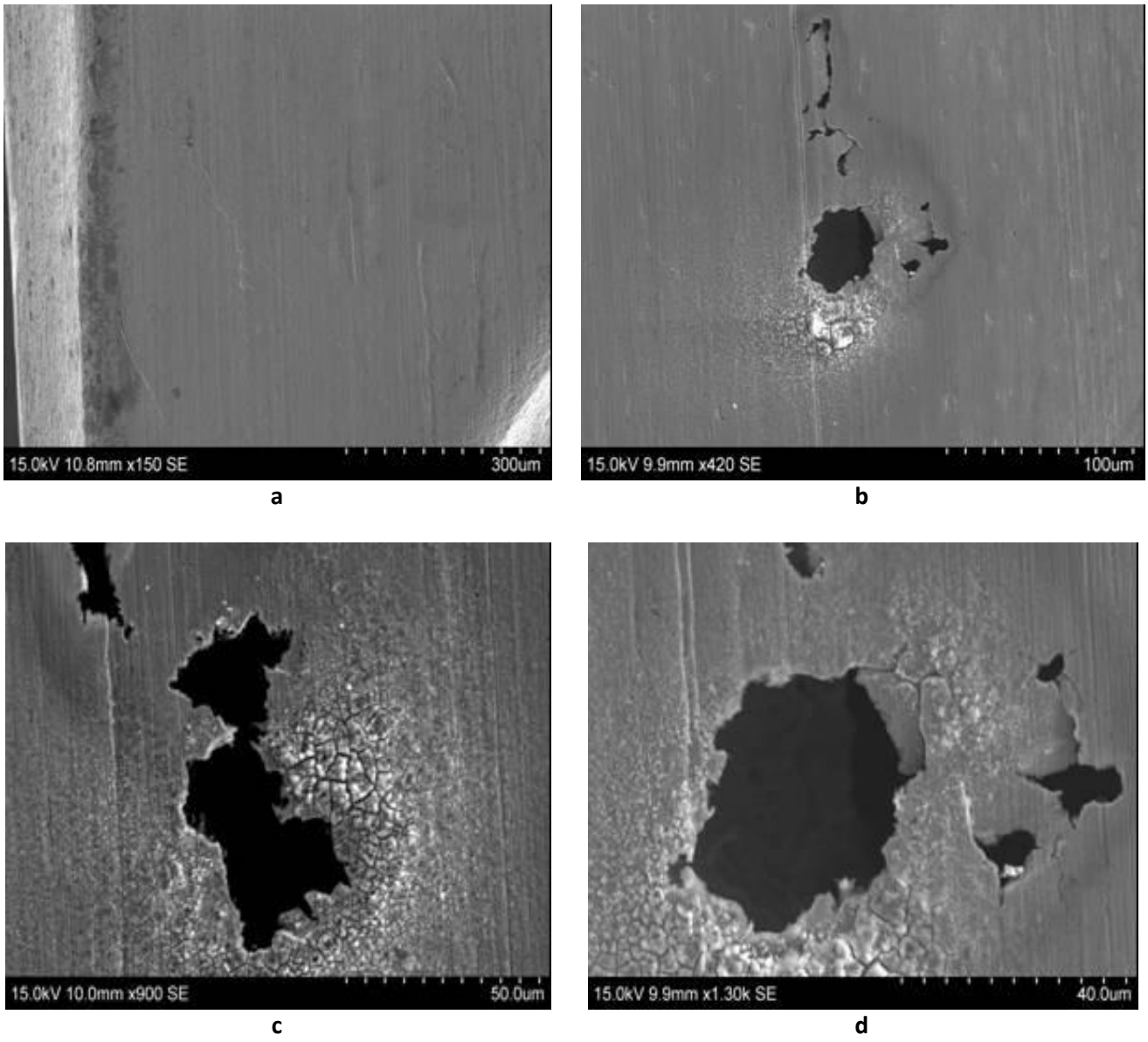

Figure 37: a) A new, never used, stainless steel plate. b) The stainless steel plate used for the 0.293 V test in the electrolyte containing 10 ppm Cl^-. c) SEM image showing pitting corrosion on the stainless steel surface after the polarization test at -0.293 V with 100 ppm Cl^-. d) SEM image showing pitting corrosion on the stainless steel surface after the polarization test at -0.293 V with 100 ppm Cl^-.

4.1.6 Coating A

The results from the polarization tests of the stainless steel plates with Coating A are presented in Figure 38, Figure 39 and Figure 40. To allow for comparability the reproducibility results are also included in Figure 38 and Figure 39. In Figure 40 one stainless steel plate without coating is included together with the gold coated stainless steel and the gold coated glass.

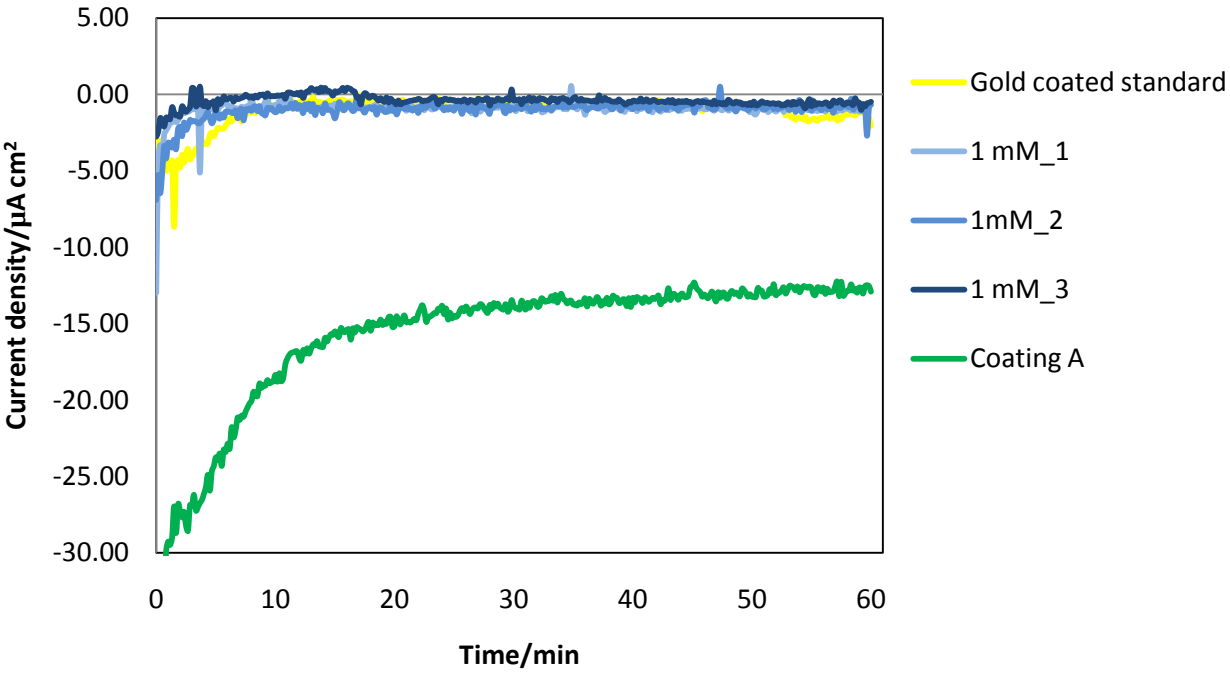

Figure 38: Coating A, test 2; -0.717 V vs. Hg/$HgSO_4$ for 1 hour

The test run at -0.717 V vs. Hg/$HgSO_4$ showed results very different from most of the other test performed during this project work. There is a very high absolute current density even after the curve has stabilized. At this potential hydrogen evolution is the dominating reaction, and the high current density indicates that one or more of the components in coating A catalyses this reaction.

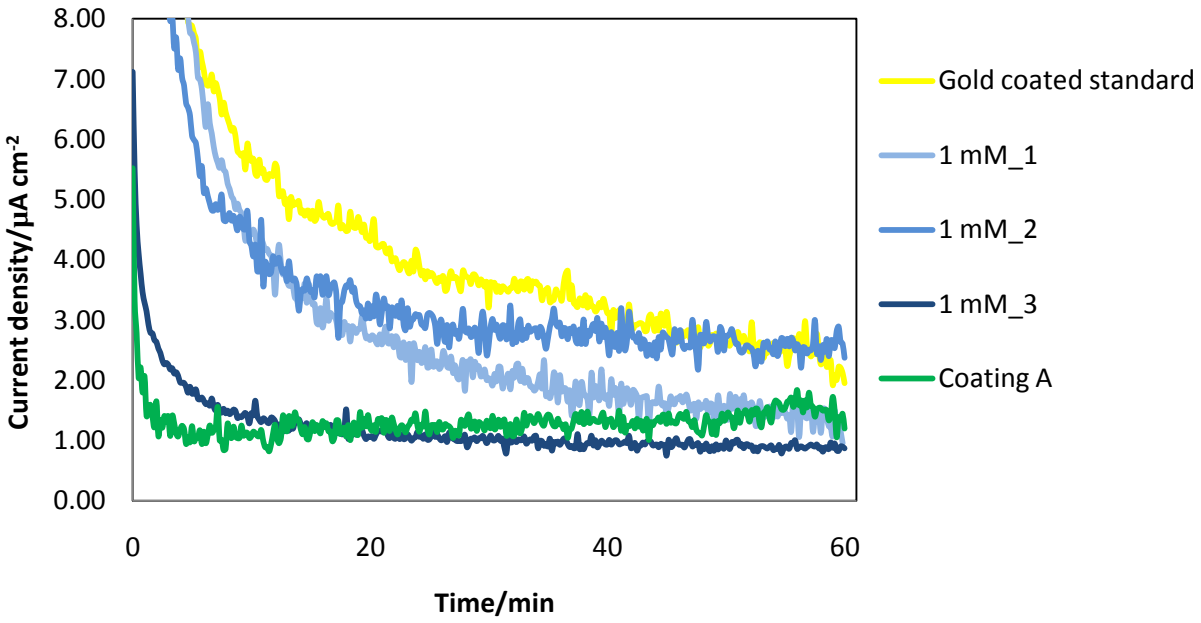

Figure 39: Coating A, test 3; 0.293 V vs. $Hg/HgSO_4$ for 1 hour

In Figure 39 the corrosion test results from the 0.293 V vs. $Hg/HgSO_4$ test are presented. The stabilized current density is in the same area of magnitude as for the non coated stainless steel and the gold coated stainless steel stainless steel plates, but lower than most of them. These results are promising, as they indicate that the corrosion is the same or lower than the stainless steel which has a corrosive protective oxide layer on the surface. Some current is produced, which could be caused by pitting corrosion, but if pitting corrosion had taken place, the current would probably be higher than for the stainless steel plates without coating.

Figure 38 and Figure 39 both showed different results from the corrosion tests of stainless steel plates with Coating A at 0.293 V vs. $Hg/HgSO_4$ and -0.717 V vs. $Hg/HgSO_4$ compared to the other tests presented in the same figures. Different explanations were presented for each of them. In Figure 40 the sweep test of stainless steel with Coating A from -0.9 V to 0.4 V vs. $Hg/HgSO_4$ is presented together with the gold coated stainless steel plate, the gold coated glass and a non-coated stainless steel plate. Earlier in the results, the sweep from the gold coated glass test has been presented as the more ideal sweep when one is trying to avoid corrosion, because the current stays close to zero throughout most of the sweep. By studying the Coating A polarization from 0.9 V to 0.4 V vs. $Hg/HgSO_4$ it is obvious that this is the one that looks most like the gold coated glass of all the tests in Figure 40. It does seem to bend of towards higher currents after passing 0 V vs. $Hg/HgSO_4$, but the results obtained from this new coating are still very promising.

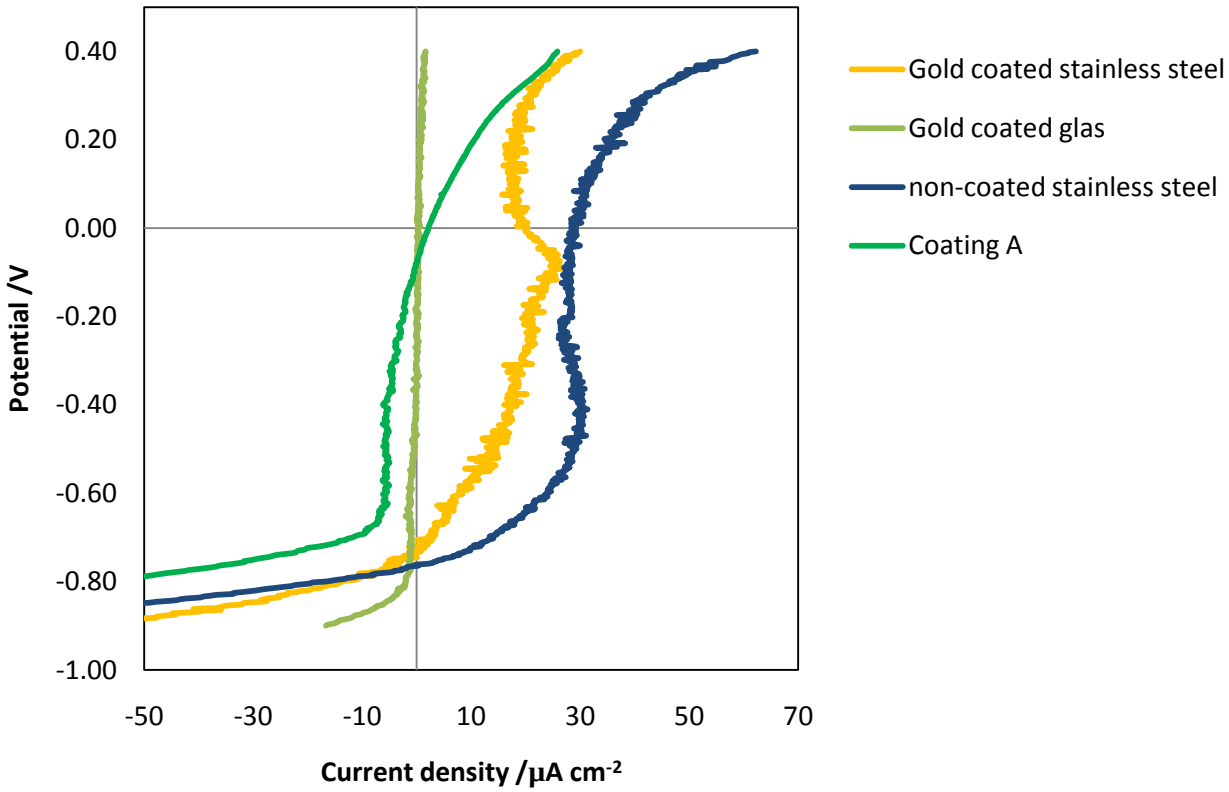

Figure 40: Coating A, test 1; -0.9V to 0.4 V vs. $Hg/HgSO_4$ with a scan rate of 2 mV s^{-1}.

The shape of both the stainless steel sweep and the cold coated stainless steel sweep have are different compared to the stainless steel with Coating A, which indicates that fewer or at least different surface reactions took place on the Coating A plate throughout the sweep. At this potential the high current density cannot be blamed on corrosion of stainless steel, but one or more reduction surface reactions have probably taken place on the bipolar plate. The components of the coating are not known, and it is thus hard to determine which surface reaction that could have caused the high current density values. These results could be important for future work with this coating, and further inspection of this coating is highly recommended.

4.1.7 Concluding discussion of the polarization tests

Stainless steel plates have been trough polarization test during this project work. Tests have been done with different coatings and also in different electrolytes. Before starting any of the polarization tests, gold coated stainless steel was chosen as standard, but this proved to not have been a good idea because the gold coating seemed to peel off very easily. The gold coated glass showed a significant lower current density compared to the gold coated steel in the sweep test (Figure 23). Both polarizations from -0.9 to 0.4 V vs. $Hg/HgSO_4$ and high potential polarization tests show that the lowest current was produced by the stainless steel plates with the new coating, Coating A. Maybe these plates should be considered as standard for the next set of polarization tests. In order to do so, a more thorough inspection and analysis of the new coating should be performed.

Most of the polarization tests at both high (0.293 V vs. $Hg/HgSO_4$) and low potentials (-0.717 V vs. $Hg/HgSO_4$) produced very small currents, sometimes almost non-existing. Some of the tests diverge from all the others, and the tests performed on non-coated stainless steel in a 1 M sulfuric acid solution (section 4.1.4) all produced higher absolute currents than the tests performed in solutions with lower molarities of sulfuric acid. This could be because the oxide layer dissolved in such a strong acid, which could have exposed the stainless steel to the corrosive environment in the electrolyte.

Another test that stood out was the test performed at 0.293 V vs. $Hg/HgSO_4$ for one hour in a 1 mM sulfuric acid solution with the addition of 100 ppm chloride (Figure 35). The current density at the end of the test was close to 300 times the current density produced in any of the reproducibility tests. There were obvious signs of pitting corrosion on the plate used for this test, and it proves how dangerous pitting corrosion can be for a material. 100 ppm is, however, too high a concentration in a PEM fuel cell, and these results should not cause any problems when operating a PEM fuel cell.

The last test that stood out from all the other polarization tests due to very high current densities was the low potential (-0.717 V vs. $Hg/HgSO_4$) test for the stainless steel with the new coating (Coating A) (Figure 38). The current density produced was about 10 times higher than any of the reproduced tests, and this indicates that one or more of the components in Coating A have functioned as catalysts for hydrogen evolution. Components in Coating A could also have been reduced in the electrolyte, but these components of the coating are not known. The polarization from -0.4 V to 0.9 V (Figure 40) done with Coating A coated plates show a strong cathodic current above the reproducible potential, which indicates that a reduction has taken place. This could be the reduction of one of the components in the coating, but the different components are not known.

DOEs target for corrosion current for bipolar plates in PEM fuel cells is less than 1 μA cm^{-2}. Both non-coated stainless steel in 0.1 mM and 1 mM (Figure 31) solutions and Coating A (Figure 39) showed current densities close to or lower than this value in the high potential (0.293 V) tests. The low current densities recorded for non-coated stainless steel are probably due to the passivated oxide layer formed on the surface of the plates, which would probably cause large changes contact reistance, and thus not pass DOEs requirements for contact resistance. The low corrosion current from Coating A is promising, and the contact reistance measurements are presented in section 4.2.6. A further discussion of both non-coated stainless steel and Coating A is presented later in the thesis, after the discussion of the ICR results.

If all the polarization tests are seen together, most of them show results as were to be expected. The oxide layer formed on the stainless steel prevented corrosion and other electrochemical reactions to take place. At a low pH and when too much chloride was added to the electrolyte, corrosion currents seemed to spike. None of these factors should however be an issue in an operating PEM fuel cell, because the chloride content in the electrolyte should never get as high as 100 ppm.

4.2 Contact resistance measurements

The interfacial contact resistance (ICR) was measured both before and after each polarization test. The graphs presented in this section show the change, or delta value, from the ICR testing before and after each polarization test. This was done because the contact resistance measured for the stainless steel plates before the polarization tests changed from test to test. The oxide layer formed on stainless steel starts to form as soon as the steel comes in contact with air, and it was thus almost impossible to get the exact same results on the pre-polarization test ICR measurements, in particular at higher pressures. This means that the graphs displaying the contact resistance in this report are not directly comparable to most of the ICR research described in the literature, but it makes the comparison within this project much more accurate. Table 6 shows the contact resistance at 140Ncm^{-2} before and after each polarization test. This makes it is possible to get some idea of the contact resistance measurements done in this project compared to previous research (section 2.5.2).

Table 6: contact resistance results at 140 Ncm^{-2} (14 bar) before and after all the polarization tests. All the contact resistance values are given in mΩ cm^2.

What was tested	Test 1: -0.9V to 0.4V vs. $Hg/HgSO_4$		Test 2: -0.717 V vs. $Hg/HgSO_4$		Test 3: 0.293 V vs. $Hg/HgSO_4$	
	Before	After	Before	After	Before	After
Gold coated stainless steel	11.53	10.65	11.1	9	11.1	14
Reproducibility 1	15.8	90	17.25	36.8	17	117.5
Reproducibility 2	19.8	131.5	16.2	37.1	19	182.5
Reproducibility 3	17	154.4	16.2	62.5	25	364
1 vs 18 hours	-	-	12	15.7	18.2	57.5
0.1mM/pH=3.87	19.15	170.5	15.85	29.3	20.85	186.5
1mM/pH=2.78	16.6	134.2	17.25	36.95	18.85	183
0.1M/pH=1.01	16	90.6	18.35	20.6	13.9	29.8
1M/pH=0.51	18.35	18.8	26.7	14.75	18.35	18.8
Addition of 2ppm fluoride	23.7	157.5	19.5	50.5	20.7	171.9
Addition of 10ppm chloride	18.8	185	21.2	46	17	201.3
Addition of 100ppm chloride	22.4	194.5	24.9	104.5	24	268
Coating A	14.4	19.8	14.5	28	14.9	15.25

4.2.1 Gold coated stainless steel- standard

As mentioned in section 3.1 gold coated stainless steel plates were chosen as standard because gold by itself has most of the qualities desired for a bipolar plate. The contact resistance measurements for the gold coated stainless steel plates are presented together with the reproducibility measurements in Figure 41, Figure 42 and Figure 43. Gold coated stainless steel shows a very small change in contact resistance when measured before and after the polarization tests. This was to be expected, as gold does not form a passivated oxide layer on the surface like stainless steel does. The gold coated steel ICR results obtained

before and after test 2 (-0.717 V vs. $Hg/HgSO_4$ for 1 hour) show slightly negative delta values (Figure 41). The reason why these delta values are negative could be uncertainties in the measurement equipment. Because the equipment was taken apart and put together again for each new test (Figure 21a-d), it was hard to get the exact same conditions for each test. What is important to note from these results, is that gold shows little or no change in contact resistance before and after the polarization test.

The ICR delta results from test 3 (0.293 V vs. $Hg/HgSO_4$ for 1 hour) and test 1 (-0.9 V to 0.4 V vs. $Hg/HgSO_4$) also show a very small absolute delta value (Figure 42). As explained above, this was expected due to Gold's ability to conduct current and at the same time avoid formations of low-conduction oxide layers.

4.2.2 Reproducibility of non-coated stainless steel

The ICR delta values from the reproducibility tests are presented in Figure 41, Figure 42 and Figure 43. These tests were done to find out whether or not the change in contact resistance after the corrosion tests could be reproduced if the conditions were the same. Test 1, 2 and 3 (Table 4) were repeated three times each and as similar as possible. Figure 41, Figure 42 and Figure 43 all show that the change in contact resistance for non-coated stainless steel is several times higher than the change for the gold coated steel. This confirms that non-coated steel is more affected by the polarization tests than the gold-coated steel.

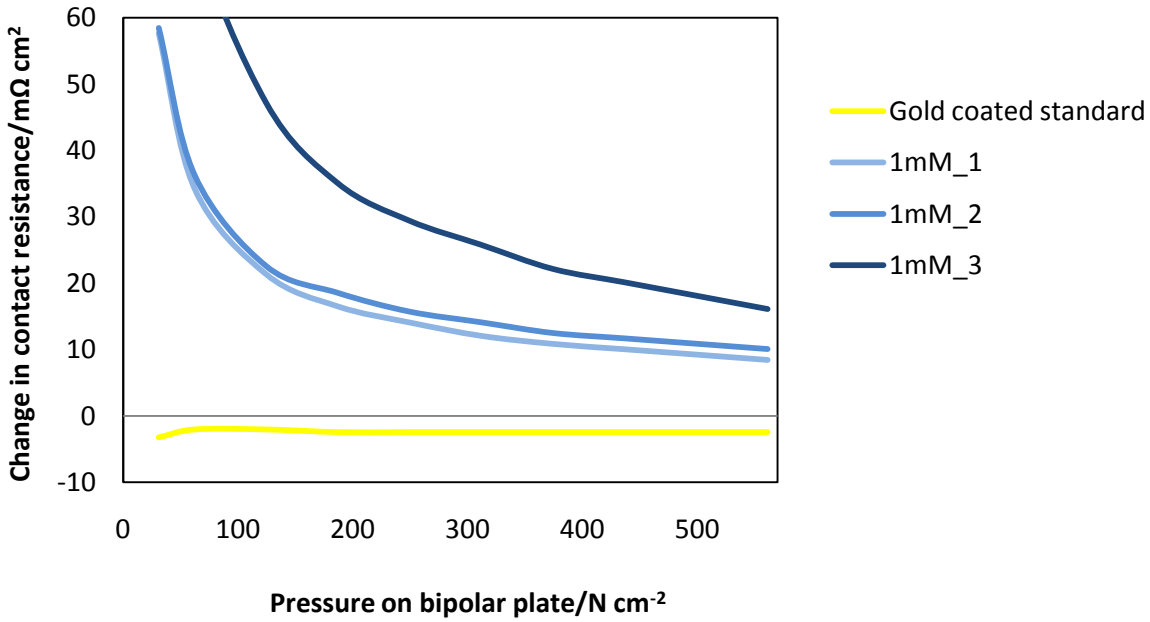

Figure 41: Reproducibility, test 2; -0.717 V vs. $Hg/HgSO_4$ for 1 hour.

The oxide layer formed on the non-coated stainless steel probably causes the change in contact resistance because the layer thickness seems to increase during the Polarization test. The fact that the stainless steel plates had been acid cleaned before the first ICR tests could increase the delta values even more, because the oxide layer starts to form as soon as

the steel is in contact with air. By acid cleaning them, this air-made oxide layer was even thinner before the plates were put trough the polarization tests.

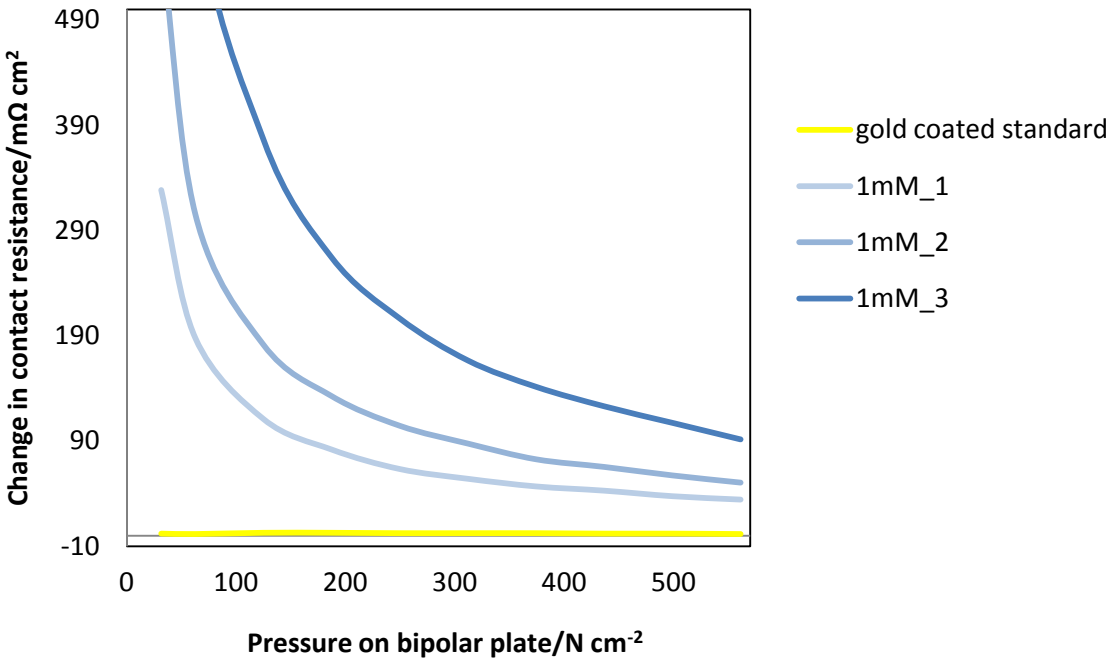

Figure 42: Reproducibility, test 3; 0.293 V vs. $Hg/HgSO_4$ for 1 hour.

There is a large difference between the non-coated stainless steel and the gold coated stainless steel in all three figures, but there is quite a big difference between the delta values of the reproduced tests as well. In Figure 42 e.g. there is a gap between two of the non-coated stainless steel curves (1mM_1 and 1mM_3) that exceeds the gap between the gold coated stainless steel and the lowest of the non-coated stainless steel at all pressures. The delta value obtained from the ICR measurements of the gold coated steel (Figure 42) are close to 0 $m\Omega cm^2$at 140 Ncm^{-2} (Table 6), while for 1 mM_1 and 1 mM_2 the delta values are 100.5 $m\Omega cm^2$ and 339 $m\Omega cm^2$ respectively.

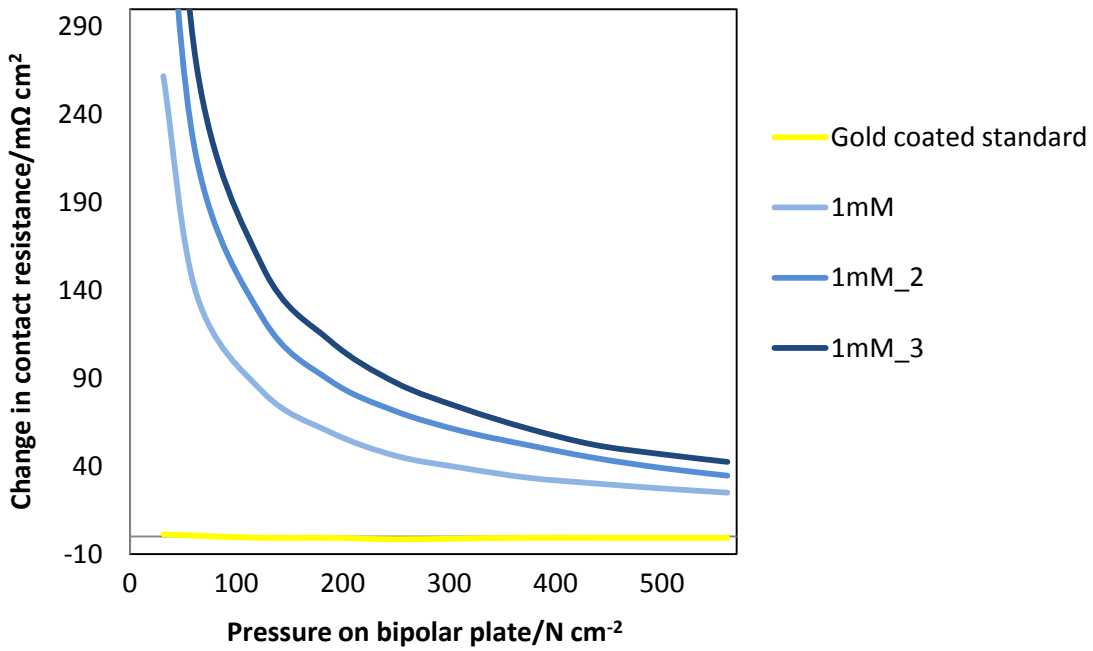

Figure 43: Reproducibility, test 1; -0.9V to 0.4 V vs. $Hg/HgSO_4$.

Even though some of the reproduced tests seem to give about the same contact resistance delta values at all pressures (1mM_1 and 1mM_2, Figure 41), this could be coincidental. If all the reproducibility tests are seen together, the reproducibility seems to be quite low compared to the difference between the reproduced tests and the gold coated stainless steel. But none of the reproduced tests show as low delta values as the gold coated stainless steel plates, which means that one can easily see which of the graphs in Figure 41 and Figure 43 that displays the gold coated plates, and which of them are displaying the reproducibility tests.

4.2.3 1 vs. 18 hours

The results from the contact resistance measurements done before and after the long term polarization tests are presented as delta values in Figure 44 and Figure 45. The ICR values for the long term tests changed less than for the 1 hour tests (1 mM_1, 1 mM_2 and 1 mM_3). The passivated oxide layer is most likely the reason for the increase in contact resistance before and after one test. This indicates that the increase in oxide layer thickness was smaller for the long term tests compared to the 1 hour tests.

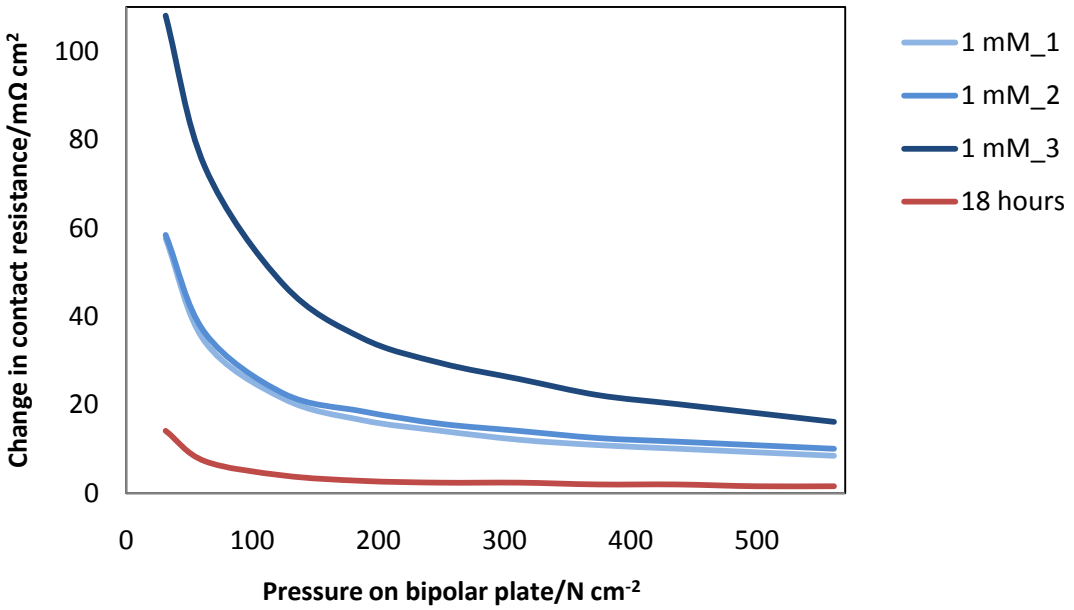

Figure 44: 1 vs. 18 hours, test 2; -0.717 V vs. $Hg/HgSO_4$ for 18 hours.

One reason for the eventual increase in oxide layer thickness could be that the 17.5 and 18 hour tests were performed very early on in the project work. As mentioned in section 4.1.3 the plates used for these tests were reused, and other polarization tests had thus been conducted with these plates earlier. It was assumed in the beginning that by cleaning the stainless steel plates in acid, the built up passivated oxide layer would come off completely, and in this way the acid washed plates would always be as new ones. This assumption might not have been right, and some of the oxide layer could have survived the acid cleaning. If this was the case, the change in contact resistance before and after each test would not have been that great, because some of the oxide layer was already there before the polarization tests were performed.

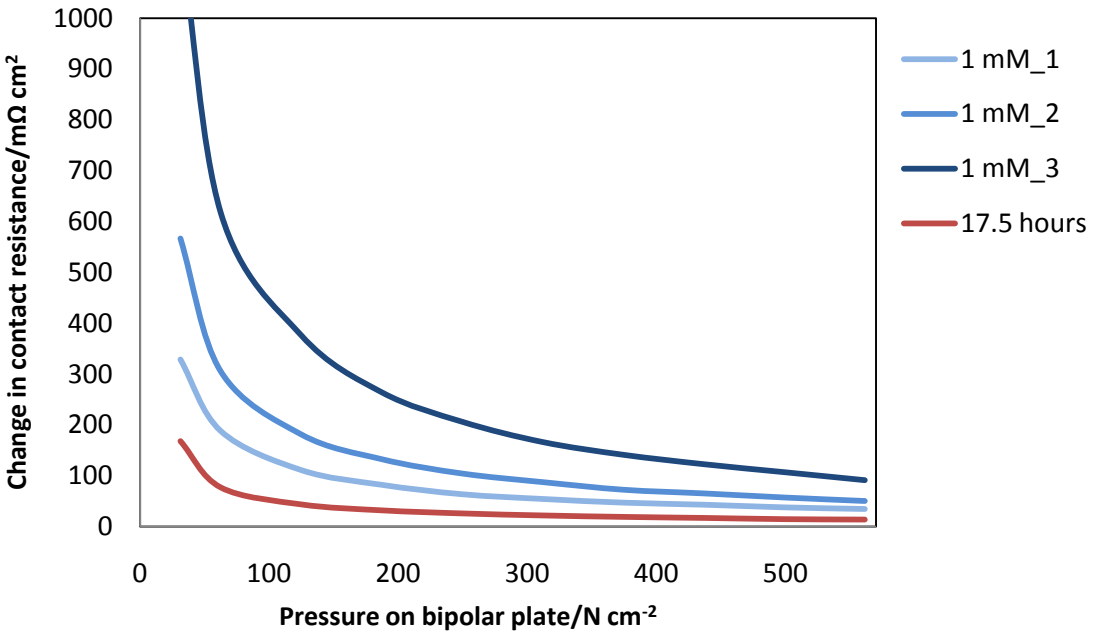

Figure 45: 1 vs. 18 hours, test 3; 0.293 V vs. $Hg/HgSO_4$ for 17.5 hours.

All the other tests described in this project were done with new stainless steel bipolar plate that had not been used in polarization tests before. The reason why the long term tests were not done all over with new stainless steel plates, was because the results obtained from the polarization tests (section 4.1.3) might not have changed that much if new plates had been used. In addition there was a time limit on this project, and the reproduction of the 18 hour tests were not prioritized because there were a lot of other tests one wished to conduct.

4.2.4 pH variations

The contact resistance measured before and after the polarization tests at different molarities are presented as delta values in Figure 46, Figure 47 and Figure 48. Figure 46 displays the changes in contact resistance before and after polarization test 2 (-0.717 V vs. $Hg/HgSO_4$ for 1 hour). The results from the ICR measurements before and after the 0.1 mM, 1 mM and 0.1 M polarization tests show a positive change, which means that the contact resistance had gone up from the before-to the after ICR measurements. The two lower molarities (0.1 mM and 1 mM) show a higher increase in contact resistance compared to the 0.1 M. This could be because the oxide layer formed on the stainless steel loses its stability at higher molarities (lower pH values). When it starts to dissolve, it gets thinner and the delta contact resistance is thus decreased. The tests done in 0.1 M H_2SO_4 could have resulted in a thinner oxide layer on the stainless steel plates, which most likely would result in a lower contact resistance.

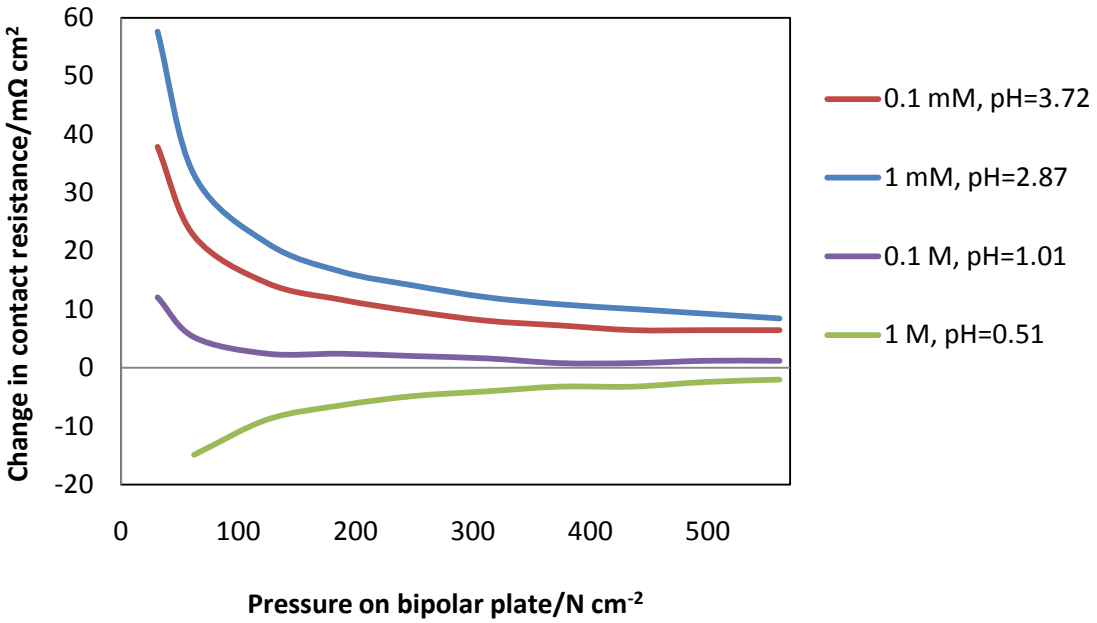

Figure 46: pH variations, test 2; -0.717 V vs. $Hg/HgSO_4$ for 1 hour.

When it comes to the delta values obtained from the 1 M test at -0.717 V vs. $Hg/HgSO_4$ for one hour, there is a negative change in contact resistance, which means that the contact resistance decreased after the polarization test. As discussed in section 4.1.5 the plates tested at a low potential in the 1 M H_2SO_4 solution looked very different from all the other plates when they were studied afterwards (Figure 33a). The polarization tests showed that the plate tested in a 1 M solution produced a much higher current than the ones tested in the solutions with other molarities. This could indicate that a completely different surface reaction has taken place. If this surface reaction resulted in a conducting layer on the stainless steel plates, the contact resistance could increase. This would explain both the polarization- and the ICR results.

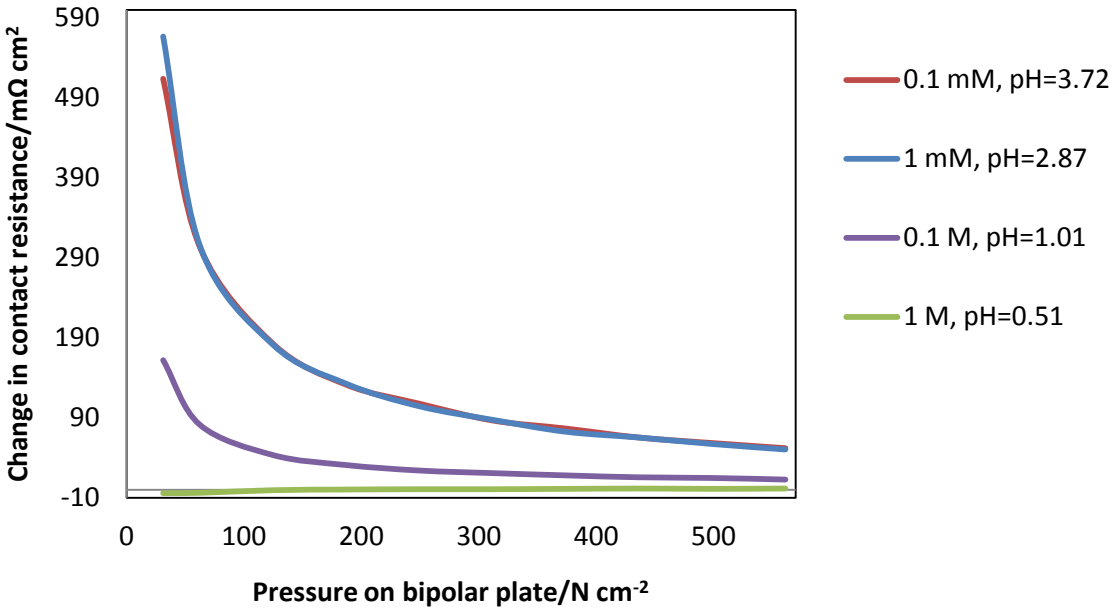

Figure 47: pH variations, test 3; 0.293 V vs. $Hg/HgSO_4$ for 1 hour.

The ICR results obtained before- and after the high potential polarization tests (0.293 V vs. $Hg/HgSO_4$ for 1 hour) are displayed in Figure 47. The same trend is found here as was found in Figure 46; the test done in 0.1mM and 1 mM H_2SO_4 show a higher change in contact resistance than the tests done in 0.1 M and 1M H_2SO_4. As was suggested from the results at low potential (Figure 46) the oxide layer is probably more unstable at higher molarities.

The delta ICR values obtained as part of the 1 M H_2SO_4 test at 0.293 V vs. $Hg/HgSO_4$ are close to zero, and in the beginning a little negative. But since the negative part of the graph is at low pressures, this might just be because of instabilities in the equipment. The potential measurements at low pressures were fluctuating throughout all tests and took a while to get stable. The plate did not look any different when it was studied after the polarization test, and it is not likely that the same surface reactions have taken place here compared to the plate tested at a low potential.

If it is assumed that the stainless steel bipolar plate tested at a high potential in a 1 M H_2SO_4 solution not reacted in the same way as the plate tested in the solution at a low potential, the low delta value in contact resistance could be explained by the same reasoning as for the 0.1 M test. If the passivated oxide layer was dissolved in the 0.1 M H_2SO_4 solution, it should be even more unstable, and maybe not even there in a 1 M solution. If the oxide layer was very thin or absent, the change in contact resistance could be close to zero.

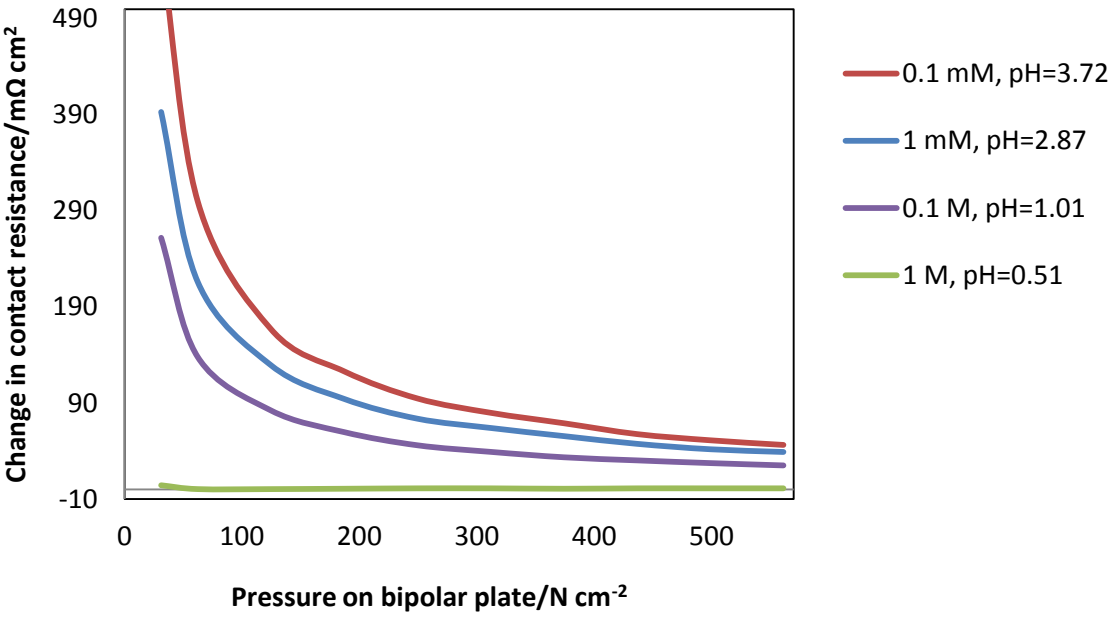

Figure 48: pH variations, test 1; -0.9V to 0.4 V vs. $Hg/HgSO_4$.

4.2.5 Addition of Fluoride and Chloride to the electrolyte

Figure 49, Figure 50 and Figure 51 present the delta results from the ICR measurement done before and after the polarization tests performed in a 1 mM solution containing fluoride and chloride together with the reproducibility results and the gold coated standard. These results were included in the figures because they lay the foundation for the comparison.

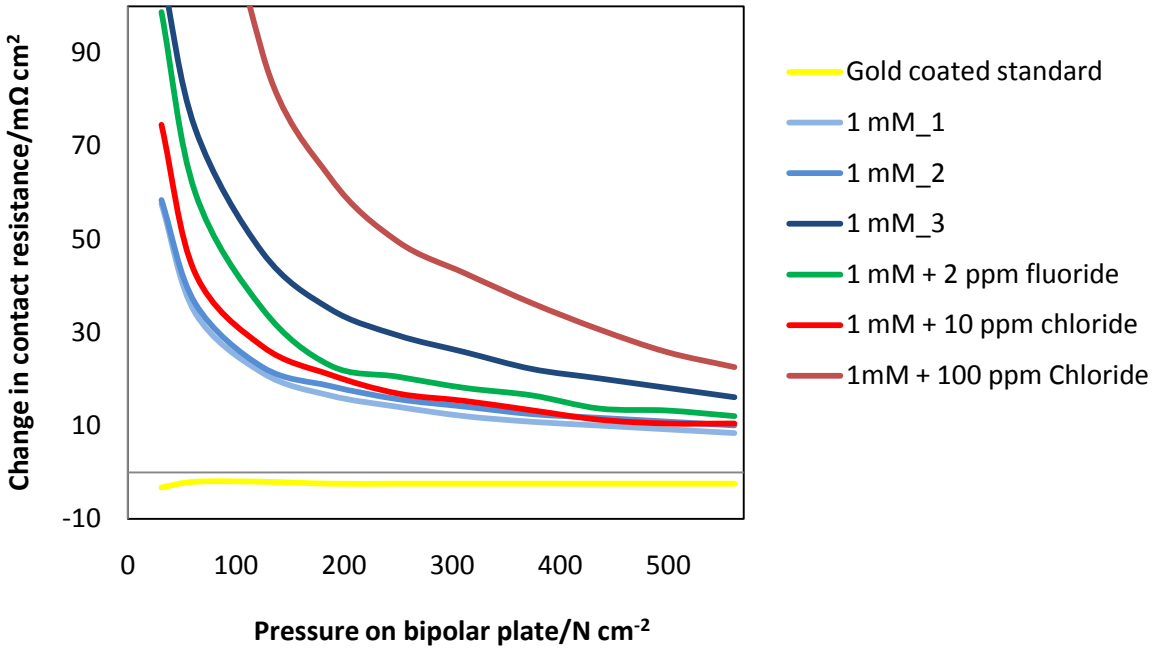

Figure 49: Addition of F^- and Cl^-, test 2; -0.717 V vs. $Hg/HgSO_4$ for 1 hour.

The polarization test results (section 4.1.5) showed that the tests performed in solutions with 2 ppm F^- and 10 ppm Cl^- produced current densities in the same order of magnitude as the reproducibility tests. The ICR measurements results from all three tests (1,2 and 3) seem to agree with the polarization test results because the 2 ppm F^- and 10 ppm Cl^- graphs fall in between the reproducibility graphs in both Figure 49 and Figure 50. This indicates that the amounts of chloride and fluoride found in a fuel cell do not affect the surface reactions taking place on the stainless steel bipolar plate.

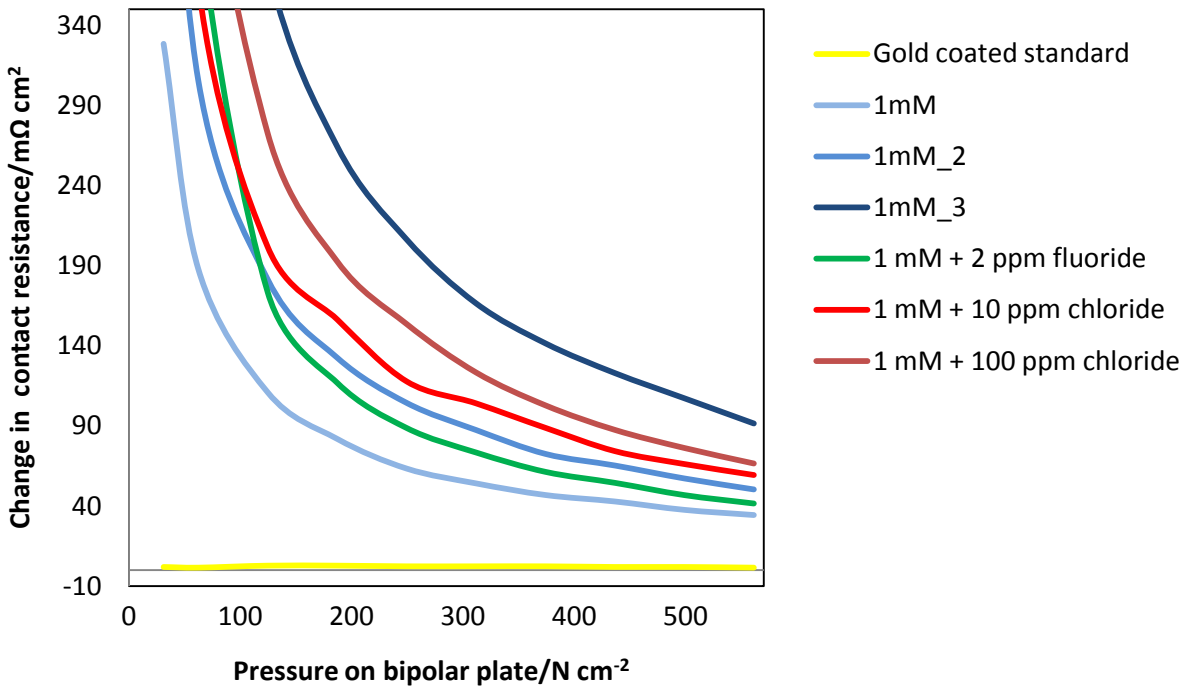

Figure 50: Addition of F^- and Cl^-, test 3; 0.293 V vs. $Hg/HgSO_4$ for 1 hour.

In section 4.1.5 the polarization test at 0.293 V vs. $Hg/HgSO_4$ in sulfuric acid containing 100 ppm Cl^- showed a very high corrosion current. The pictures taken of the plates in the SEM confirmed severe pitting all over the bipolar plate. The ICR results obtained before and after this polarization test do not show an increase or decrease in contact resistance compared to the other test presented in Figure 50. Pitting corrosion takes place in very small areas of the stainless steel, and the small areas of exposed iron compounds from the pitting should not contribute to a decrease in contact resistance. The oxide layer on the stainless steel plate does not have to be any thinner than on the reproducibility tested plates because the pitting only affects very small areas of the plates. This could in turn explain why the contact resistance measurements of the 100 ppm Cl^- test do not seem all that different from the other tests presented in Figure 50.

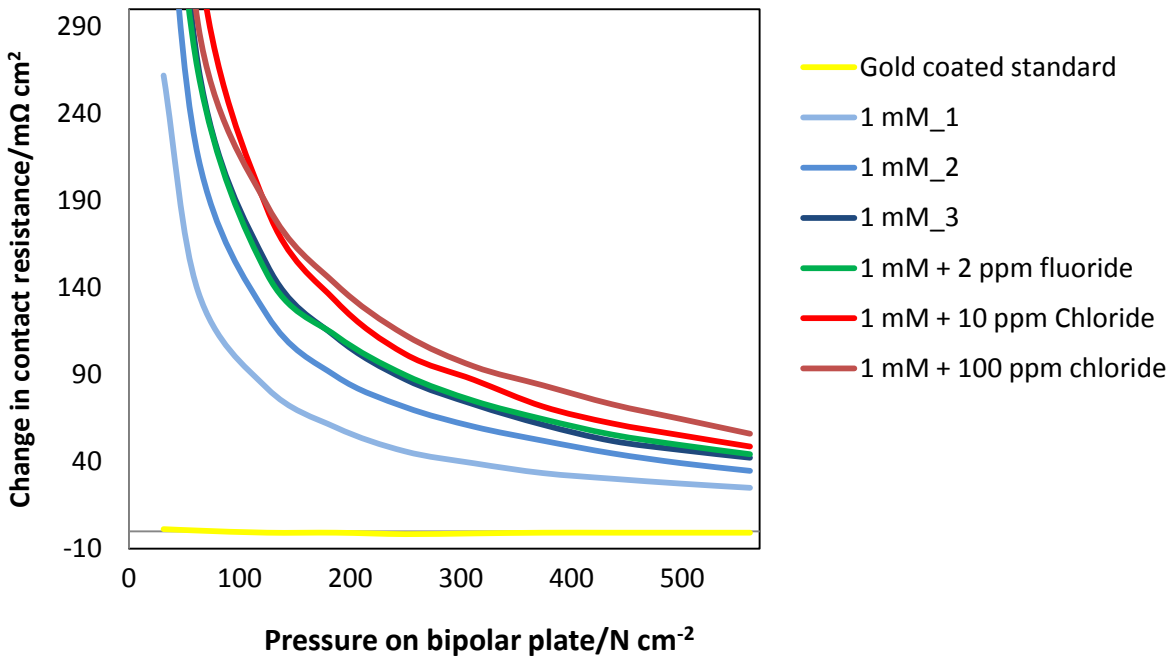

Figure 51: Addition of F- and Cl-, test 1; -0.9 V to 0.4 V vs. $Hg/HgSO_4$.

The delta values of the contact resistance from the 100 ppm Cl^- ICR tests in Figure 49 and Figure 51 are slightly higher than the rest of the tests presented in the same figures. There does not seem to be any obvious reasons for this, and it might just be the same instability that has been found in e.g. the reproducibility results. The 100 ppm Cl^- sweep test (Figure 51) delta ICR values are only slightly higher than the rests of the tests, while the delta ICR values 100 ppm Cl^- test at -0.717 V vs. $Hg/HgSO_4$ looks to be a little more separated from the rest of the results in this graph. This does not necessarily mean anything considering that the absolute delta values in Figure 49 are much lower than in the values in Figure 51.

4.2.6 Coating A

In section 4.1.6 the polarization test results from the stainless steel plates with Coating A were presented and discussed. Results different from what had been found in all the other tests throughout this project were presented there. In the following three figures (52-54), the results from the ICR measurements are presented as delta values. In all three figures the curves from the Coating A tests are lower than the reproducibility tests, which shows that the change in contact resistance was lower for the plates with Coating A than for the non coated stainless steel plates.

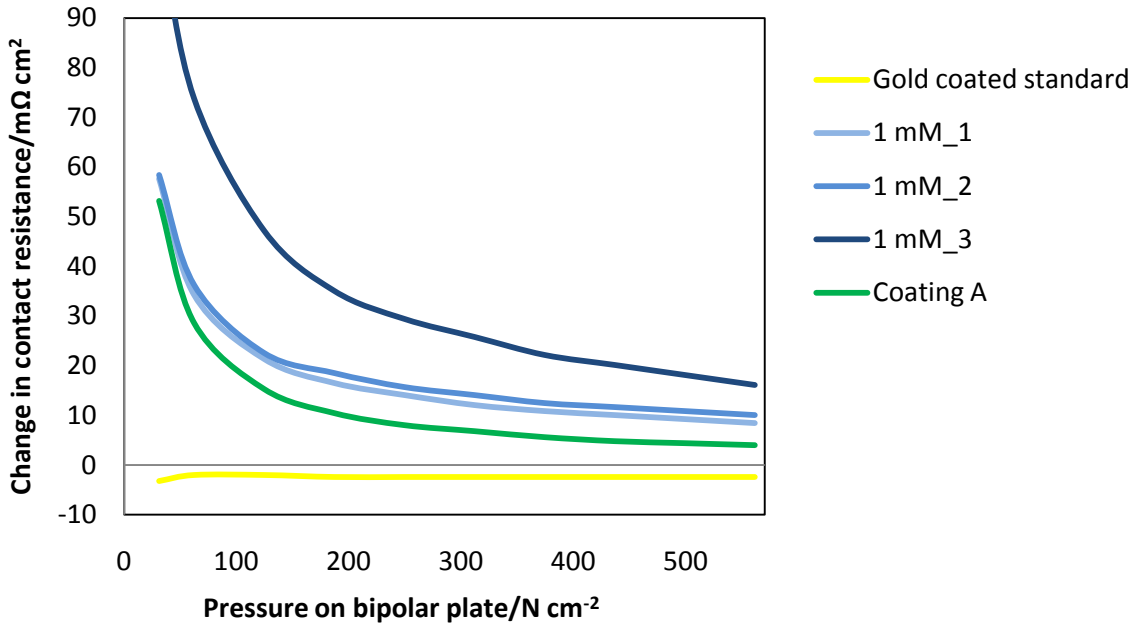

Figure 52: Coating A, test 2; -0.717 V vs. $Hg/HgSO_4$ for 1 hour.

The y-axis scales used in Figure 52, Figure 53 and Figure 54 are a little different because the contact resistance did not change much for any of the plates at -0.717 V vs. $Hg/HgSO_4$. However, if we look at the absolute values at 140 N cm^{-2} (Table 6) it is evident that all the ICR tests done before and after the polarization tests for the stainless steel plates with Coating A are in the same range, as opposed to for the non-coated stainless steel. This could be because stainless steel with Coating A showed little or no change after being put through any of the three standard polarization tests used during this research. If this is the case, Coating A is could be a promising alternative to the bare stainless steel plates as bipolar. If there is little or no change in contact resistance, there is most likely no oxide layer that prohibits the current to flow in between two stainless steel plates.

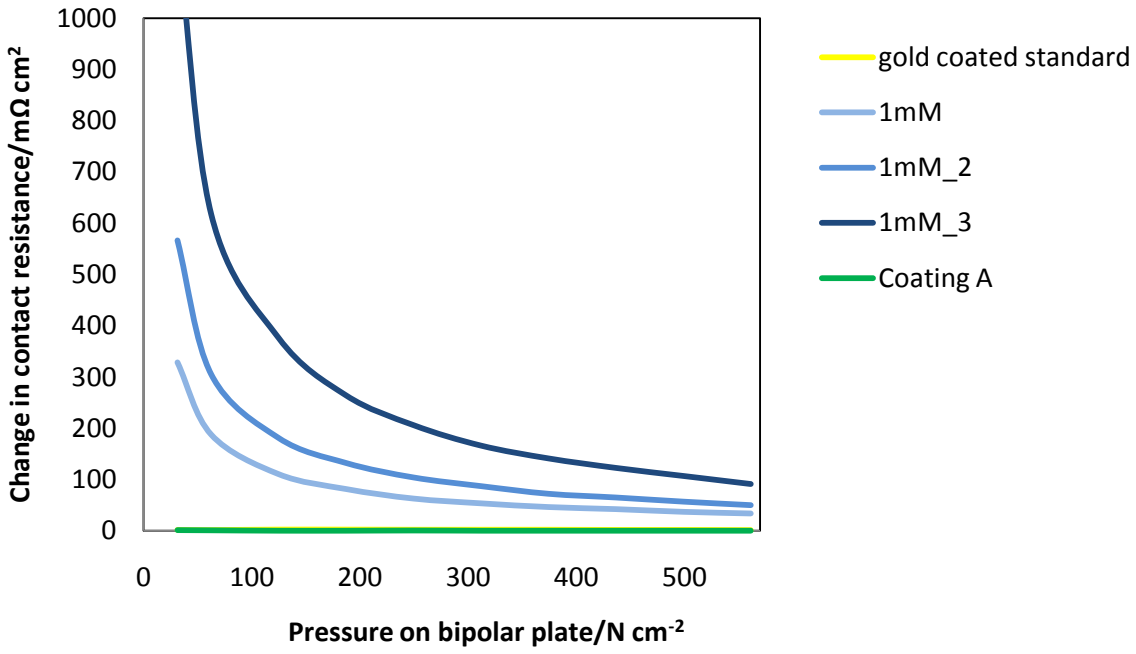

Figure 53: Coating A, test 3; 0.293 V vs. $Hg/HgSO_4$ for 1 hour.

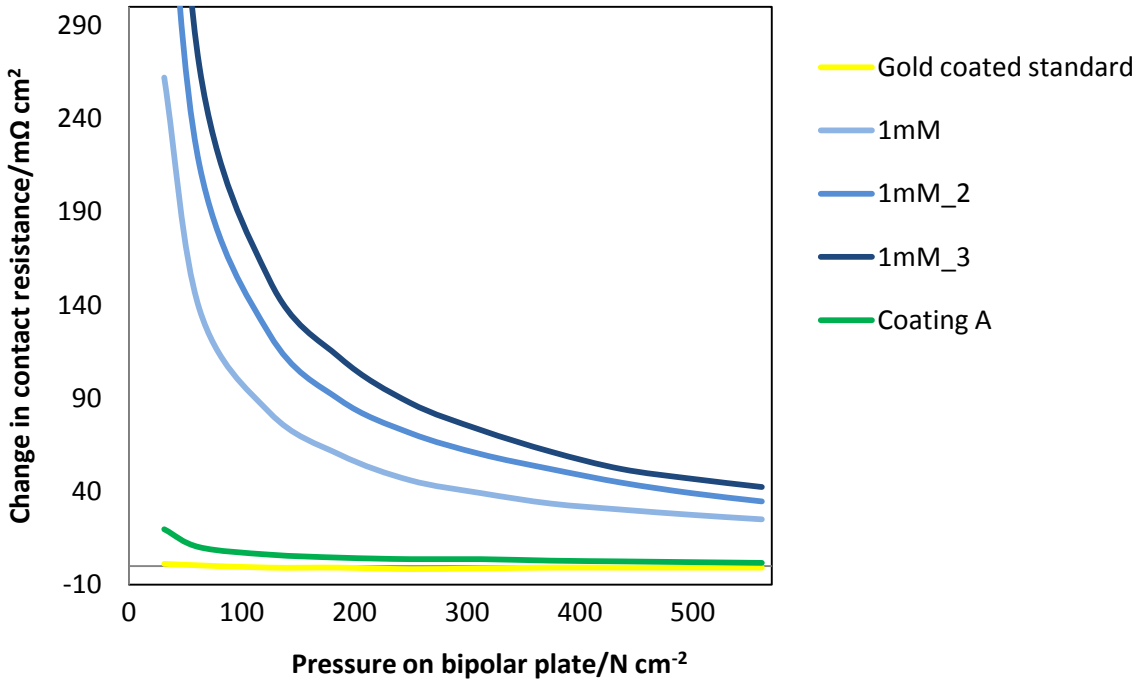

Figure 54: Coating A, test 1; -0.9 to 0.4 V vs. $Hg/HgSO_4$.

4.2.7 Concluding discussion of the contact resistance measurements

The delta results from all the contact resistance tests have been discussed, and it is clear that there is some instabilities and uncertainties about how reproducible and accurate these results are. But if the instabilities are put aside, there are still some results that deviate from the rest of the results. In section 4.1.7 it was concluded that the gold coated stainless steel plates did not work well as standard for the polarization tests, most likely due to pitting corrosion. For the ICR tests, the gold coated plates did produce good results, and with the low ICR delta values gold showed to be a very good standard for the contact resistance measurements. The non-coated stainless steel showed ICR results around 100 mΩ cm^2 (Table 6) after the polarization tests, which is around one order of magnitude higher than DOEs target for contact resistance (Table 1). This rules out stainless steel as bipolar plate material. By use of equation 5 it is found that 100 mΩ corresponds to 100 mV if the current is set to 1 A. This shows that the contact resistance matters for the fuel cell, even if the measured ICR values are small.

$$U = R_{contact} \cdot I \qquad (5)$$

Gold was not the only coating that did well in the contact resistance tests. The new coating, Coating A, showed little or no change in contact resistance at both the high potential (Figure 53) and sweep polarization tests (Figure 54). The changes in contact resistances before and after the high potential test (Figure 53) are actually lower than for the gold coated steel. The ICR values of Coating A measured after the polarization tests are all higher than DOEs target of 10mΩ cm^2, but not more than 18 mΩ cm^2 at the highest. This suggests that the new coating produces better ICR results than the gold coated plate, and with the low current densities recorded during the high potential polarization test (section 4.1.6 and 4.1.7), Coating A is close to satisfying DOE's targets for both contact resistance and corrosion current. The results from the polarization test at -0.717 V vs. $Hg/HgSO_4$ (Figure 38) and the corresponding ICR measurements (Figure 52) show that something has happened to the coating which needs to be further investigated if this Coating is to be used in future work.

Low changes in contact resistance were also found when the stainless steel plates used for the 0.1 M and the 1 M polarization tests were ICR tested (Figure 46, Figure 47 and Figure 48). These results are, however, not necessarily as promising as for the gold coated steel and the steel with coating A. The reason for the low change in contact resistance for the stainless steel after being tested in 0.1 M and 1 M solutions is probably because the oxide layers had started to dissolve during the polarization tests. This could in turn mean that the plates were more exposed to the corrosive environment, and the currents in Figure 30, Figure 31 and Figure 32 are higher for the 0.1 M and 1 M tests compared to the low molarity tests (0.1 mM and 1 mM) The absolute values of the contact resistances are all higher than DOEs requirements (Table 6). The connection between the polarization results and the contact resistance results will be further discussed in section 4.3.

4.3 Concluding discussion

The following discussion sums up and ties up the discussion of the polarization tests and the contact resistance measurements.

4.3.1 Gold coated stainless steel

The results from the polarization tests and corresponding ICR measurements of gold coated stainless steel did not all produce the results that were predicted when these plates were chosen as standard. The ICR tests showed that the contact resistance of the gold coated stainless steel changed very little after going through polarization tests (Figure 41, Figure 42 and Figure 43), which is promising. The polarization test results showed that the gold coated stainless steel plates produced current densities in the same order of magnitude as the non-coated stainless steel plates. This was not what was expected when gold was chosen as standard for the polarization tests, because gold coated steel was expected to show as low corrosion currents (i.e. the results obtained from gold on glass, Figure 23). The reason for the high currents was suggested to be that the gold coating not adhered well enough to the stainless steel surface. This could in turn have caused pitting corrosion, increasing the release of ions to the electrolyte and thus have caused the current to rise. Because of the high current densities the gold coated stainless steel should not have been used as an ideal standard for the polarization tests, but it proved to be a good standard for the ICR tests.

4.3.2 Reproducibility of non coated stainless steel

The results obtained from the reproducibility polarization tests and corresponding ICR measurements all gave results that indicated certain instabilities from test to test. The polarization tests (Figure 25, Figure 26 and Figure 27) showed variations in current densities between tests in the same order of magnitude as the absolute values of the current densities. The change in contact resistance showed the same trend between the reproduced tests, where the difference in contact resistance from one test to another in some areas of the graphs exceeded the absolute value of the contact resistance in that area (Figure 41, Figure 42 and Figure 43, section 4.2.2). Several reasons were suggested for these results, including temperature instabilities, problems with the power grid and composition variations in the stainless steel. The noise is probably not scaled with the measured current density, and the noise is thus more distinct when the current density is low. Even though the polarization test at high potential showed current densities close to DOE's requirements for bipolar plates in PEM fuel cells, the measured contact resistance was around one order of magnitude higher than DOE's requirements. These results correspond well with the assumption that a passivated oxide layer formed on the stainless steel plates during the polarization tests, as this would have caused low currents and great changes in contact resistance.

4.3.3 1 vs. 18 hours

The long term tests were performed to show that the chosen length of one hour for the rest of the polarization tests was reasonable. Both the polarization- and ICR results showed some divergence from the 1 hour tests. The current densities of the long term polarization tests (Figure 28 and Figure 29) both took longer to stabilize than for any of the 1 hour tests.

The ICR delta values did not either coincide with the 1 hour tests results (Figure 44 and Figure 45). Even though delta curves made from ICR results before and after the 1 hour tests showed some variations in current density, the long term delta values from both test 1 (-0.717 V vs. $Hg/HgSO_4$) and 2 (0.293 V vs. $Hg/HgSO_4$) where lower than all the 1 hour delta values. Thicker oxide layers were suggested as reasons for the divergence between the long term and the 1 hour polarization and ICR tests. As the plates used for the 18 hour tests had been used before, there might have been oxide layers on the surfaces even after cleaning them in acid. This could in turn have resulted in smaller changes in contact resistance compared to the 1 hour tests where new plates were used for each test.

4.3.4 pH variations

The polarization tests performed in the 1 M electrolyte (Figure 30, Figure 31 and Figure 32) all showed higher current densities compared to the tests performed in the electrolytes with other pH values (0.1 M, 1 mM and 0.1 mM). It was suggested that this increase was caused by destabilization of the passivated oxide layer. If this layer had dissolved either partially or completely as a result of the low pH in the electrolyte, the surface would have become more vulnerable to further corrosion. The corresponding changes in contact resistance for the same plates were close to zero for all three tests (Figure 46, Figure 47 and Figure 48). The contact resistance even seemed to decrease after the polarization test at -0.717 V vs. $Hg/HgSO_4$, which indicates that the surface oxide layer had become even thinner after the polarization tests than it was before. Regardless of what reactions took place on the stainless steel surface, both the ICR measurements and the polarization tests indicate that the oxide layer was dissolved in the 1 M sulfuric acid solution. This could cause the stainless steel to lose its corrosion resistance and corrode uniformly with time.

The ICR measurements performed after the tests done in the 0.1 M solution showed that the increase in contact resistance after all three tests (-0.717 V, 0.293 V and -0.9 to 0.4 V vs. $Hg/HgSO_4$) were substantially lower than the increase after the 0.1 mM and 1 mM tests. The corresponding results from the polarization tests also show an increase in current densities compared to the 0.1 mM and 1 mM tests, although for the 0.293 V vs. $Hg/HgSO_4$ test this increase was fairly small. This puts the results from the 0.1 M ICR and polarization tests in between the 1 M tests and the tests performed in the 0.1 mM and 1 mM solutions. If the oxide layer was partially dissolved in 1 M solution, it might also havestarted to dissolve in the 0.1 M solution. Both the contact resistance measurements and the polarization test results support this assumption.

For the tests performed in the lower molarity solutions (0.1 mM and 1 mM) it is hard to separate both the polarization and ICR results, because they are very similar. For test 1, 2 and 3 (Table 4) in the 0.1 mM and 1 mM solutions, the current densities were much lower compared to both the 0.1 M and 1 M solutions, and the changes in contact resistances were higher than for the high molarity solution tests. This could mean that the oxide layer formed on the surface of the stainless steel plates during the polarization tests were more stable in the 0.1 mM and 1 mM solution than in the 0.1 M and 1 M tests. This would explain both the high change in contact resistance and the low current densities.

What is evident from the polarization tests performed at different molarities and the ICR measurements done before and after each polarization test is that it does matter which molarity the tests are performed in. There are great differences in both the delta values of the contact resistance measurements and the current densities produced in the solutions with different acidities. From the results obtained during this project work it is suggested that the pH value chosen for polarization tests done in a simulated fuel cell environment should be as close to the real pH measured in the operating PEM fuel cell (Figure 18). Previous research has often been done in low pH electrolytes, usually with a pH of 1 (Table 3). Lowering of the pH might not just speed up the reactions that normally takes place on a stainless steel plates in an operating fuel cell. New reactions might take place on the plates, which would have never taken place in a real PEM fuel cell operated under normal conditions. One should thus be careful when changing the pH, and maybe consider other factors to alternate in order to accelerate the corrosion and degrading of the stainless steel plates.

4.3.5 Addition of Fluoride and Chloride to the electrolyte

The addition of 2 ppm fluoride and 10 ppm chloride to the 1 mM H_2SO_4 electrolyte did not result in substantial changes for neither the polarization tests nor the ICR measurements compared to the tests done in electrolytes without these ions (Figure 34, Figure 35 and Figure 36). The change in contact resistance also coincided well with the results from the reproduced tests. In the literature describing similar polarization testing, the effect off 2 ppm F^- and 10 ppm Cl^- was not determined (section 2.4.3), but the research described in this thesis indicates that the effect is small or non-existing.

The polarization tests done on the stainless steel plates in a 1 mM solution containing 100 ppm Cl^- were done to see if an increase in chloride concentration had any affect at all on the stainless steel. The results from both the polarization tests and the ICR measurements showed that this was in fact the case. A great increase in current density was recorded for the polarization at 0.293 V vs. $Hg/HgSO_4$, and clear signs of pitting corrosion was found by further investigation of the plates in the SEM (Figure 37). The other polarization and ICR measurements done in the solution containing 100 ppm Cl^- did not give results very different from corresponding tests done in sulfuric acid solution without any additions. Even though results obtained in the 0.293 V vs. $Hg/HgSO_4$ test were interesting, they were not very

relevant for further work with PEM fuel cells as 100 ppm Cl^- is a lot more chloride than what is expected to be found in an operating PEMFC.

4.3.6 Coating A

The new coating showed very promising results from the ICR measurements, and the delta values were all very low (Figure 52, Figure 53 and Figure 54). The polarization tests, on the other hand, did not show the same trend for both high and low voltages (Figure 38, Figure 39 and Figure 40). The polarization test done at high potential (0.293 V vs. $Hg/HgSO_4$) showed corrosion currents lower than most of the reproducibility tests and also lower than the corresponding test done on gold coated stainless steel. The corrosion currents of Coating A in the high potential test were close to DOE's target of less than 1 $\mu A\ cm^{-2}$, and the ICR values (Table 6) were also close to DOE's target of less than 10 $m\Omega\ cm^2$.

The polarization test set to run between -0.9 V and 0.4 V showed a very low current throughout the entire test, but there was a high cathodic current as the potential moved above the reversible potential for hydrogen evolution. This indicates that one or more of the components in the coating were reduced during the polarization. Because the composition of the coating was unknown, it was hard to determine which reduction reaction this could have been.

The polarization test done at -0.717 V vs. $Hg/HgSO_4$ on the stainless steel plates with Coating A showed a current density much higher than any of the reproducibility tests and even the test of the gold coated plate. One or several of the unknown components in the coating could have functioned as catalysts for hydrogen evolution, which could in turn have increased the current density. The corresponding ICR results showed a small decrease in contact resistances, but the absolute values were close to 0. This indicates that whatever reaction took place to cause high current densities during the polarization test, did not change the contact resistance remarkably.

5. Conclusion

Different results were obtained from the different polarization tests and corresponding ICR measurements throughout the project, and some of the results were more predictable than others. Gold coated stainless steel plates showed good results in the ICR tests, but high currents densities were recorded during the polarization tests. This current was probably caused by pitting corrosion in some areas of the stainless steel plates because the gold did not adhere well enough to the stainless steel surface. The gold coated glass showed very low current densities in the sweep test, and proved that the gold coated steel did not behave as gold by itself.

The reproducibility results showed that both the polarization tests and the contact resistance tests were hard to reproduce fully, but this can in part be excused by the fact that the measured absolute values of both current and contact resistance were very low for most of the tests. The noise was probably not scaled to the current density, and it was thus very distinct as the current densities were low. This makes it hard to get accurate measurements, and thus decreases the probability of getting good reproducibility.

The long term polarization tests showed that the current density did stabilize over time, but it took a little longer than what was expected. The ICR measurements showed a low increase in contact resistance, which could be because the stainless steel plates were reused. By reusing the plates the oxide layer formed in one polarization test might not have been entirely removed when they were cleaned in hydrochloric acid before the next test. If this was the case, the contact resistance would not change as much as it did when new stainless steel plates where used. This makes it hard to draw any conclusions from the long term results, but the current densities measured in most of the 1 hour polarization tests stabilized within the first 20 minutes, which indicates that 1 hour should be sufficient duration for each test.

The polarization tests performed at different molarities showed higher current densities, and the corresponding measured change in contact resistance showed lower changes in contact resistances for the tests performed in 0.1 M and 1 M solutions compared to the tests performed in the 0.1 mM and 1 mM solutions. This indicates that the passivated oxide layer created during the polarization test was disintegrated at higher molarities, which was also expected as the formation of chromium oxides depends on the pH in the electrolyte (section 2.4.1). If the oxide layer got thin enough or was completely removed, the surface of the stainless steel could easily react with the electrolyte and corrosion reactions could take place which are unlikely to take place in an operating fuel cell. If one is to follow the results obtained during this project work, tests in electrolytes with lower pH than what is found in an operating PEM fuel cell should not be conducted to accelerate the reactions on the stainless steel plates. Other factors should be altered if the objective is to accelerate reactions taking place in an operating fuel cell.

The polarization tests performed in the 1 mM solution containing either 2 ppm F^- or 10 ppm Cl^- did not result in currents higher than for the reproduced tests, and the change in contact resistance was also very similar to the results obtained from the reproducibility measurements. The stainless steel plates used for the test done in the electrolyte containing 100 ppm chloride showed clear signs of pitting corrosion after the 0.293 V vs. $Hg/HgSO_4$ test. The 100 ppm tests were conducted to see whether or not the higher chloride amount would have any effect on the stainless steel, but these high amounts are not probable to exist within an operating PEM fuel cell

Towards the end of the project a new coating called Coating A was run through the three standardized polarization tests with corresponding ICR measurements. The coating showed very promising results for tests 1 and 3 (0.9 V to 0.4 V and 0.293 V vs. $Hg/HgSO_4$), with relatively low current densities and very small changes in contact resistance. A high cathodic current was observed above the reversible potential for hydrogen evolution, which was suggested to be caused by one or more reduction reactions of components in Coating A. The change in contact resistance was also low after the polarization test done at -0.717 V vs. $Hg/HgSO_4$, but the current density produced during this test was very high. At this potential hydrogen evolution is the most likely reaction to occur, and the high current density indicates that components in Coating A were more catalytic towards hydrogen evolution compared to non-coated stainless steel. The composition of Coating A was not known, but the high hydrogen evolution and the possible reduction reactions should be further investigated if the coating is to be used in future projects.

Out of all the tests performed during this project work, very few of the contact resistance measurements were satisfying according to DOE's requirements of less than 10 mΩ cm^2 (Table 1). Gold coated stainless steel showed the best results, with values down to 10 mΩ cm^2 (Table 6). For Coating A, the contact resistance was around 14 mΩ cm^2 at its lowest. All the other ICR measurements were above DOE's requirements, which means that non-coated stainless steel is not suited as bipolar plate material. DOE's requirements for corrosion current is less than 1 μA cm^{-2}, which was obtained by the high voltage tests performed in 0.1 mM and 1 mM solutions as well as the high voltage test of Coating A. The plates with Coating A were however the only plates that satisfied DOE's requirements for both corrosion current and contact resistance.

6. Further work

Different results were presented in this thesis, and as with all projects one discovers improvements in the procedures as the project progresses. Some of the routines created during the project work are recommended to be carried on in projects building on this one. In order to get reproducible results new plates should be used for each test, at least if non-coated stainless steel is used. It is also recommended that the plates are cleaned in hydrochloric acid before the pre polarization ICR measurement.

The potentials chosen for the standardized tests at the start of the project were chosen because they were close to the anodic potential (-0.717 V vs. $Hg/HgSO_4$), and the open circuit potential (-0.293 V vs. $Hg/HgSO_4$). The objective of the polarization tests was to see whether or not the stainless steel plates corroded and at -0.717 V vs. $Hg/HgSO_4$ this is highly unlikely to happen. In the future the low potential test should be conducted at a higher potential, to avoid high current density caused by hydrogen evolution. This way corrosion might be easier to detect.

It is recommended that a further investigation of the reproducibility be done if accurate results are necessary. This was not an objective in the work done for this thesis, as there was a time limit for the project. Tests could be done using a different potentiostat, as there could be small changes in accuracy between each machine. Tests could also be performed at a different location, where the power grid does not affect the potential. Convection controlled tests could also be performed. It was assumed that some of the noise observed was a result of the low absolute values of the current density, which is difficult to do anything about.

Coating A showed promising ICR measurements and low currents were produced at higher potentials. The composition of the coating was not known, which made it difficult to determine which reaction(s) took place at low potentials. In order to use this coating in the future, more details about it and its composition should be obtained. Investigation of the coating by use of EDS and X-Ray Diffraction (XRD) should also be considered.

7. Literature

1. *40 fires foundation. How a fuel cell works*. 10.11.2010 10.34; Available from: http://40fires.org/Wiki.jsp?page=How%20a%20Fuel%20Cell%20Works.
2. Wang, H.L., M.A. Sweikart, and J.A. Turner, *Stainless steel as bipolar plate material for polymer electrolyte membrane fuel cells.* J. Power Sources, 2003. **115**(2): p. 243-251.
3. Hermann, A., T. Chaudhuri, and P. Spagnol, *Bipolar plates for PEM fuel cells: A review.* Int. J. Hydrog. Energy, 2005. **30**(12): p. 1297-1302.
4. Hamilton, P.J. and B.G. Pollet, *Polymer Electrolyte Membrane Fuel Cell (PEMFC) Flow Field Plate: Design, Materials and Characterisation.* Fuel Cells, 2010. **10**(4): p. 489-509.
5. Kongstein, O.E., A. Ødegård, and T. Tingelöf, *Report: Materials for bipolar plates in PEM fuel cells.* 2011.
6. Larminie, J. and A. Dicks, *Fuel cell systems explained*. 2003, Chichester: Wiley. xxii, 406 s.
7. Hamann, C.H., A. Hamnett, and W. Vielstich, *Electrochemistry*. 2007, Weinheim: Wiley. XVIII, 531 s.
8. Shao, Y., G. Yin, and Y. Gao, *Understanding and approaches for the durability issues of Pt-based catalysts for PEM fuel cell.* J. Power Sources, 2007. **171**(2): p. 558-566.
9. *Fuel cell R & D, Energy Efficiency and Renewable Energy Program.*
10. Tawfik, H., Y. Hung, and D. Mahajan, *Metal bipolar plates for PEM fuel cell - A review.* J. Power Sources, 2007. **163**(2): p. 755-767.
11. Jones, D.A., *Principles and Prevention of Corrosion*. 1996: Simon and Schuster.
12. Bardal, E., *Korrosjon og korrosjonsvern*. 2001. p. 125-136.
13. *The full wiki*. [cited 2011 23-05-11]; Available from: http://www.thefullwiki.org/Chromium.
14. *Different types of corrosion*. Available from: http://www.corrosionclinic.com/types_of_corrosion/pitting_corrosion.htm.
15. Makkus, R.C., A.H.H. Janssen, F.A. de Bruijn, and R.K.A.M. Mallant, *Use of stainless steel for cost competitive bipolar plates in the SPFC.* J. Power Sources, 2000. **86**(1-2): p. 274-282.
16. Ihonen, J., F. Jaouen, G. Lindbergh, and G. Sundholm, *A novel polymer electrolyte fuel cell for laboratory investigations and in-situ contact resistance measurements.* Electrochim. Acta, 2001. **46**(19): p. 2899-2911.
17. Lee, Y.B. and D.S. Lim, *Electrical and corrosion properties of stainless steel bipolar plates coated with a conduction polymer composite.* Curr. Appl. Phys., 2010. **10**: p. S18-S21.
18. Wang, L., D.O. Northwood, X. Nie, J. Housden, E. Spain, A. Leyland, and A. Matthews, *Corrosion properties and contact resistance of TiN, TiAlN and CrN coatings in simulated proton exchange membrane fuel cell environments.* J. Power Sources, 2010. **195**(12): p. 3814-3821.
19. Kumagai, M., S.T. Myung, S. Kuwata, R. Asaishi, and H. Yashiro, *Corrosion behavior of austenitic stainless steels as a function of pH for use as bipolar plates in polymer electrolyte membrane fuel cells.* Electrochim. Acta, 2008. **53**(12): p. 4205-4212.

20. Yoon, W., X.Y. Huang, P. Fazzino, K.L. Reifsnider, and M.A. Akkaoui, *Evaluation of coated metallic bipolar plates for polymer electrolyte membrane fuel cells.* J. Power Sources, 2008. **179**(1): p. 265-273.
21. Rivas, S.V., M.R. Belmonte, P.-Q.J. T., M.A. Cortes, L.E. Morón, and G. Orozco, *Corrosion Performance of Stainless Steel and Inconel in Simulated Fuel-Cell media.* ECS Transactions 2007(3): p. 13-30.
22. Ofstad, A.B., M.S. Thomassen, J.L. Gomez de la Fuente, F. Seland, S. Møller-Holst, and S. Sunde, *Assesment of Platinum Dissolution from a Pt/C Fuel Cell Catalyst: An Electrochemical Quartz Crystal.* Journal of Electrochemical Society, 2010(157): p. B621-B627.
23. Andre, J., L. Antoni, and J.P. Petit, *Corrosion resistance of stainless steel bipolar plates in a PEFC environment: A comprehensive study.* Int. J. Hydrog. Energy, 2010. **35**(8): p. 3684-3697.
24. Bard, A.J. and L.R. Faulkner, *Electrochemical Methods*. 1980: John wiley and Sons.
25. Hjelen, J., *Scanning elektron-mikroskopi*. 1989.

Appendix A: Picture of the polarization equipment

Figure A1: Picture of the polarization testing equipment.

Appendix B: Electrolyte calculations

1mM H_2SO_4 in a 2 liter solution:

$$M_{H_2SO_4} = 98.078 \frac{g}{mol}$$

Concentration of given H_2SO_4: 96%

Molarity: $1 \cdot 10^{-3} \frac{mol}{L}$

Mass H_2SO_4 (L) per liter solution:

$$m = \frac{c \cdot M}{96\%} = 1 \cdot 10^{-3} \frac{mol}{L} \cdot 98.078 \frac{g}{mol} = 0.102164 \frac{g}{L}$$

For a 2 liter solution:

$$m_{2L} = 0.102164\ g \cdot 2 = 0.2043291667\ g$$

Table B1: The calculated molarities of the different solutions.

Molarity	0.1mM	1mM	0.1M	1M
Amount H_2SO_4 in a 2 liter solution[g].	*0.02043291667*	*0.2043291667*	*20.43291667*	*204.3291667*
Approximate. pH (not measured)	*4*	*3*	*1*	*0*

Addition of Fluoride and Chloride to the 1mM H_2SO_4 solution:

Because the amount of H_2SO_4 and additives are so small compared to the 2 liters of water, this was not be taken into consideration when calculating the amount of additives.

2ppm F^-

$$M_{NaF}=41.99\frac{g}{mol} \quad \text{and} \quad M_{F^-}=19\frac{g}{mol}$$

For a 1 liter solution, 2 ppm F^- is:

$$m_{F^-}=2\cdot10^{-6}\frac{kg}{kg}=2\cdot10^{-3}\frac{g}{kg}$$

Given in grams per liter, assuming the density of water to be $1000\frac{g}{L}$:

$$2\cdot10^{-3}\frac{g}{kg}=2\cdot10^{-3}\frac{g}{kg}$$

For 2 liters:

$$2\cdot10^{-3}\frac{g}{L}\cdot 2=4\cdot10^{-3}\frac{g}{L}$$

Total amount of NaF in a 2 ppm F^- solution:

$$m_{NaF}=4\cdot10^{-3}\ g\cdot\frac{41.99\frac{g}{mol}}{19\frac{g}{mol}}=8.84\cdot10^{-3}\ g$$

10 ppm Cl^-

$$M_{NaCl}=58.44\frac{g}{mol} \quad \text{and} \quad M_{Cl^-}=35.45\frac{g}{mol}$$

For a 1 liter solution, 2 ppm F^- is:

$$m_{Cl^-}=1\cdot10^{-5}\frac{kg}{kg}=1\cdot10^{-2}\frac{g}{kg}$$

Given in grams per liter assuming the density of water to be $1000\frac{g}{L}$:

$$1\cdot10^{-2}\frac{g}{kg}=1\cdot10^{-2}\frac{g}{L}$$

For 2 liters:

$$1\cdot10^{-2}\frac{g}{L}\cdot2=2\cdot10^{-2}\frac{g}{L}$$

Total amount of NaF in a 2 ppm F^- solution:

$$m_{NaCl}=2\cdot10^{-2}\ g\cdot\frac{58.44\ \frac{g}{mol}}{35.45\ \frac{g}{mol}}=3.297\cdot10^{-2}\ g$$

Appendix C: The start up procedure of the program used to run the potentiostat

Figure C1: The start up window of the Thales program.

The first window in the Thales program is shown in figure C1. The green button was pushed to enter the program. In the next window (figure C2), POL was chosen to start the polarization part of the program. Figure C3 shows the window where the conditions for the polarization test were set. Phase 1 (*polarization*) was used for the tests run at constant potentials, which was applied along with the length of the tests and intervals between each measurement (Figure C3). Phase 3 (*linear scan*) was used for the test run between -0.9 V and 0.4 V, and the potentials were applied along with the scan rates (Figure C3).

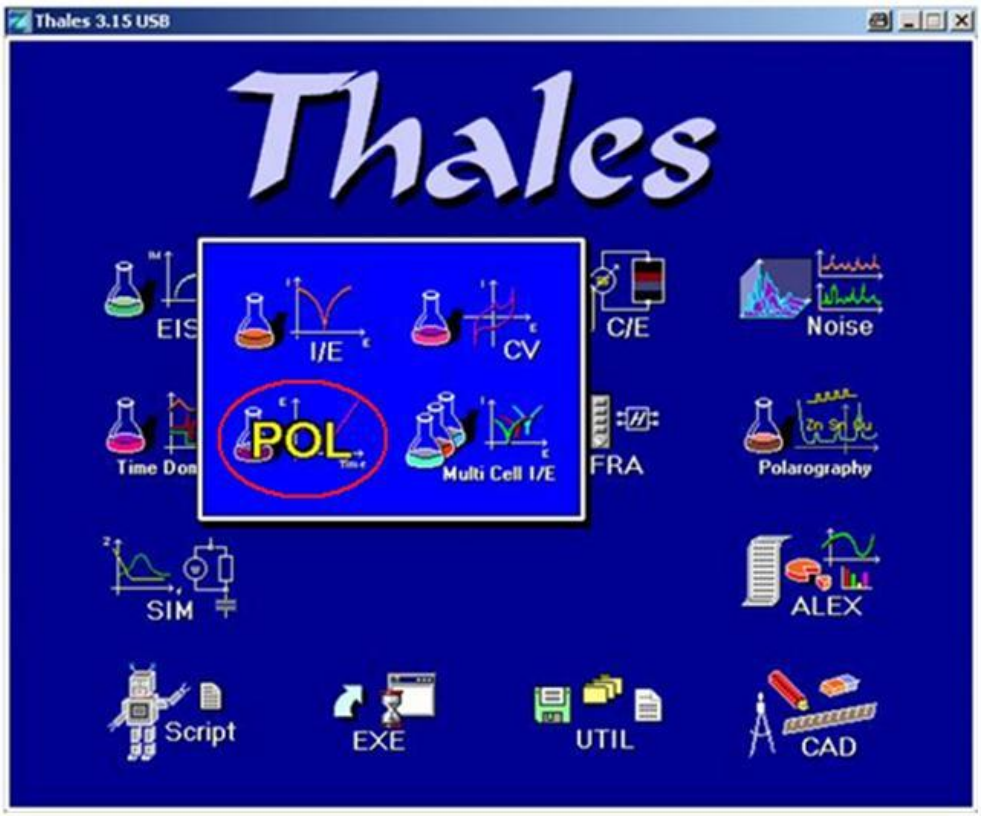

Figure C2: The window where polarization testing was chosen.

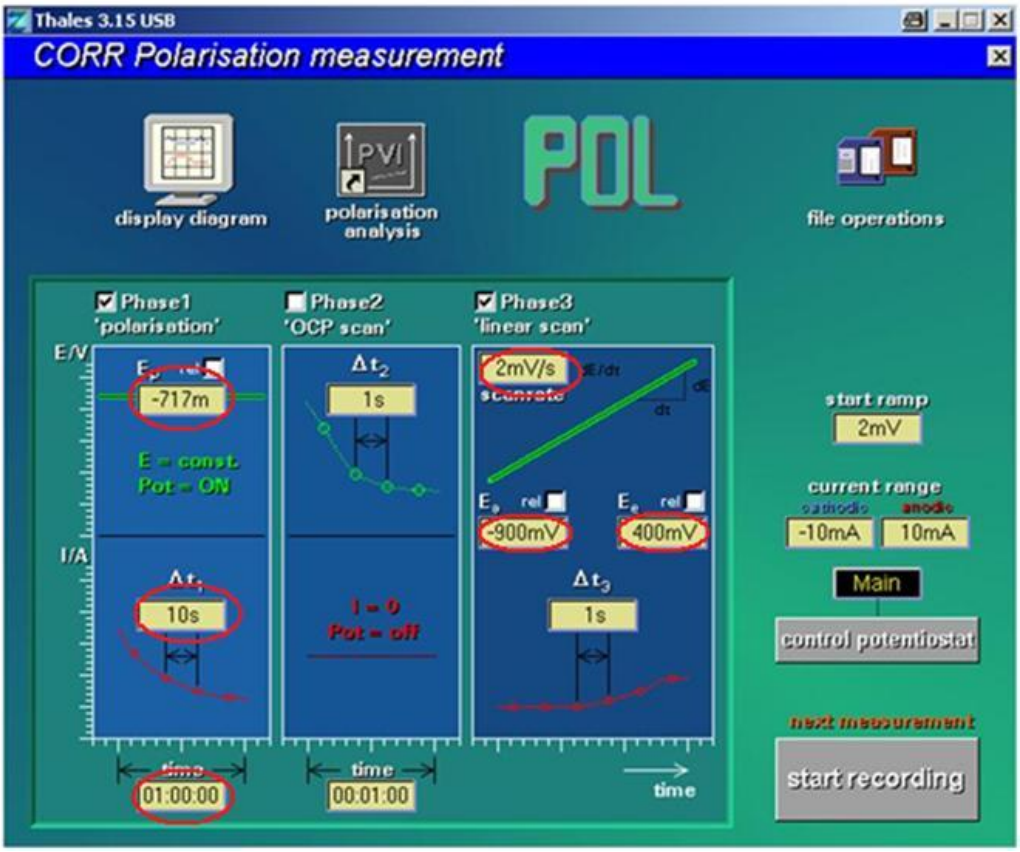

Figure C3: The window where the different tests were chosen and conditions were applied.

Appendix D: All the corrosion tests performed during this project

Table D1: Overview: All the tests done during the research described in this report.

Date (2011)	Coating	Test number	Molarity [mol/L]	Additives to the electrolyte	Comment
11.01	-	1+2+3	1 mM	-	-
13.01	-	1+2+3	1 mM	-	-
18.01	-	1+2+3	1 mM	-	-
24.01	-	2	1 mM	-	-
24.01	-	3	1 mM	-	-
26.01	-	4	1 mM	-	1 vs. 18 hours
31.01	-	4	1 mM	-	1 vs. 18 hours
01.02	-	2	1 mM	-	-
02.02	-	4	1 mM	-	1 vs. 18 hours
03.02	-	5	1 mM	-	1 vs. 18 hours
08.02	-	2	0.1 M	-	pH- variations
09.02	-	3	0.1 M	-	pH- variations
10.02	-	2	0.1 M	-	pH- variations
10.02	-	1	0.1 M	-	pH- variations
11.02	-	3	1 M	-	pH- variations
11.02	-	2	1 M	-	pH- variations
16.02	-	2	0.1 mM	-	pH- variations
16.02	-	3	0.1 mM	-	pH- variations
18.02	-	1	0.1 mM	-	pH- variations
01.03	-	2	1 M	-	pH- variations
01.03	-	3	1 M	-	pH- variations
01.03	-	1	1 M	-	pH- variations
07.03	-	2	0.1 mM	-	pH- variations
07.03	-	3	0.1 mM	-	pH- variations
08.03	-	3	0.1 mM	-	pH- variations
09.03	-	2	1 mM	-	Reproducibility
09.03	-	2	1 mM	-	Reproducibility
14.03	-	2	1 mM	-	Reproducibility
14.03	-	3	1 mM	-	Reproducibility
15.03	-	3	1 mM	-	Reproducibility
16.03	-	3	1 mM	-	Reproducibility
18.03	Gold	2	1 mM	-	Gold standard
21.03	Gold	3	1 mM	-	Gold standard
21.03	-	2	1 mM	-	-
22.03	-	3	1 mM	-	-
22.03	-	1	1 mM	-	-
25.03	-	2	0.1 M	-	pH- variations

25.03	-	3	0.1 M	-	pH- variations
28.03	-	1	0.1 M	-	pH- variations
30.03	Gold	1	1 mM	-	Gold standard
01.04	-	1	1 mM	-	-
05.04	-	1	1 mM	2 ppm F^-	Additives
05.04	-	2	1 mM	2 ppm F^-	Additives
06.04	-	3	1 mM	2 ppm F^-	Additives
07.04	-	1	1 mM	2 ppm F^-	Additives
07.04	-	2	1 mM	10 ppm Cl^-	Additives
07.04	-	1	1 mM	10 ppm Cl^-	Additives
08.04	-	3	1 mM	10 ppm Cl^-	Additives
11.04	-	1	1 mM	10 ppm Cl^-	Additives
11.04	-	2	1 mM	10 ppm Cl^-	Additives
12.04	-	1	1 mM	-	Reproducilbility
12.04	-	1	1 mM	-	Reproducilbility
02.05	-	1	1 mM	100 ppm Cl^-	Additives
04.05	-	2	1 mM	100 ppm Cl^-	Additives
11.05	-	3	1 mM	-	Reproducilbility
11.05	Coating A	2	1 mM	-	Coating A
11.05	Coating A	1	1 mM	-	Coating A
12.05	Coating A	3	1 mM	-	Coating A
12.05	-	3	1 mM	100 ppm Cl^-	Additives
12.05	-	3	1 mM	-	Reproducilbility

Appendix E: Calculation of contact resistance

Areas and applied current:

Surface area piston:

$$A_{piston} = 3.1414 \cdot 4 \cdot 4\ cm^2 = 50.256\ cm^2$$

Surface area stainless steel plate (one side):

$$A_{plate\_1} = 16.08\ cm^2$$

Actual contact area between plate and Piston:

$$A_{plate\_2} = 8.059\ cm^2$$

Current applied: 2 A

Calculation of the force excited on the plate:

Pressure applied from the piston: 1 bar

Force from piston:

$$F_{Piston} = P_{Piston} \cdot A_{Piston} = 1bar \cdot 50.256\ cm^2 = 50.256\ bar\ cm^2$$

Pressure on plate:

$$P_{plate} = \frac{F_{Piston}}{A_{plate}} = \frac{50.256\ bar\ cm^2}{8.059\ cm^2} = 6.236\ bar = 62.36\ N\ cm^{-2}$$

Calculation of the contact resistance:

Potential measured at 1 bar: 11.3 mV

Resistance from potential and current:

$$R = \frac{V}{I} = \frac{11.3\ mV}{2A} = 5.65\ m\Omega$$

Contact resistance:

$$R_{contact} = R \cdot A_{plate(oneside)} = 5.65\ m\Omega \cdot 8.059\ cm^2 = 45.53335\ m\Omega\ cm^2$$